

CERN-TH/2000-296

BARI-TH/2000-394

QCD SUM RULES, A MODERN PERSPECTIVE

PIETRO COLANGELO

*Istituto Nazionale di Fisica Nucleare, Sezione di Bari, Italy*ALEXANDER KHODJAMIRIAN^a*Theory Division, CERN, CH-1211 Geneva 23, Switzerland*

An introduction to the method of QCD sum rules is given for those who want to learn how to use this method. Furthermore, we discuss various applications of sum rules, from the determination of quark masses to the calculation of hadronic form factors and structure functions. Finally, we explain the idea of the light-cone sum rules and outline the recent development of this approach.

*to be published in the Boris Ioffe Festschrift
"At the Frontier of Particle Physics / Handbook of QCD",
edited by M. Shifman (World Scientific, Singapore, 2001)*

^aOn leave from Yerevan Physics Institute, 375036 Yerevan, Armenia

Contents

1	Introduction	3
2	Understanding SVZ sum rules	4
2.1	Correlation function of quark currents	4
2.2	Summing up hadrons: the unitarity relation	7
2.3	Deriving the dispersion relation	8
2.4	Applying the Borel transformation	10
2.5	Calculating the correlation function in QCD: the perturbative part	11
2.6	Vacuum condensates and operator product expansion	14
2.7	What do we know about the vacuum condensates ?	20
2.8	Use of quark-hadron duality	22
2.9	SVZ sum rules at work	25
3	Applications and development of the method	29
3.1	Light quark masses: m_u, m_d, m_s	30
3.2	Heavy quark masses: m_c, m_b	34
3.3	Heavy-light mesons	35
3.4	B_c meson	38
3.5	Ioffe currents and sum rules for baryons	39
3.6	Three-point correlation functions: form factors and decay am- plitudes	42
3.7	Hadron structure functions	48
3.8	Matrix elements of effective operators	51
3.9	QCD sum rules in HQET	52
4	Light-Cone Sum Rules	54
4.1	The basics of the method	54
4.2	Light-cone distribution amplitudes	62
4.3	LCSR for the pion form factor	64
4.4	Strong Couplings	67
4.5	Heavy-to-light form factors and couplings	69
5	Summary	74

1 Introduction

The method of QCD sum rules, developed more than twenty years ago by Shifman, Vainshtein and Zakharov (SVZ),¹ has become a widely used working tool in hadron phenomenology.^b The advantages of this method are well known. Instead of a model-dependent treatment in terms of constituent quarks, hadrons are represented by their interpolating quark currents taken at large virtualities. The correlation function of these currents is introduced and treated in the framework of the operator product expansion (OPE), where the short- and long-distance quark-gluon interactions are separated. The former are calculated using QCD perturbation theory, whereas the latter are parametrized in terms of universal vacuum condensates or light-cone distribution amplitudes. The result of the QCD calculation is then matched, via dispersion relation, to a sum over hadronic states. The sum rule obtained in this way allows to calculate observable characteristics of the hadronic ground state. Inversely, the parameters of QCD such as quark masses and vacuum condensate densities can be extracted from sum rules which have experimentally known hadronic parts. What is also very important, the interactions of quark-gluon currents with QCD vacuum fields critically depend on the quantum numbers (spin-parity, flavor content) of these currents. Therefore, interpolating hadrons with currents, one is able to understand why the hadrons with different quantum numbers are not alike.² Numerous properties of hadrons with various flavor content have been calculated by the sum rule method. The results are encouraging and in most cases reveal a remarkable agreement with the experimental data. Therefore, whenever one needs to determine an unknown hadronic parameter, the QCD sum rule prediction is among the reliable ones.

However, the accuracy of this method is limited, on one hand, by the approximations in the OPE of the correlation functions and, on the other hand, by a very complicated and largely unknown structure of the hadronic dispersion integrals. The latter are usually approximated by employing the quark-hadron duality approximation. Consequently, the applicability of sum rules and the uncertainties of their predictions must be carefully assessed case by case.

QCD sum rules are discussed in many reviews^{3–10} (the list can be further continued) emphasizing various aspects of the method. In this review we try to present and update the subject in a more concise, i.e. close to encyclopedic style, explaining the basics, presenting the most interesting applications, overviewing the recent developments and assessing the current and future po-

^b The mere fact that the original SVZ work¹ has already got more than 2200 citations reflects the amount of papers employing QCD sum rules.

tential of sum rules. In several cases we compare the predictions of this method with the results of lattice QCD. Our purpose is to convince the reader that the analytical QCD sum rules are to a large extent complementary to the numerical lattice simulations of hadrons. It is a very special occasion to write a review on QCD sum rules in honor of B.L. Ioffe who contributed to this field with landmark results, considerably enlarging the spectrum of hadronic problems treated within this method.

The content of the review is as follows. Section 2 is an elementary introduction written for readers who have no experience in QCD sum rules and would like to grasp the basics of the method. In Section 3 we present an overview of the current status of many important applications and discuss the possible improvements and the perspectives for new investigations. In Section 4 we consider the light-cone version of QCD sum rules, explaining the idea, outlining the derivation and presenting the main applications. Section 5 contains a summary.

2 Understanding SVZ sum rules

2.1 Correlation function of quark currents

The QCD Lagrangian

$$\mathcal{L}_{QCD} = -\frac{1}{4}G_{\mu\nu}^a G^{a\mu\nu} + \sum_q \bar{\psi}_q(i \not{D} - m_q)\psi_q, \quad (1)$$

where $G_{\mu\nu}^a$ is the gluon field-strength tensor and ψ_q are the quark fields with different flavors: $q = u, d, s, c, \dots$, is discussed in detail in many chapters of this book. It is our common belief that this Lagrangian governs all properties of hadrons and hadronic processes. However, a direct use of Eq. (1) and of the corresponding Feynman rules is possible only within the limited framework of perturbation theory. At least some of the quarks or gluons in a hadronic process have to be highly virtual. This condition guarantees the smallness of the corresponding effective quark-gluon coupling $\alpha_s = g_s^2/4\pi$ and, thereby, a legitimacy of the perturbative expansion. Usually, high virtuality is achieved in a scattering of hadrons at large momentum transfer. However, even for these specially configured hard scattering processes, a perturbative calculation of quark-gluon Feynman diagrams is not sufficient, because the quarks participating in the hard scattering are confined inside hadrons. Hence, one has to combine the perturbative QCD result with certain wave functions or momentum distributions of quarks in hadrons. To calculate these characteristics, one needs to know the QCD dynamics at distances of order of the hadron

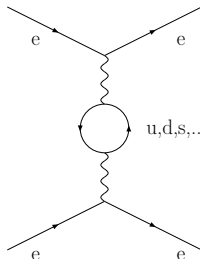


Figure 1: Quark-antiquark creation and annihilation by the virtual photon in the electron-electron scattering.

size: $R_{hadr} \sim 1/\Lambda_{QCD}$, the scale at which perturbation theory in α_s is not applicable.

In order to avoid long-distance problems, one could consider processes with *no* initial and final hadrons, and with all quarks propagating at short distances (during short times). Such configurations are not that hypothetical as it may seem. They are realized in nature, when the quark-antiquark pair is produced and absorbed by an external source, e.g. by a virtual photon in the electron-electron elastic scattering, as shown in Fig. 1. The propagation of the intermediate quark-antiquark pair in this process adds a very small (order of $\alpha_{em} = e^2/4\pi$) quantum correction to the cross section of $e^-e^- \rightarrow e^-e^-$. Nevertheless, taken separately, the amplitude of the quark-pair creation and annihilation is an extremely useful object from the QCD point of view. The formal expression for this amplitude can be written as

$$\Pi_{\mu\nu}(q) = i \int d^4x e^{iq \cdot x} \langle 0 | T \{ j_\mu(x) j_\nu(0) \} | 0 \rangle = (q_\mu q_\nu - q^2 g_{\mu\nu}) \Pi(q^2), \quad (2)$$

where q is the four-momentum of the virtual photon with $q^2 < 0$, $j_\mu = \bar{\psi} \gamma_\mu \psi$ is the colorless quark current with a given flavor $\psi = u, d, s, c, \dots$ (for simplicity, we have omitted the electromagnetic coupling from this definition). In the amplitude (2), the initial and final states contain no hadrons and are therefore identified with the vacuum state of QCD. The Lorentz-structure of the r.h.s. of Eq. (2) is dictated by the conservation of the electromagnetic current: $\partial_\mu j^\mu = 0$, so that the single invariant amplitude $\Pi(q^2)$ encodes all dynamical effects.

The amplitude $\Pi_{\mu\nu}$ represents an important example of a two-point *corre-*

lation function (correlator) of quark currents. If the four-momentum squared transferred to the quarks is large, $Q^2 \equiv -q^2 \gg \Lambda_{QCD}^2$, this correlation function turns into the genuine short-distance object we are looking for. This is simply because the integral in Eq. (2) is dominated by small spatial distances and time intervals:

$$|\vec{x}| \sim x_0 \sim 1/\sqrt{Q^2} \ll R_{hadr} . \quad (3)$$

This condition can be directly inferred from a general analysis of Eq. (2) in the case of massless quarks, an approximation justified for the light u, d, s quarks. After contraction of the Lorentz indices, the vacuum average in Eq. (2) can only depend on the space-time interval $x^2 = x_0^2 - \vec{x}^2$:

$$\langle 0 | T\{j_\mu(x)j^\mu(0)\} | 0 \rangle = \int d\tau e^{i\tau x^2} f(\tau) , \quad (4)$$

where the Fourier transform of this functional dependence is introduced. Using the representation (4) and shifting the variable x , one obtains from Eq. (2):

$$3q^2\Pi(q^2) = -i \int d\tau \int d^4x e^{i\tau x^2} e^{iQ^2/4\tau} f(\tau) . \quad (5)$$

The integrand on the r.h.s. of this equation is suppressed if at least one of the exponential functions rapidly oscillates. Therefore, dominant contributions to $\Pi(q^2)$ stem from the regions where both $\tau \sim 1/x^2$ and $\tau \sim Q^2$. To fulfill these two conditions simultaneously, one has to demand

$$x^2 \sim 1/Q^2 , \quad (6)$$

so that, at $Q^2 \rightarrow \infty$ the quarks propagate near the light-cone, $x^2 \sim 0$. This condition is necessary but not yet sufficient for the short-distance dominance. To demonstrate the latter it is convenient to choose the reference frame $q_0 = 0$, so that $\vec{q}^2 = Q^2$, and the exponent in Eq. (2) is simply equal to $\exp(-i\vec{q} \cdot \vec{x})$. Again, to avoid a fast oscillating integrand one needs

$$|\vec{x}| \sim 1/\sqrt{Q^2} , \quad (7)$$

which, together with Eq. (6), yields Eq. (3). Hence, at large Q^2 the quarks in the diagram in Fig. 1 propagate predominantly at short distances and during short time intervals. Due to the asymptotic freedom of QCD, the quark-gluon interactions are then suppressed. Therefore, as a first approximation, one may calculate the correlation function (2) representing virtual quarks by the free-quark propagators inferred directly from the Lagrangian (1). In the case of heavy quark currents ($\psi = c, b$), the situation is even simpler because the

quark mass $m_{c,b} \gg \Lambda_{QCD}$ introduces an intrinsic large energy scale. One has an asymptotically free quark-antiquark fluctuation already at small $q^2 \ll 4 m_{c,b}^2$. In this case, the characteristic distances in the correlation function are determined by the inverse heavy quark mass $|\vec{x}| \sim x_0 \sim 1/(2 m_{c,b})$.

2.2 Summing up hadrons: the unitarity relation

Before turning to the actual calculation of $\Pi_{\mu\nu}$, let us discuss how this object is related to physically observed hadrons. Note that the invariant amplitude $\Pi(q^2)$ is an analytic function of q^2 defined at both negative (spacelike) and positive (timelike) values of q^2 and, formally, even at complex values of this variable. At positive q^2 the underlying electromagnetic process is the cross-channel of the electron-electron scattering, i.e. the annihilation $e^+e^- \rightarrow e^+e^-$ with the total c.m. energy $E_{e^+} + E_{e^-} = \sqrt{q^2}$. If q^2 is shifted from large negative to positive values, the average distance between the points 0 and x in the quark amplitude (2) grows. The long-distance quark-gluon interactions become important and, eventually, the quarks form hadrons. In particular, a quark-antiquark pair created by the current j_μ with the spin-parity $J^P = 1^-$ materializes as a neutral vector meson. For the currents $\bar{u}\gamma_\mu u$ and $\bar{d}\gamma_\mu d$, one has to respect the isospin symmetry, because the mass difference $m_d - m_u \sim O(\text{MeV})$ is much smaller than the QCD scale Λ_{QCD} . The ground-state vector mesons with the isospin $I = 1$ and $I = 0$ are ρ and ω with the quark content $(\bar{u}u - \bar{d}d)/\sqrt{2}$ and $(\bar{u}u + \bar{d}d)/\sqrt{2}$, respectively. The lightest vector meson created by the current $\bar{s}\gamma_\mu s$ is ϕ . For the heavy quark currents $\bar{c}\gamma_\mu c$ and $\bar{b}\gamma_\mu b$, the ground states are J/ψ and Υ , respectively. Physically, vector mesons are observed in a form of resonances in e^+e^- annihilation at energies $\sqrt{q^2} = m_V$, ($V = \rho, \omega, \phi, J/\psi, \Upsilon, \dots$). Not only the ground-state, but also excited vector mesons and a continuum of two- and many-body hadron states with the quantum numbers of V contribute to $\Pi_{\mu\nu}$.

A rigorous way to quantify a very complicated hadronic content of $\Pi_{\mu\nu}$ at $q^2 > 0$ is provided by the *unitarity relation* obtained by inserting a complete set of intermediate hadronic states in Eq. (2):

$$2\text{Im}\Pi_{\mu\nu}(q) = \sum_n \langle 0 | j_\mu | n \rangle \langle n | j_\nu | 0 \rangle d\tau_n (2\pi)^4 \delta^{(4)}(q - p_n), \quad (8)$$

where the summation goes over all possible hadronic states $|n\rangle$ created by the quark current j_μ including sums over polarizations, and $d\tau_n$ denotes the integration over the phase space volume of these states.

The one-particle, vector meson contribution to the hadronic sum (8) is

$$\frac{1}{\pi} \text{Im } \Pi_{\mu\nu}^V(q^2) = (q_\mu q_\nu - m_V^2 g_{\mu\nu}) f_V^2 \delta(q^2 - m_V^2), \quad (9)$$

where the total decay width of V is neglected for simplicity, and the decay constant f_V is defined by the matrix element of the current j_μ between the vacuum and the vector-meson states:

$$\langle V(q) | j_\mu | 0 \rangle = f_V m_V \epsilon_\mu^{(V)*}, \quad (10)$$

$\epsilon_\mu^{(V)}$ being the polarization vector of V ($\epsilon^V \cdot q = 0$). Note that f_V is a typical hadronic parameter determined by the long-distance dynamics.

The contributions of continuum hadronic states to the unitarity relation (8) are more involved. Each individual state $|n\rangle$ yields a continuous imaginary part at $q^2 > m_n^2$, m_n being the sum of hadron masses in this state. Moreover, the corresponding hadronic matrix elements for multiparticle states $\langle n | j_\mu | 0 \rangle$ are not just constants but depend on q^2 .

For convenience, we single out the ground-state vector-meson contribution on the r.h.s. of the unitarity relation (8) and introduce a compact notation for the rest of contributions including excited vector mesons and continuum states:

$$\frac{1}{\pi} \text{Im } \Pi(q^2) = f_V^2 \delta(q^2 - m_V^2) + \rho^h(q^2) \theta(q^2 - s_0^h), \quad (11)$$

where s_0^h is the threshold of the lowest continuum state. Notice that in the light quark channels this threshold, set by two- and three-pion states, is lower than m_V . In the heavy quark channels the pattern is different. There are several heavy quarkonium resonances below the threshold of the heavy flavored meson pair production and, therefore, Eq. (11) has to be slightly modified: $\text{Im } \Pi^V(q^2) \rightarrow \sum_V \text{Im } \Pi^V(q^2)$ including the sum over all below-threshold quarkonium states.

2.3 Deriving the dispersion relation

From the above discussion we learned that the correlation function (2) is an object of *dual* nature. At large negative q^2 it represents a short-distance quark-antiquark fluctuation and can be treated in perturbative QCD, whereas at positive q^2 it has a decomposition in terms of hadronic observables. The next step is to derive a dispersion relation linking $\Pi(q^2)$ at an arbitrary point $q^2 < 0$ to the hadronic sum (8). For that, one employs the Cauchy formula for the

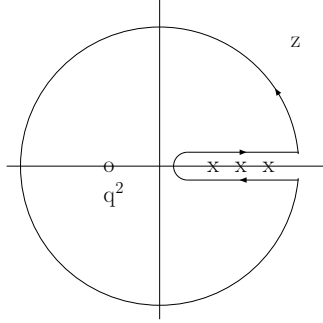


Figure 2: The contour in the plane of the complex variable $q^2 = z$. The open point indicates the $q^2 < 0$ reference point of the QCD calculation. Positions of hadronic thresholds at $q^2 > 0$ are indicated by crosses.

analytic function $\Pi(q^2)$, choosing the contour shown in Fig. 2:

$$\begin{aligned} \Pi(q^2) &= \frac{1}{2\pi i} \oint_C dz \frac{\Pi(z)}{z - q^2} = \frac{1}{2\pi i} \oint_{|z|=R} dz \frac{\Pi(z)}{z - q^2} \\ &+ \frac{1}{2\pi i} \int_0^R dz \frac{\Pi(z + i\epsilon) - \Pi(z - i\epsilon)}{z - q^2}. \end{aligned} \quad (12)$$

The radius R of the circle in this contour can be put to infinity. This simplifies the r.h.s. of Eq. (12) considerably, because, if the correlation function vanishes sufficiently fast at $|q^2| \sim R \rightarrow \infty$, (if $\lim_{|q^2| \rightarrow \infty} \Pi(q^2) \sim 1/|q^2|^\epsilon$, with any $\epsilon > 0$) the integral over the circle tends to zero. Below we shall discuss a necessary modification of Eq. (12) if $\Pi(q^2)$ does not vanish. The second integral on the r.h.s. of Eq. (12) can be replaced by an integral over the imaginary part of $\Pi(q^2)$. One makes use of the fact that $\Pi(q^2)$ is real at $q^2 < t_{min} = \min\{m_V^2, s_0^h\}$. Hence, according to the Schwartz reflection principle: $\Pi(q^2 + i\epsilon) - \Pi(q^2 - i\epsilon) = 2i \operatorname{Im}\Pi(q^2)$ at $q^2 > t_{min}$. After this replacement, we obtain the *dispersion relation*:

$$\Pi(q^2) = \frac{1}{\pi} \int_{t_{min}}^{\infty} ds \frac{\operatorname{Im} \Pi(s)}{s - q^2 - i\epsilon}. \quad (13)$$

The infinitesimal $-i\epsilon$ will not be shown explicitly hereafter. As we shall see in the next subsection, the correlation function (2) is ultraviolet divergent. Consequently, the imaginary part $\text{Im}\Pi(s)$ does not vanish at $s \rightarrow \infty$ and the dispersion integral (13) diverges. A standard way to cure this problem is to subtract from $\Pi(q^2)$ first few terms of its Taylor expansion at $q^2 = 0$. For the correlation function (2) one subtraction is sufficient:

$$\overline{\Pi}(q^2) = \Pi(q^2) - \Pi(0). \quad (14)$$

The dispersion relation (13) is modified in the following way:

$$\overline{\Pi}(q^2) = \frac{q^2}{\pi} \int_{t_{min}}^{\infty} ds \frac{\text{Im}\Pi(s)}{s(s-q^2)}. \quad (15)$$

Using the hadronic representation (11), one finally obtains

$$\Pi(q^2) = \frac{q^2 f_V^2}{m_V^2(m_V^2 - q^2)} + q^2 \int_{s_0^h}^{\infty} ds \frac{\rho^h(s)}{s(s-q^2)} + \Pi(0). \quad (16)$$

Notice that in our case $\Pi(0) = 0$, due to the gauge invariance of the electromagnetic interaction. Nevertheless, we retain $\Pi(0)$ in Eq. (16), having in mind a generic case, where a subtraction constant or a finite polynomial in q^2 appear in the resulting dispersion relation.

The dispersion relations similar to Eq. (16) are central objects of our review. With the correlation functions calculated in QCD in a certain approximation, these relations establish *sum rules*, i.e. nontrivial constraints on the sums over hadronic parameters.

2.4 Applying the Borel transformation

The sum rules in the form (16) are not yet very useful, e.g. for estimating the parameters of the lowest-lying hadronic state. They are in general plagued by the presence of unknown subtraction terms. More importantly, little is known about the spectral function $\rho^h(s)$ of excited and continuum states. The situation can be substantially improved¹ if one applies to both sides of Eq. (16) the Borel transformation

$$\Pi(M^2) \equiv \mathcal{B}_{M^2} \Pi(q^2) = \lim_{\substack{-q^2, n \rightarrow \infty \\ -q^2/n = M^2}} \frac{(-q^2)^{(n+1)}}{n!} \left(\frac{d}{dq^2} \right)^n \Pi(q^2). \quad (17)$$

Two important examples are :

$$\mathcal{B}_{M^2}(q^2)^k = 0, \quad \mathcal{B}_{M^2} \left(\frac{1}{(m^2 - q^2)^k} \right) = \frac{1}{(k-1)!} \frac{\exp(-m^2/M^2)}{M^{2(k-1)}}, \quad (18)$$

at $k > 0$. Transformations of more complicated functions can be found in the literature.^{11,12} Applying Eqs. (17) and (18) to Eq. (16), a more convenient form of the sum rule is obtained:

$$\Pi(M^2) = f_V^2 e^{-m_V^2/M^2} + \int_{s_0^h}^{\infty} ds \rho^h(s) e^{-s/M^2}. \quad (19)$$

The Borel transformation removes subtraction terms in the dispersion relation and exponentially suppresses the contributions from excited resonances and continuum states heavier than V . In the case of the heavy quark-antiquark currents, instead of the Borel transformation, it is more useful to apply a simpler procedure of n -times differentiation of Eq. (16) at $q^2 = q_0^2 \leq 0$:

$$M_n(q_0^2) \equiv \frac{1}{n!} \frac{d^n}{dq^{2n}} \Pi(q^2) |_{q^2=q_0^2} = \frac{f_V^2}{(m_V^2 - q_0^2)^{n+1}} + \int_{s_0^h}^{\infty} ds \frac{\rho^h(s)}{(s - q_0^2)^{n+1}}. \quad (20)$$

One gains a power suppression of heavier states and again removes the subtraction terms.

2.5 Calculating the correlation function in QCD: the perturbative part

We now turn to the next important step in the sum rule derivation and describe how the QCD calculation of the correlation function (2) is done. As explained in subsection 2.1, at very large $Q^2 = -q^2$ the function $\Pi_{\mu\nu}$ can be approximated by the free-quark loop diagram shown in Fig. 3a. In a generic case of a single quark flavor with the mass m , one has to contract all quark fields in (2) considering the quark propagators in the free-quark approximation:

$$S_0^{ij}(x, y) = -i \langle 0 | T \{ \psi^i(x) \bar{\psi}^j(y) \} | 0 \rangle = \delta^{ij} \int \frac{d^4 p}{(2\pi)^4} e^{-ip \cdot (x-y)} \frac{\not{p} + m}{p^2 - m^2}, \quad (21)$$

where the quark color indices are explicitly shown. After integrating over x , shifting to $D \neq 4$ dimensions and taking traces, we obtain

$$q^2 \Pi^{(0)}(q^2) = -\frac{12i}{(D-1)} \int_0^1 dv \int \frac{d^D p}{(2\pi)^D} \frac{(2-D)(p^2 - q^2 v(1-v)) + Dm^2}{(p^2 + q^2 v(1-v) - m^2)^2}. \quad (22)$$

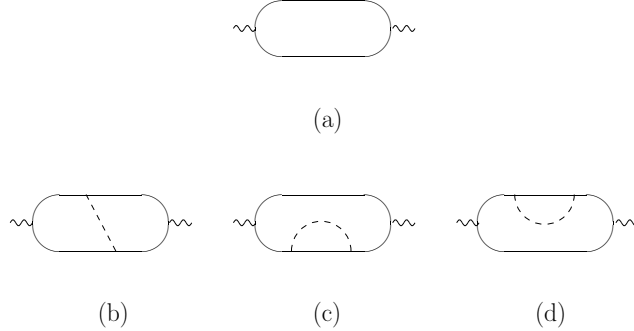


Figure 3: Diagrams determining the correlation function (2): the free-quark loop (a), the perturbative QCD corrections (b,c,d). Solid lines denote quarks, dashed lines gluons, wavy line external currents.

One may now proceed, performing the momentum integration in D dimensions. However, at this point we prefer to modify the standard procedure, and apply the Borel transformation before the integration in p is done. The divergence disappears and the limit $D \rightarrow 4$ can safely be restored. After the Wick rotation to the Euclidean space $p^2 \rightarrow -p^2 \equiv z$ and the angular integration in the four-dimensional integral, one obtains, in the massless quark case,

$$\mathcal{B}_{M^2}(q^2 \Pi^{(0)}(q^2)) = \int_0^\infty dz f^{(0)}(z), \quad (23)$$

where

$$f^{(0)}(z) = \frac{1}{2\pi^2} z \int_0^1 \frac{dv}{v(1-v)} \left(-1 + \frac{2z}{v(1-v)M^2} \right) \exp \left\{ -\frac{z}{M^2 v(1-v)} \right\}. \quad (24)$$

The numerical result for $f^{(0)}(z)$ is shown in Fig. 4. We see that the average $\langle z \rangle$ characterizing the quark virtuality in the loop diagram, is of the order of M^2 , and that the region of small z , e.g., $z \leq 0.1 M^2$ is strongly suppressed. Thus, at sufficiently large M^2 , the quarks are predominantly far off-shell. In the case of heavy c, b quarks it is more useful to differentiate Eq. (22) n times over q^2 at $q^2 = 0$, revealing that the dominant contribution stems from $|p^2| \sim m_{c,b}^2/n$.

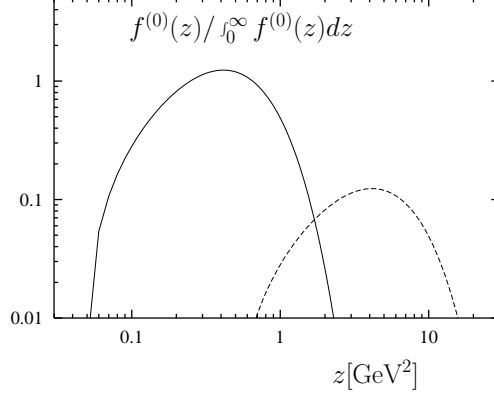


Figure 4: The distribution of the quark virtuality in the loop diagram after the Borel transformation at $M^2 = 1 \text{ GeV}^2$ (solid line) and $M^2 = 10 \text{ GeV}^2$ (dashed line).

Thus, an average high virtuality of heavy quarks is guaranteed, if n is not very large.

The most convenient final expression of $\Pi^{(0)}(q^2)$ is in the form of the dispersion integral:

$$\Pi^{(0)}(q^2) = \frac{q^2}{\pi} \int ds \frac{\text{Im } \Pi^{(0)}(s)}{s(s - q^2)} \quad (25)$$

with the imaginary part

$$\text{Im } \Pi^{(0)}(s) = \frac{1}{8\pi} v(3 - v^2) \theta(s - 4m^2), \quad (26)$$

where $v = \sqrt{1 - 4m^2/s}$. One should be careful in interpreting the imaginary parts of quark-loop diagrams. In QCD quarks are confined (the full quark propagators have no poles). Hence, the imaginary part (26) is a purely mathematical object. The free-quark approximation $\Pi^{(0)}(q^2)$ is especially simple in the light-quark case $m^2 \ll Q^2$, yielding

$$\Pi^{(0)}(q^2) \simeq \frac{q^2}{4\pi^2} \int_{4m^2}^{\infty} \frac{ds}{s(s - q^2)} \simeq -\frac{1}{4\pi^2} \ln \frac{Q^2}{4m^2} + O\left(\frac{m^2}{Q^2}\right), \quad (27)$$

where the $O(m^2/Q^2)$ correction is numerically important only in the s -quark case.

To improve the free-quark approximation, one has to calculate the $O(\alpha_s)$ perturbative correction corresponding to the diagrams in Figs. 3b,c,d. Since we already convinced ourselves that the average quark virtualities in the loop are of $O(M^2)$, it is conceivable to use QCD perturbation theory for these diagrams taking the quark-gluon coupling α_s at the scale M . The calculation of two-loop diagrams is technically quite involved but, fortunately, the result can be directly taken from QED, employing the Schwinger interpolation formula¹³ for the $O(\alpha_{em})$ radiative correction to the electron polarization operator. One has simply to replace $\alpha_{em} \rightarrow \alpha_s C_F$ ($C_F = 4/3$). After adding the $O(\alpha_s)$ correction, the perturbative part of the correlation function, $\Pi^{(pert)}(q^2)$, is given by the dispersion relation (25) with the imaginary part

$$\text{Im } \Pi^{(pert)}(s) = \text{Im } \Pi^{(0)}(s) \left\{ 1 + \alpha_s C_F \left[\frac{\pi}{2v} - \frac{v+3}{4} \left(\frac{\pi}{2} - \frac{3}{4\pi} \right) \right] \right\}. \quad (28)$$

In the case of u, d, s quark currents, the $O(\alpha_s)$ correction in (28) reduces to α_s/π and is numerically small. Virtual gluon exchanges are potentially important for the correlation functions of heavy quark-antiquark currents since the α_s/v term in (28) becomes anomalously large at $v \ll 1$, i.e., at s close to the threshold $4m^2$. The α_s/v terms can be traced back to Coulomb-type interactions between quarks and antiquarks. In the nonrelativistic approximation, it is possible¹⁴ to sum up all $(\alpha_s/v)^n$ terms in the correlation function, taking into account not only the one-gluon exchange but the whole ladder of such exchanges. This summation is usually applied to the correlation functions of $\bar{b}\gamma_\mu b$ currents related to Υ resonances.^c

A careful reader may have noticed that in all perturbative diagrams considered here the regions of small quark and gluon virtualities are automatically included, e.g., the integration in (24) spreads over small quark virtualities. The QCD perturbation theory is invalid in this region and the free propagators cannot be used. Nevertheless, one may still argue that no large numerical error is being introduced, as long as M^2 is kept large. For instance, in the integral (23) the region with $z \leq \mu^2$ contributes with a suppression of $O(\mu^4/M^4)$.

2.6 Vacuum condensates and operator product expansion

The fact that the perturbative part of $\Pi_{\mu\nu}$ has been reliably calculated does not yet imply that *all* important contributions to the correlation function have

^cAt $O(\alpha_s)$ accuracy one should take care of a proper definition of the heavy quark mass which is a scale-dependent parameter in perturbative QCD. In Eq. (28) the so called ‘‘pole’’ mass is used. We do not discuss this important issue here, and refer to the chapters by Uraltsev and Chetyrkin in this book.

been taken into account. The complete calculation¹ has to include the effects due to the fields of soft gluons and quarks populating the QCD vacuum. The problem of vacuum fields in QCD with its many interesting aspects is discussed elsewhere in this book. We only mention that vacuum fluctuations in QCD are due to the complicated nonlinear nature of the Lagrangian (1). The ultimate solution of QCD equations of motion and the resulting complete picture of the vacuum fields are unknown. Various nonperturbative approaches (instanton models, lattice simulation of QCD, etc.) indicate that these fields fluctuate with typical long-distance scales $\Lambda_{vac} \sim \Lambda_{QCD}$. It is clear that the quark-antiquark pair created by the external current at one point and absorbed at another point interacts with the vacuum fields. This interaction is beyond QCD perturbation theory and has to be taken into account separately.

A practical way to calculate the vacuum-field contributions to the correlation functions relies on the following qualitative arguments. At large $Q^2 \gg \Lambda_{QCD}^2$, the average distance between the points of the quark-antiquark emission and absorption is essentially smaller than the characteristic scale of the vacuum fluctuations. Therefore, propagating in the QCD vacuum, the quark-antiquark pair acts as a short-distance probe of long-distance fields and perceives static, averaged characteristics of these fields. At the same time, the emission of quarks and antiquarks does not significantly disturb the vacuum state. Hence, in the first approximation, quarks with large momenta $\sim \sqrt{Q^2}$ scatter over external static fields composed of soft vacuum gluons and quarks. The corresponding diagrams are shown in Fig. 5. In the case of light quarks, there are several important effects: the vacuum gluons are emitted and absorbed by virtual quarks (Figs. 5a,b,c), the quarks and antiquarks are interchanged with their vacuum counterparts (Fig. 5d) and, finally, a combined quark-gluon interaction takes place (Figs. 5e,f). For the heavy quarks only the interactions with the vacuum gluons are important.

A quantitative framework which follows this picture and incorporates both short- and long-distance contributions was developed¹ in a form of a generalized Wilson OPE. To apply this method to the correlation function (2), one has to expand the product of two currents in a series of local operators:

$$\begin{aligned}
& i \int d^4x e^{iq \cdot x} T\{\bar{\psi}(x)\gamma_\mu\psi(x), \bar{\psi}(0)\gamma_\nu\psi(0)\} \\
& = (q_\mu q_\nu - q^2 g_{\mu\nu}) \sum_d C_d(q^2) O_d,
\end{aligned} \tag{29}$$

so that

$$\Pi(q^2) = \sum_d C_d(q^2) \langle 0 | O_d | 0 \rangle. \tag{30}$$

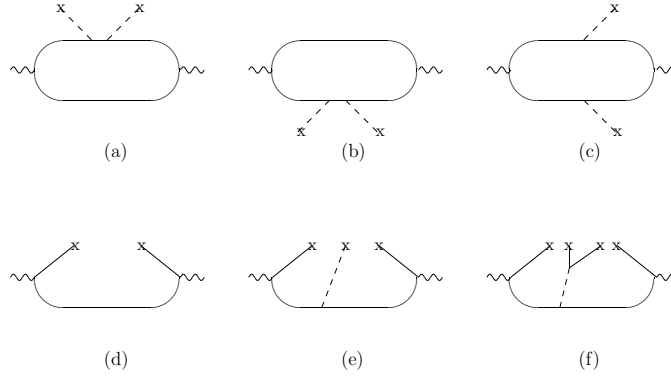


Figure 5: Diagrams corresponding to the gluon (a,b,c), quark (d), quark-gluon (e) and four-quark (f) condensate contributions to the correlation function (2).

In this expansion, the operators are ordered according to their dimension d . The lowest-dimension operator with $d = 0$ is the unit operator associated with the perturbative contribution: $C_0(q^2) = \Pi^{pert}(q^2)$, $\langle 0 | O_0 | 0 \rangle \equiv 1$. The QCD vacuum fields are represented in (30) in a form of the so called *vacuum condensates*, the vacuum expectation values of the $d \neq 0$ operators, composed of quark and gluon fields, $\bar{\psi}$, ψ and $G_{\mu\nu}^a$. The contributions of high-dimensional condensates corresponding to the diagrams with multiple insertions of vacuum gluons and quarks, are suppressed by large powers of Λ_{vac}^2/Q^2 . Therefore, even at intermediate $Q^2 \sim 1 \text{ GeV}^2$, the expansion (30) can safely be truncated after a few terms.

One may interpret the OPE (30) in the following way. The product of quark currents acts as a quasi-local “antenna” having a small size $O(1/\sqrt{Q^2})$ and probing the static vacuum fields. This interaction depends on the properties of the “antenna”, i.e. on the quantum numbers and flavor content of the quark currents. In Eq. (30), this dependence is accumulated in the Wilson coefficients $C_d(q^2)$ receiving dominant contributions from the regions of short distances (large momenta). In addition, the current-vacuum interaction is determined by the long-distance dynamics represented in Eq. (30) by the universal condensates $\langle 0 | O_d | 0 \rangle$ with $d \neq 0$, which are independent of the properties of the quark currents. The separation of distances is a key point in the OPE (30). Representing $\Pi(q^2)$ in this form, one introduces a certain scale μ which separates the regions of short and long distances. The interactions at

momenta $p^2 > \mu^2$ are included in the coefficients $C_d(q^2)$, while the effects at $p^2 < \mu^2$ are absorbed into the vacuum condensates. The scale μ should be large enough in order to justify the calculation of C_d in QCD perturbation theory. In practice, using the standard methods of the Feynman-diagram technique, an explicit separation of distances is impossible in the quark-loop diagrams. One is forced to take into account both the soft parts of perturbative diagrams and the long-distance condensate effects simultaneously. This yields a certain amount of double counting, which is, fortunately, in many cases numerically insignificant, because the condensate contributions turn out to be much larger than the soft “tails” of perturbative diagrams. Moreover, if one does not go beyond the two-loop diagrams in Figs. 3b-3d and uses the leading-order Wilson coefficients C_d for $d \neq 0$, it is possible to rearrange the OPE including the soft ($p^2 < \mu^2$) contributions of the perturbative diagrams in the definition of the condensates. This “practical version” of OPE is discussed in more detail in a recent review.⁸

The list of the operators with low dimension entering Eq. (29) starts with

$$O_3 = \bar{\psi}\psi \quad (31)$$

and

$$O_4 = G_{\mu\nu}^a G^{a\mu\nu}, \quad (32)$$

whose vacuum averages are known as the quark and gluon condensates, respectively. It is important that in QCD there are no colorless operators with lower dimensions, $d = 1, 2$.

The operators with $d = 5, 6$ are

$$O_5 = \bar{\psi}\sigma_{\mu\nu}\frac{\lambda^a}{2}G^{a\mu\nu}\psi, \quad (33)$$

$$O_6^\psi = (\bar{\psi}\Gamma_r\psi)(\bar{\psi}\Gamma_s\psi), \quad (34)$$

where $\Gamma_{r,s}$ denote various combination of Lorentz and color matrices, and

$$O_6^G = f_{abc}G_{\mu\nu}^a G_\sigma^{b\nu} G^{c\sigma\mu}. \quad (35)$$

The vacuum averages of the above operators are, correspondingly the quark-gluon, four-quark and three-gluon condensates. The condensates with $d > 6$ usually play a minor role in the most QCD sum rule applications and we will not consider them in detail.

One should mention that, in addition to rather mild effects of the quark scattering over the vacuum fields, there exist specific vacuum fluctuations at

short distances $\sim 1/\sqrt{Q^2}$, which absorb the whole momentum of the external quark current. These effects, known as “direct instantons,”^d violate the condensate expansion. For the vector currents considered here, short-distance nonperturbative effects may appear¹ only at very high dimensions ($d > 10$) and do not play any role in the truncated OPE. However, in the correlation functions of pseudoscalar ($J^P = 0^-$) and scalar ($J^P = 0^+$) quark and/or gluon currents, direct instantons are enhanced and important already at intermediate Q^2 .

To proceed with the derivation of the QCD answer for $\Pi_{\mu\nu}$, one has to evaluate the Wilson coefficients of the condensate terms in (30). For illustration, we demonstrate how the simplest contribution of the quark condensate is calculated. The relevant diagram is shown in Fig. 3d. One factorizes out all contributions to $\Pi_{\mu\nu}$ containing one antiquark and one quark field, the remaining quark fields being contracted in the free-quark propagators:

$$\begin{aligned} \Pi_{\mu\nu}^{(\bar{\psi}\psi)}(q) = i \int d^4x e^{iq \cdot x} \langle 0 | \{ \bar{\psi}^i(x) \gamma_\mu S^{ij}(x, 0) \gamma_\nu \psi^j(0) \\ + \bar{\psi}^j(0) \gamma_\nu S^{ji}(0, x) \gamma_\mu \psi^i(x) \} | 0 \rangle . \end{aligned} \quad (36)$$

In the above, the fields ψ and $\bar{\psi}$ have to be treated as external vacuum fields with negligible momenta as compared with the momenta of the freely propagating off-shell quarks. In other words, it is possible to expand $\bar{\psi}(x)$ and $\psi(x)$ around $x = 0$:

$$\begin{aligned} \psi(x) &= \psi(0) + x^\rho \overrightarrow{D}_\rho \psi(0) + \dots , \\ \bar{\psi}(x) &= \bar{\psi}(0) + \bar{\psi}(0) \overleftarrow{D}_\rho x^\rho + \dots , \end{aligned} \quad (37)$$

where D_ρ is the covariant derivative, and the higher orders in this expansion are only relevant for the operators with $d \geq 5$. Substituting (37) in (36), one encounters the following vacuum matrix elements:

$$\langle 0 | \bar{\psi}_\alpha^i \psi_\beta^j | 0 \rangle = A \delta^{ij} \delta_{\alpha\beta} , \quad (38)$$

$$\langle 0 | \bar{\psi}_\alpha^i \overrightarrow{D}_\rho \psi_\beta^j | 0 \rangle = B \delta^{ij} (\gamma_\rho)_{\beta\alpha} , \quad \langle 0 | \bar{\psi}_\alpha^i \overleftarrow{D}_\rho \psi_\beta^j(x) | 0 \rangle = \overline{B} \delta^{ij} (\gamma_\rho)_{\beta\alpha} , \quad (39)$$

where α, β are the bispinor indices, and the r.h.s. represent the most general decompositions in color and Dirac matrices, obeying color and spin conservation. The constants A, B and \overline{B} are easily obtained by multiplying both sides

^d They can be modeled employing the QCD instanton solution. Instanton-induced effects are discussed in the chapter by Shuryak in this book.

of Eqs. (38) and (39) by $\delta^{ij}\delta_{\alpha\beta}$ and $\delta^{ij}(\gamma^\rho)_{\alpha\beta}$, respectively, and taking traces. The result is :

$$A = \frac{1}{12} \langle 0 | \bar{\psi}\psi | 0 \rangle, \quad (40)$$

$$B = \frac{1}{48} \langle 0 | \bar{\psi} \vec{D} \psi | 0 \rangle = -\frac{im}{48} \langle 0 | \bar{\psi}\psi | 0 \rangle, \quad \bar{B} = -B. \quad (41)$$

In the last two relations the Dirac equation for the quark field $\vec{D} \psi(x) = -im\psi(x)$ was applied. Substituting the expansion (37) in (36) and using the expressions (38) and (39) for the matrix elements, one obtains, after the integration over x :

$$\Pi_{\mu\nu}^{(\bar{\psi}\psi)}(q) = (q_\mu q_\nu - q^2 g_{\mu\nu}) \frac{2m}{q^4} \langle 0 | \bar{\psi}\psi | 0 \rangle, \quad (42)$$

yielding the Wilson coefficient

$$C_3(q^2) = \frac{2m}{q^4}. \quad (43)$$

The proportionality of the above expression to the quark mass is expected on general grounds. The quark condensate violates chiral symmetry and its contribution should vanish in the chiral limit $m = 0$.

The derivation of higher dimensional terms of the OPE (30) is more involved. A very useful tool, simplifying the calculational procedure, is the Fock-Schwinger gauge for the gluon field:

$$(x - x_0)_\mu A^{a\mu}(x) = 0. \quad (44)$$

In this gauge, the gluon 4-potential A_μ^a is directly expressed in terms of the gluon field-strength tensor $G_{\mu\nu}^a$. This, and many other aspects of the calculational technique are explained in the review¹¹ serving as a very useful handbook for QCD sum rule practitioners (see also Ref. 15).

The final result for the OPE, with all Wilson coefficients up to $d = 6$ taken into account, reads:

$$\begin{aligned} \Pi(q^2) = & -\frac{1}{4\pi^2} \left(1 + \frac{\alpha_s}{\pi}\right) \ln \frac{-q^2}{4m^2} + \frac{2m \langle \bar{\psi}\psi \rangle}{q^4} + \frac{\alpha_s \langle G_{\mu\nu}^a G^{a\mu\nu} \rangle}{12\pi q^4} \\ & + \frac{m^3}{3q^8} \langle g_s \bar{\psi} \sigma_{\mu\nu} \frac{\lambda^a}{2} G^{a\mu\nu} \psi \rangle + \frac{2\pi\alpha_s}{q^6} \left[\langle (\bar{\psi} \gamma_\mu \gamma_5 \frac{\lambda^a}{2} \psi) (\bar{\psi} \gamma^\mu \gamma_5 \frac{\lambda^a}{2} \psi) \rangle \right. \\ & \left. + \frac{2}{9} \langle (\bar{\psi} \gamma_\mu \frac{\lambda^a}{2} \psi) (\bar{\psi} \gamma^\mu \frac{\lambda^a}{2} \psi) \rangle \right], \end{aligned} \quad (45)$$

where the shorthand notation $\langle O \rangle \equiv \langle 0 | O | 0 \rangle$ is introduced. The above expression is valid for the light quarks $\psi = u, d, s$. In this case the quark-gluon condensate contribution (diagram in Fig. 5e) is suppressed by an extra factor m^2/Q^2 . Note that the three-gluon condensate term vanishes for the correlators of massless quarks.¹⁶ The accuracy of the OPE for $\Pi(q^2)$ is not limited by the above expression. Currently, $\Pi^{(pert)}$ is known up to $O(\alpha_s^3)$,¹⁷ and the $O(\alpha_s)$ corrections to many of the coefficients C_n at $d \neq 0$ are also available. If the quark is heavy ($\psi = c, b$), the quark condensate terms are suppressed^e and one has, to $d = 4$ accuracy:¹

$$\Pi(q^2) = \frac{q^2}{\pi} \int_{4m^2}^{\infty} ds \frac{\text{Im} \Pi^{(pert)}(s)}{s(s - q^2)} + \frac{\langle \alpha_s G_{\mu\nu}^a G^{a\mu\nu} \rangle}{48\pi q^4} f(a), \quad (46)$$

where $a = 1 - 4m^2/q^2$,

$$f(a) = \frac{3(a+1)(a-1)^2}{2a^{5/2}} \ln \frac{\sqrt{a}+1}{\sqrt{a}-1} - \frac{3a^2 - 2a + 3}{a^2},$$

and $\text{Im} \Pi^{(pert)}(s)$ is given in (28). Note that at $q^2 = 0$ the gluon condensate term has a suppression factor $1/(4m_{c,b}^2)^2$ with respect to the perturbative part. The Wilson coefficients of $d = 6, 8$ terms in the OPE for the heavy quark correlator, corresponding to diagrams with three and four vacuum gluons (e.g. the three-gluon condensate contribution) have also been calculated.¹⁸

2.7 What do we know about the vacuum condensates ?

The vacuum condensates introduced in the OPE are purely nonperturbative parameters, hence, their numerical values (the condensate densities) cannot be directly calculated and have to be determined by other methods, to be briefly summarized now.

The quark condensate plays a special role being responsible for the observed spontaneous breaking of the chiral symmetry in QCD (discussed in the chapters by Leutwyler, by Diakonov and Petrov, and by Meissner in this book). For this reason, the value of the quark condensate density was known long before it was used in QCD sum rules:

$$\langle \bar{\psi}\psi \rangle = -\frac{f_\pi^2 m_\pi^2}{2(m_u + m_d)} \simeq -(240 \pm 10 \text{ MeV})^3, \quad (47)$$

^eHeavy quarks do not develop their own vacuum condensates, being far off-shell at the momentum scale Λ_{vac} , and the interactions of virtual heavy quarks with the light-quark condensates appear in higher order in α_s .

for $\psi = u, d$ and, in SU(3)-flavor approximation, also for $\psi = s$. The above value corresponds to the normalization scale $\mu = 1 \text{ GeV}$.^f

From first principles, very little is known about other condensates. Some attempts exist to calculate them on the lattice or in the models of the instanton vacuum. At present, it is still more safe, as it was done in the original work,¹ to determine the condensate densities empirically, by fitting certain QCD sum rules to experimental data. Being universal, the condensates extracted from one sum rule can be used in many others.

The gluon condensate density was originally derived from the sum rule (20) for the correlation function of $j_\mu = \bar{c}\gamma_\mu c$ currents. The hadronic spectral density was saturated by the experimentally known masses m_V and decay constants f_V of the charmonium levels $V = J/\psi, \psi', \dots$, employing quark-hadron duality (explained in the next subsection) for the heavier states. Substituting the correlation function (46) in the l.h.s. of (20), and fitting it to the r.h.s. at not very large n (in order to safely neglect $d \geq 6$ terms) the gluon condensate density,

$$\langle \frac{\alpha_s}{\pi} G_{\mu\nu}^a G^{a\mu\nu} \rangle = (0.012 \text{ GeV}^4) \pm 30\%, \quad (48)$$

has been obtained.¹ Note that the above quantity is scale-independent. The estimate (48) has survived after many years, although claims urging to revise it appear from time to time in the literature. In fact, an independent check of Eq. (48) has been carried out¹⁹ by considering SVZ sum rules for two different correlators in the pion channel, one of them sensitive to the gluon condensate and the other one to the quark condensate.

The quark-gluon condensate is “invisible” in the sum rules for vector mesons and has to be extracted from the correlation functions for baryon currents (they are considered in Sec. 3). The conventional parametrization is

$$\langle g_s \bar{\psi} \sigma_{\mu\nu} \frac{\lambda^a}{2} G^{a\mu\nu} \psi \rangle = m_0^2 \langle \bar{\psi} \psi \rangle, \quad (49)$$

where the numerical value of m_0^2 has been estimated long ago²⁰ and is still accepted:

$$m_0^2(1 \text{ GeV}) = 0.8 \pm 0.2 \text{ GeV}^2. \quad (50)$$

Four-quark condensates with different combinations of Γ_r matrices (one of the corresponding diagrams is shown in Fig. 5f) can be treated in the factorization approximation¹ which relies on the dominance of the intermediate

^f The condensate density is logarithmically dependent on the normalization scale if the underlying operator, in this case $\bar{\psi}\psi$, has a nonvanishing anomalous dimension. A natural choice is the scale μ separating the long and short distances in OPE.

vacuum state and allows to reduce each separate four-quark condensate to the square of the quark condensate. The general factorization formula reads:

$$\langle \bar{\psi} \Gamma_r q \bar{\psi} \Gamma_s \psi \rangle = \frac{1}{(12)^2} \{ (Tr \Gamma_r)(Tr \Gamma_s) - Tr(\Gamma_r \Gamma_s) \} \langle \bar{\psi} \psi \rangle^2. \quad (51)$$

Applying it to the four-quark condensate terms in (45) one obtains, instead of the two terms in the square bracket, a more compact expression $\frac{112}{81} \langle \bar{\psi} \psi \rangle^2$. The product of the four-quark condensate and α_s in (45) has a negligible scale-dependence.

The three-gluon condensate contribution is not important for most of the interesting sum rules. An order of magnitude estimate of its density based on the instanton model is ¹

$$\langle g_s^3 f_{abc} G_{\mu\nu}^a G_{\sigma}^{b\nu} G^{c\sigma\mu} \rangle \simeq 0.045 \text{ GeV}^6. \quad (52)$$

In the context of a recent development, let us mention the estimates of $d = 7$ condensates obtained in the model of the instanton vacuum ²¹ and using a factorization ansatz.²²

One should admit that the accuracy of the condensate densities obtained from sum rules and/or invoking factorization is not very high and there is still room for a considerable improvement. Because of that, one cannot fully benefit from the improved Wilson coefficients available from perturbative calculations. On the other hand, as we already noticed, perturbative loop diagrams include regions of soft momenta. Therefore, any update of condensates has to be combined with a more delicate procedure identifying and separating these regions in the perturbative coefficients, in spirit of the “practical version” of OPE. Regardless to their particular relevance for SVZ sum rules, the vacuum condensates are important nonperturbative characteristics of QCD in general, thus deserving dedicated studies.

2.8 Use of quark-hadron duality

Let us continue our derivation. Performing the Borel transformation of the Eq. (45), the QCD answer for $\Pi(M^2)$ in the sum rule (19) can now be obtained. The result reads:

$$f_V^2 e^{-m_V^2/M^2} + \int_{s_0^h}^{\infty} ds \rho^h(s) e^{-s/M^2} = \frac{1}{4\pi^2} \left(1 + \frac{\alpha_s(M)}{\pi} \right) \int_0^{\infty} ds e^{-s/M^2} \\ + \frac{2m \langle \bar{\psi} \psi \rangle}{M^2} + \frac{\langle \frac{\alpha_s}{\pi} G_{\mu\nu}^a G^{a\mu\nu} \rangle}{12M^2} - \frac{112\pi \alpha_s \langle \bar{\psi} \psi \rangle^2}{81 M^4}. \quad (53)$$

In the above, the four-quark condensates are factorized and α_s is taken at the scale M .⁹

In addition, it is possible to estimate the integral over the excited and continuum states in Eq. (53) using the following arguments. In the deep spacelike region $q^2 \rightarrow -\infty$, where all power-suppressed condensate contributions can safely be neglected, the limit $\Pi(q^2) \rightarrow \Pi^{(pert)}(q^2)$ is valid yielding an approximate equation of the corresponding dispersion integrals:

$$q^2 \int_{t_{min}}^{\infty} ds \frac{\text{Im}\Pi(s)}{s(s-q^2)} \simeq q^2 \int_{4m^2}^{\infty} ds \frac{\text{Im}\Pi^{(pert)}(s)}{s(s-q^2)}, \quad (54)$$

(again at $q^2 \rightarrow -\infty$). In order to satisfy the above relation, known as the *global quark-hadron duality*,^h the integrands on both sides of it should have the same asymptotics:

$$\text{Im}\Pi(s) \rightarrow \text{Im}\Pi^{(pert)}(s) \quad \text{at } s \rightarrow +\infty, \quad (55)$$

where, in our case, $\text{Im}\Pi(s)$ is given by Eq. (11) and $\text{Im}\Pi^{(pert)}(s)$ by Eq. (28). One could still allow $\text{Im}\Pi(s)$ to oscillate around the perturbative QCD limit. Eq. (55) is an example of the *local* quark-hadron duality. From (54) and (55) it is postulated that at sufficiently large $Q^2 = -q^2$ the following approximation is valid:

$$q^2 \int_{s_0^h}^{\infty} ds \frac{\rho^h(s)}{s(s-q^2)} \simeq \frac{1}{\pi} q^2 \int_{s_0}^{\infty} ds \frac{\text{Im}\Pi^{(pert)}(s)}{s(s-q^2)}, \quad (56)$$

where s_0 is an effective threshold parameter which does not necessarily coincide with s_0^h . After the Borel transformation one obtains:

$$\int_{s_0^h}^{\infty} ds \rho^h(s) e^{-s/M^2} \simeq \frac{1}{\pi} \int_{s_0}^{\infty} ds \text{Im}\Pi^{(pert)}(s) e^{-s/M^2}. \quad (57)$$

The relation (56) and its Borel transformed version (57) represent the quark-hadron duality approximation used in SVZ sum rules to replace the integrals over excited and continuum states. The threshold parameter s_0 which, in

⁹To do it more precisely, the Borel transformation has to be applied to the logarithmic dependence of α_s on the scale q^2 .

^hFor a more detailed discussion of quark-hadron duality see the chapter by Shifman in this book.

general, has to be fitted, is expected to be close to the mass squared of the first excited state of V .

The assumption (56) is certainly weaker than local duality, because it involves integrals and, in particular, it is insensitive to oscillations of $\rho^h(s)$ around $\text{Im } \Pi^{(pert)}(s)$. Moreover, at very large Q^2 , for the positive definite correlation functions, such as (2), the validity of (56) is simply a mathematical consequence of the global duality. On the other hand, employing the duality approximation (56) in sum rules at intermediate Q^2 (or, equivalently, Eq. (57) at intermediate M^2) one also relies on the validity of the local duality approximation (56), starting from a certain finite s_0 . The latter assumption is not a strict consequence of the asymptotic freedom. It is therefore fair to call Eq. (56) “semilocal” duality. In this situation, the Borel transformation performed in the sum rule (53) is of a great importance, because, due to the exponential suppression of the integral on the l.h.s., the sensitivity to the duality approximation (57) of this integral is not high.

It is also important to recall that quark-hadron duality was confirmed in the channels accessible in e^+e^- annihilation and in τ lepton decays, where the spectral density $\rho^h(s)$ of excited and continuum states was measured and the hadronic dispersion integrals were compared with their perturbative QCD counterparts. For example, using the experimental data on $J/\psi, \psi', \dots \rightarrow l^+l^-$ decay widths, the quark-hadron duality for the charmonium channel was shown to hold to good accuracy.²³

Using the duality approximation (57) in Eq. (53), one can simply subtract the integral over $\rho^h(s)$ from the perturbative part on the r.h.s. This is the last step in the derivation procedure outlined and explained in the previous subsections. Our goal is achieved: the SVZ sum rule for the parameters of the ground-state hadron V can now be written explicitly. For definiteness, let us choose the case $V = \rho$. It corresponds to the correlation function (2), where the $I = 1$ combination of u and d quark currents is taken:

$$j_\mu^{(\rho)} = \frac{1}{2}(\bar{u}\gamma_\mu u - \bar{d}\gamma_\mu d) \quad (58)$$

with the decay constant defined as in Eq. (10):

$$\langle \rho^0(p) | j_\nu^{(\rho)} | 0 \rangle = \frac{f_\rho}{\sqrt{2}} m_\rho \epsilon_\nu^{(\rho)*} . \quad (59)$$

The resulting sum rule reads:

$$f_\rho^2 = M^2 e^{m_\rho^2/M^2} \left[\frac{1}{4\pi^2} \left(1 - e^{-s_0^{\rho}/M^2} \right) \left(1 + \frac{\alpha_s(M)}{\pi} \right) \right]$$

$$+ \frac{(m_u + m_d)\langle\bar{\psi}\psi\rangle}{M^4} + \frac{1}{12} \frac{\langle\frac{\alpha_s}{\pi} G_{\mu\nu}^a G^{a\mu\nu}\rangle}{M^4} - \frac{112\pi}{81} \frac{\alpha_s \langle\bar{\psi}\psi\rangle^2}{M^6} \Big], \quad (60)$$

s_0^ρ being the duality threshold for the ρ meson channel.

2.9 SVZ sum rules at work

Historically, Eq. (60) was one of the first successful applications of the method. Recently, this sum rule was reanalyzed⁸ highlighting many interesting theoretical details. Here we will follow a more pragmatic procedure, trying to reveal the predictive power and the actual accuracy of the method.

We start with discussing the choice of the Borel parameter. The sum rule (60) is not applicable at too small M^2 because the missing terms with higher-dimensional condensates and, potentially, also the short-distance non-perturbative effects, all proportional to large powers of $1/M^2$, may become too important to be neglected. Usually, the low limit on M^2 is adopted by demanding that in the truncated OPE the condensate term with the highest dimension remains a small fraction of the sum of all terms. This limit keeps the convergence of the condensate expansion under control and guarantees that one does not introduce a large error neglecting the higher-dimensional terms. At too large M^2 the quark-hadron duality approximation cannot be trusted. Therefore, one also has to choose an upper limit on M^2 , so that the exponentially suppressed contribution of the states above s_0^ρ remains a small part of the total dispersion integral. The value of s_0^ρ is not completely arbitrary, being correlated with the onset of excited states in the channel of the current j_μ^ρ . According to the experimental data, the resonance activity related to the first excited states in the ρ channel shows up at $s \sim 1.5 \div 2.0 \text{ GeV}^2$, hence s_0 in this vicinity can be expected. We have checked that in the sum rule (60), in the range

$$0.5 < M^2 < 1.2 \text{ GeV}^2, \quad (61)$$

the $d = 6$ four-quark contribution is less than 10% and, simultaneously, the $s > s_0^\rho$ part of the dispersion integral is less than 30 % of the total r.h.s.. One should emphasize that in certain sum rules the *Borel window* similar to Eq. (61) simply does not exist, that is, the lower limit of M^2 overshoots the upper one. The channels where the sum rules fail are usually plagued by “direct instantons”, and therefore the physical reason of the failure is understandable.

After the range of M^2 is determined, we can fit the decay constant f_ρ and the threshold parameter s_0^ρ from Eq. (60) by demanding the maximal stability of f_ρ within this range. The mass m_ρ is fixed by its experimental value.ⁱ The

ⁱThe SVZ method has enough predictive potential to yield also the ρ meson mass m_ρ by

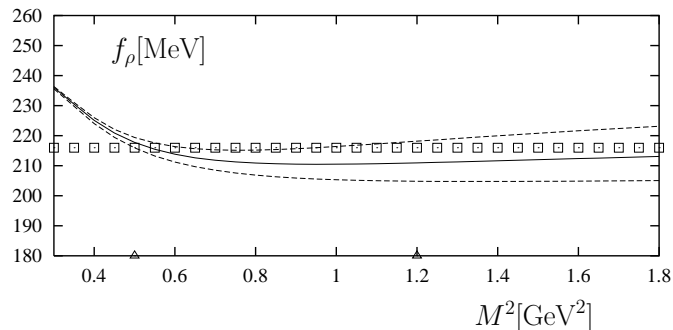


Figure 6: ρ meson decay constant f_ρ calculated from the SVZ sum rule (60) as a function of the Borel parameter M^2 , fixing the threshold at $s_0^\rho=1.7$ GeV^2 (solid line). For comparison, the results at $s_0^\rho=1.5$ GeV^2 and $s_0^\rho=2.0$ GeV^2 are shown by the lower and upper dashed lines, respectively. The central experimental value is indicated by boxes, the triangles on the M^2 axis mark the allowed range of the Borel parameter.

resulting numerical values of f_ρ are shown in Fig. 6 as a function of M^2 , at the central values of the condensates (47),(48) and at $\alpha_s(1\text{GeV}) = 0.5$. Within the interval (61), the maximally stable f_ρ corresponds to $s_0 = 1.7$ GeV^2 .

In order to assess the predictive power of the sum rule (60), it is necessary to estimate the theoretical uncertainties. They originate from the following sources:

(a) dependence on the Borel parameter. The sum rule is an approximate relation, therefore it is not surprising that the final numerical result for the constant parameter f_ρ changes with M^2 . As can be seen in Fig. 6, the variation of f_ρ within the Borel window is small,

$$f_\rho^{Borel} = 210 \div 217 \text{ MeV}, \quad (62)$$

and one can claim the success of the sum rule (60). Indeed, a large instability with respect to the variation of M^2 would indicate absence of important condensate contributions or may cast doubt over the reliability of the duality approximation. Apparently, all values of f_ρ in the interval (62) can be equally trusted as sum rule predictions, therefore, the variation within the Borel window has to be included in the total theoretical uncertainty.

combining the sum rule (60) with the same sum rule differentiated over $1/M^2$. We do not discuss this procedure here, concentrating on the determination of hadronic matrix elements such as f_ρ .

(b) inaccurate knowledge of the condensate densities. Varying them within errors indicated in Eqs. (47) and (48) we obtain a small, $\pm 1\%$ change of the prediction (62).

(c) neglect of the $d \geq 6$ terms in OPE. We assume that the neglected condensate terms are altogether not larger than the $d = 6$ contribution. This yields less than $\pm 5\%$ uncertainty in f_ρ .

(d) limited accuracy of perturbative contributions. Varying the scale of α_s and adding the known higher-order corrections to the perturbative part one again observes a small, about $\pm 3\%$, variation of f_ρ . Absence of $O(\alpha_s)$ corrections to $d \neq 0$ Wilson coefficients has a negligible impact on the result.

Adding the individual uncertainties (a)–(d) linearly, which is a rather conservative attitude, we get about $\pm 10\%$ in total and obtain the following interval for the SVZ sum rule prediction:

$$f_\rho = 213 \pm 20 \text{ MeV}, \quad (63)$$

where the form of writing is just for convenience and there is no preferable central value. The uncertainties (c),(d) may somewhat decrease after future theoretical work. Note that the variation of s_0^ρ should not be counted as an independent uncertainty, since this parameter is fitted from the sum rule together with f_ρ . On the other hand, it is helpful to have several alternatives for the quark-hadron duality ansatz, including the radial excited or continuum states and increasing the effective threshold. In the ρ channel one can try different models, e.g., $\rho + \rho'$ +continuum with higher s_0^ρ , including also the finite widths of these resonances. The results for f_ρ are practically very close to what one obtains with the simplest SVZ construction: $\rho + \text{continuum}$. Our estimate (63) is in a good agreement with the experimental number

$$f_\rho^{exp} = 216 \pm 5 \text{ MeV} \quad (64)$$

obtained from the measured leptonic width ²⁴ $\Gamma(\rho^0 \rightarrow e^+e^-) = 6.77 \pm 0.32 \text{ keV}$.

Another illustration of the method is provided by the SVZ sum rule for the pion decay constant f_π , defined as

$$\langle \pi(p) | j_\mu^{(\pi)} | 0 \rangle = -ip_\mu f_\pi, \quad (65)$$

where

$$j_\mu^{(\pi)} = \bar{u} \gamma_\mu \gamma_5 d \quad (66)$$

is the axial-vector current interpolating the pion. The sum rule¹ obtained from the correlation function of two $j_\mu^{(\pi)}$ currents looks very similar to Eq. (60):

$$f_\pi^2 = M^2 \left[\frac{1}{4\pi^2} \left(1 - e^{-s_0^\pi/M^2} \right) \left(1 + \frac{\alpha_s(M)}{\pi} \right) \right]$$

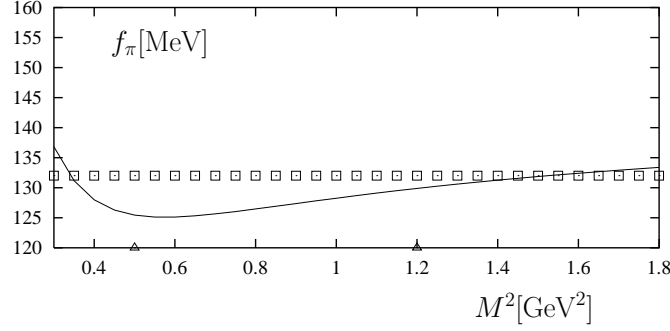


Figure 7: The decay constant f_π calculated from the SVZ sum rule at $s_0=0.7 \text{ GeV}^2$ (solid line). For comparison, the experimental value is indicated with boxes, the triangles at the M^2 axis mark the allowed range of the Borel parameter.

$$+ \frac{1}{12} \left[\frac{\langle \frac{\alpha_s}{\pi} G_{\mu\nu}^a G^{a\mu\nu} \rangle}{M^4} + \frac{176\pi \alpha_s \langle \bar{\psi}\psi \rangle^2}{M^6} \right], \quad (67)$$

but, importantly, differs in the sign of the four-quark condensate term. This difference between the nonperturbative interactions of the currents $j_\mu^{(\rho)}$ and $j_\mu^{(\pi)}$ with the QCD vacuum, to a large extent explains why the hadrons in the vector and axial channels are not alike, i.e. why there is a single ρ resonance in the first channel and a combination of pion with a_1 meson in the second.¹ The sum rule prediction with the estimated uncertainty,

$$f_\pi = 127 \pm 15 \text{ MeV}, \quad (68)$$

is in excellent agreement with the experimental number $f_\pi = 132 \text{ MeV}$. Many other “classical” examples of the SVZ method can be found in the original papers¹ or in the reviews.⁴

There are two important messages from the above analysis. The first one is that QCD sum rules are (and will remain) approximate and their accuracy cannot be improved beyond certain limits. The second message is more encouraging. Within the SVZ method one is able to estimate the theoretical uncertainty of the predicted hadronic parameter. Similar estimates are impossible, e.g., in many quark models of hadrons, where the inputs are nonuniversal and have no direct relation to QCD.

3 Applications and development of the method

In the past two decades, QCD sum rules have been applied to many problems of hadron physics, with an accuracy, in several cases, substantially improved with respect to the original analyses. An incomplete list of applications includes:

- determination of the light (u , d , s) and heavy (c , b) quark masses;
- masses and decay constants of light and heavy mesons and baryons;
- form factors of mesons and baryons ;
- valence quark distributions and spin structure functions of the nucleon; structure functions of the photon, ρ meson and pion;
- hadronic matrix elements relevant for the description of $K^0-\bar{K}^0$, $B_d-\bar{B}_d$, $B_s-\bar{B}_s$ mixing;
- strong couplings and magnetic moments of mesons and baryons;
- calculation of the parameters of effective theories, such as chiral perturbation theory (χ PT), heavy quark effective theory (HQET), nonrelativistic QCD (NRQCD);
- spectroscopy and properties of non $q\bar{q}$ hadrons (gluonia, hybrids);
- hadrons in nuclear matter, properties of hadronic matter at high temperature and density.

It is hardly possible to include in one review an exhaustive detailed presentation of all important results obtained in twenty years of investigations. For the interested reader, a lot of important information, not covered here, is accumulated in the papers listed in the bibliography. In this Section we focus only on a part of the topics listed above, with an emphasis on the results which seem to be particularly important for current and future experimental studies.^{*j*} Our intention is also to discuss the possibilities to improve these results and to outline the problems that still need to be solved.

Before starting the presentation, let us again emphasize that QCD sum rules are approximate relations. The predictions obtained from their analyses are characterized by uncertainties which are estimated by varying the input parameters (α_s , condensates, Borel parameters, etc.) in the allowed ranges. For a convenient comparison with the results obtained by other methods, we

^{*j*} For an earlier survey, see the Appendix on QCD sum rules in the “The BaBar physics book”²⁵ Some of the results collected there are updated here.

will quote the sum rule predictions as: central value \pm uncertainty. The latter cannot be considered as a statistical error. It just indicates the range of variation of the result from the (central value $-$ uncertainty) to the (central value $+$ uncertainty).

3.1 Light quark masses: m_u , m_d , m_s

A precise determination of the quark masses is a task of paramount importance for the Standard Model and its extensions. Chiral perturbation theory allows to determine the ratios of the light quark masses:

$$\frac{m_s}{m_d} = 18.9 \pm 0.8, \quad \frac{m_u}{m_d} = 0.553 \pm 0.043, \quad \frac{m_s}{\frac{1}{2}(m_u + m_d)} = 24.4 \pm 1.5, \quad (69)$$

obtained at the next-to-leading order from the measured masses of the pseudoscalar mesons.²⁶ The determination of the individual quark masses has attracted a lot of attention in the QCD sum rule community. The correlators of the divergence of light quark (u , d) axial-vector currents have been studied to calculate $m_u + m_d$. In addition, correlators of the divergence of vector and axial-vector strange currents have been analyzed to determine m_s , using experimental information on $K\pi$ and $K\pi\pi$ resonances.

Let us present in more detail this set of results. For further use, it is important to mention that the quark masses depend on the normalization scale μ through the renormalization group equation:

$$\mu \frac{d}{d\mu} m_q(\mu) = -\gamma(\alpha_s) m_q(\mu). \quad (70)$$

The scale dependence can be expressed as:

$$m_q(\mu) = \hat{m}_q R(\mu), \quad (71)$$

where \hat{m}_q is a renormalization invariant parameter and

$$R(\mu) = \left(\frac{\beta_0}{2} \frac{\alpha_s(\mu)}{\pi} \right)^{2\gamma_0/\beta_0} \left\{ 1 + \left(2\frac{\gamma_1}{\beta_0} - \frac{\beta_1\gamma_0}{\beta_0^2} \right) \frac{\alpha_s(\mu)}{\pi} + \mathcal{O}(\alpha_s^2) \right\}; \quad (72)$$

γ_i and β_i are the first coefficients of the mass anomalous dimension γ and of the QCD β function, respectively; in the \overline{MS} scheme, for three colors and N_f flavors, they read:

$$\gamma_0 = 2, \quad \gamma_1 = \frac{101}{12} - \frac{5}{18} N_f, \quad (73)$$

and

$$\beta_0 = 11 - \frac{2}{3}N_f, \quad \beta_1 = 51 - \frac{19}{3}N_f. \quad (74)$$

In order to determine $m_u + m_d$ one can study the two-point correlation function

$$\Psi_5(q^2) = i \int d^4x e^{iq \cdot x} \langle 0 | T \{ j_5(x) j_5^\dagger(0) \} | 0 \rangle, \quad (75)$$

j_5 being the divergence of the axial current (66): $j_5 = \partial_\mu (\bar{u} \gamma^\mu \gamma_5 d)$. The correlator (75) is particularly sensitive to the u and d quark masses, since $j_5 = (m_u + m_d) \bar{u} i \gamma_5 d$.

In the perturbative contribution to (75) up to 4-loop corrections^{17,27} are available. In the condensate expansion terms up to $d = 6$ has been taken into account. The hadronic spectral function is expressed in terms of the pion pole and of higher resonances, and is constrained to satisfy the behavior predicted by chiral perturbation theory at the (3π) threshold.

In Table 1 we present a set of the results for $\overline{m}_u + \overline{m}_d$, in the \overline{MS} scheme at $\mu = 1$ GeV (see also Refs. 28–30). In the same Table we also include recent lattice QCD determinations, which are typically provided for the combination $(\overline{m}_u + \overline{m}_d)/2$ at $\mu = 2$ GeV; the corresponding values at $\mu = 1$ GeV are obtained using Eqs. (72)–(74). One observes that, although the uncertainty has not

$(\overline{m}_u + \overline{m}_d)(\mu = 1 \text{ GeV})$ (MeV)	Ref.	comments
15.2 ± 2.0	DR87 ³¹	LO
15.6 ± 3.4	N89 ³²	“
12.8 ± 2.5	P98 ³³	$\mathcal{O}(\alpha_s^3)$
9.5 ± 1.6	G97 ³⁴	(quenched) lattice QCD
12.6 ± 1.3	BGLM00 ³⁵	“
11.6 ± 1.1	A00 ³⁶	“

Table 1: QCD sum rule results for $\overline{m}_u + \overline{m}_d$ ($\mu = 1$ GeV), compared to the recent lattice QCD determinations (renormalized to the same scale).

substantially improved in the years, the most recent sum rule determination of $\overline{m}_u + \overline{m}_d$ predicts a value smaller than the previous ones. This is related to the account of higher order QCD corrections and to the improvement of the

hadronic spectral function. Notice that, being combined with the chiral ratios in Eq. (69), the results in Table 1 allow one to individually determine m_u , m_d and m_s .

A similar analysis can be applied to determine the strange quark mass. One considers the two-point correlator of the divergences of the strangeness changing vector current $j_S = \partial_\mu(\bar{s}\gamma^\mu u)$:

$$\Psi(q^2) = i \int d^4x e^{iq \cdot x} \langle 0 | T \{ j_S(x) j_S^\dagger(0) \} | 0 \rangle, \quad (76)$$

which is sensitive to m_s , since $j_S = i(m_s - m_u)\bar{s}u$.

It is worth describing this calculation in some detail. In QCD, the second derivative of the correlation function (76), $\Psi''(q^2) = (\partial^2/(\partial q^2)^2)\Psi(q^2)$, is obtained from the dispersion relation:

$$\Psi''(q^2) = \frac{2}{\pi} \int_0^\infty ds \frac{\text{Im } \Psi(s)}{(s - q^2)^3}. \quad (77)$$

The hadronic spectral function $\rho(s) = \frac{1}{\pi} \text{Im } \Psi(s)$ can be obtained inserting a set of intermediate states with strangeness $|S| = 1$, $J^P = 0^+$ and $I = \frac{1}{2}$ in the correlator (76), starting from the two-particle states: $|K\pi\rangle$, $|K\eta\rangle$, $|K\eta'\rangle$, etc. The $|K\pi\rangle$ contribution to $\rho(s)$ can be written as

$$\rho^{K\pi}(s) = \frac{3}{32\pi^2} \frac{\sqrt{(s - s_+)(s - s_-)}}{s} |d(s)|^2 \theta(s - s_+), \quad (78)$$

where $s_\pm = (M_K \pm M_\pi)^2$. The function $d(s)$ is the scalar $K \rightarrow \pi$ form factor; in the low- s region it admits a linear expansion, with the parameters fixed by the one-loop chiral perturbation theory. Above the $K\pi$ threshold, the function $d(s)$, hence $\rho^{K\pi}(s)$, can be reconstructed assuming the dominance of the scalar, $|S| = 1$, $K_0^*(1430)$ and $K_0^*(1950)$ resonances.^{38,39} This procedure, however, only partially uses the experimental information on the scalar $K\pi$ system, where a sizeable non-resonant component is observed.⁴⁰ Another possibility for reconstructing $\rho^{K\pi}(s)$ consists in using the Omnés formula to account for information on the scalar $K\pi$ system from the measured $I = \frac{1}{2}$ $K\pi$ scattering phase shift. With this procedure, the normalization condition of $\rho^{K\pi}(s)$ at the $K\pi$ threshold is automatically satisfied.⁴¹

Due to the positivity of the spectral function $\rho(s)$, the procedures described above yield either a lower bound on m_s , if only the low hadronic states are taken into account, or a determination of m_s , if the rest of contributions is approximated by duality. Concerning the perturbative contribution to the

sum rule, early calculations included $\mathcal{O}(\alpha_s^2)$ corrections; currently the $\mathcal{O}(\alpha_s^3)$ expression is used.^{39,41} Also the condensates up to $d = 6$ are included in the OPE. The results of this set of determinations are collected in Table 2.⁴³ The main uncertainty in the determination of m_s is due to the procedure of reconstructing the spectral function $\rho(s)$.⁴⁵

One could also use the correlator of the divergences of the strangeness changing axial current, proportional to $m_s + m_u$. The corresponding sum rule has been investigated,^{38,46} but the result for m_s has a larger uncertainty caused by an insufficient information on $K\pi\pi$ resonances needed to reconstruct the hadronic spectral function.

$\overline{m}_s(\mu = 1 \text{ GeV}) \text{ (MeV)}$	Ref.	comments
171 ± 15	CDPS95 ³⁷	$\mathcal{O}(\alpha_s^2)$ + resonances
189 ± 32	JM95 ³⁸	“
203.5 ± 20	CPS97 ³⁹	$\mathcal{O}(\alpha_s^3)$ + resonances
140 ± 20	CDNP97 ⁴¹	$\mathcal{O}(\alpha_s^3)$ + Omnès
160 ± 30	J98 ⁴²	“
159 ± 11	M99 ⁴⁴	FESR + Omnès
155 ± 25	DPS99 ⁴⁶	axial current div.
$200 \pm 40 \pm 30$	CKP98 ⁴⁷	τ decays
164 ± 33	PP99 ⁴⁸	“
$176 \pm 37 \pm 13$	KKP00 ⁴⁹	“
$158.6 \pm 18.7 \pm 16.3 \pm 13.3$	KM00 ⁵⁰	“
184 ± 26	E97 ⁵¹	(unquenched) lattice QCD
124 ± 21	G97 ³⁴	(quenched) lattice QCD
139 ± 9	A99 ⁵²	“
138 ± 5	G99 ⁵³	“
146 ± 12	BGLM00 ³⁵	“
128 ± 5	G00 ⁵⁴	“
144 ± 5	A00 ³⁶	“
117 ± 9	A00 ³⁶	(unquenched) lattice QCD

Table 2: QCD sum rule results for $\overline{m}_s(\mu = 1 \text{ GeV})$ compared to recent lattice QCD determinations (renormalized to $\mu = 1 \text{ GeV}$).

In Table 2 we also collect the outcome of the analysis of strange and nonstrange hadronic τ decays. In this case, m_s is determined retaining in the OPE the SU(3)-flavor breaking contributions, which depend on the strange

quark mass. The spread of the results is mainly caused by differences in the treatment of the higher-order perturbative terms. The sum rule results can be compared with recent lattice QCD determinations of m_s , also given in Table 2, both in quenched approximation and for dynamical fermions.

The compilation of results presented above clearly demonstrates the unique ability of QCD sum rules to analytically determine the light-quark masses, employing various correlation functions and systematically including, order by order, the contributions of the perturbative series and of the nonperturbative condensates. The main limitation is caused by an insufficient knowledge of the hadronic spectral function in the scalar and pseudoscalar channels. In principle, this difficulty can be solved when detailed experimental data become available.

3.2 Heavy quark masses: m_c , m_b

The study of the charmonium system was probably one of the first applications of the QCD sum rule method.¹ The c quark mass can be determined, if one considers the two-point correlation function of two $\bar{c}\gamma_\mu c$ currents (discussed in Sec. 2), and uses for the hadronic spectral density the experimental data on the e^+e^- cross section into charm-anticharm states, in particular the precise information on the masses and the electronic widths of the $J^P = 1^-$ charmonium levels (J/ψ , ψ' , \dots). So far, the sum rule was analyzed including the perturbative QCD two-loop corrections. The nonperturbative contribution mainly depends on the gluon condensate $\langle\alpha_s G^2\rangle$, while the contributions of other vacuum condensates are believed to be small numerically.

m_c (GeV)	$\overline{m}_c(\overline{m}_c)$ (GeV)	Ref.	comments
1.46 ± 0.05		DGP94 ⁵⁶	Borel
1.42 ± 0.03	$1.23^{+0.02}_{-0.04} \pm 0.03$	N94 ⁵⁷	Borel, moments
	$1.525 \pm 0.040 \pm 0.125$	APE98 ⁵⁹	lattice QCD
	1.33 ± 0.08	FNAL98 ⁶⁰	“
	$1.20 \pm 0.04 \pm 0.11 \pm 0.2$	NRQCD99 ⁶¹	lattice NRQCD

Table 3: QCD sum rule determinations of the c quark mass and recent lattice QCD results.

In Table 3 we present two results for the charmed quark pole mass m_c ,⁵⁵ together with the recent lattice QCD determinations. The difference between the two analyses is that in the first one⁵⁶ the pole mass is directly computed, while in the second one⁵⁷ the \overline{MS} running quark mass \overline{m}_c is determined, and then related to the pole mass. The two results are in agreement with each

other, and with the estimate ¹ $m_c(p^2 = -m_c^2) = 1.26$ GeV (having about ± 0.1 GeV uncertainty) obtained in the original SVZ analysis. It would be important to update the sum rule determination of the charm quark mass, including the $O(\alpha_s^2)$ perturbative correction ⁵⁸ and the three- and four-gluon condensate contributions.¹⁸

In recent years, there has been an impressive progress in the determination of the b -quark mass, from the analysis of the two-point correlation function of $\bar{b}\gamma_\mu b$ currents. In this analysis, the hadronic spectral function is obtained taking into account six $\Upsilon(nS)$ resonances, their masses and leptonic decay constants being precisely measured in e^+e^- annihilation. The current activity aims at working with the highest possible moments of sum rules, where NRQCD is a good approximation. In this framework one is able to perform the Coulomb resummation, taking into account relativistic and radiative corrections order by order. Notice that the gluon condensate contributions are negligible in the heavy quarkonium system.

In Table 4 we present a summary of recent determinations,⁶² together with an average of the lattice QCD results.⁶³ From this Table we see that the preferred interval for the sum rule results is $m_b \simeq 4.8 \pm 0.1$ GeV.

A detailed discussion of NRQCD and its application to the b quark mass problem is beyond our task, and the interest reader is addressed to more specialized reviews.⁶⁴ We only notice that there exists an alternative approach, based on taking the first few moments of the standard SVZ sum rules. In this case, the b -quark mass is determined in a purely relativistic way. The drawback is the sensitivity to the tail of the hadronic spectral function corresponding to the open beauty production at energies larger than the resonance masses. This spectral function can be handled by employing the duality approximation, combining it with the experimentally measured inclusive $e^+e^- \rightarrow \bar{b}b$ cross section. This kind of analysis was employed in the early papers ⁴ and still deserves attention, having in mind the possibility of including the recently calculated $O(\alpha_s^2)$ correction ⁵⁸ which will improve the accuracy of the perturbative part.

The task of an accurate evaluation of the b quark mass is very important. As we shall see in the following, a precise determination of m_b will critically reduce the uncertainty in various sum rules for B mesons.

3.3 Heavy-light mesons

The decay constants $f_{D_{(s)}}$ and $f_{B_{(s)}}$ of the heavy-light mesons $D_{(s)}$, $B_{(s)}$ are defined by the matrix element of the heavy flavored axial-vector current

$$\langle 0 | \bar{q} \gamma_\mu \gamma_5 Q | H(p) \rangle = i f_H p_\mu, \quad (79)$$

m_b (GeV)	$\overline{m_b}(\overline{m_b})$ (GeV)	Ref.	Method
4.72 ± 0.05	4.19 ± 0.06 4.20 ± 0.10 4.20 ± 0.06 4.25 ± 0.08	DP92 ⁶⁵	standard SVZ
4.62 ± 0.02		N94 ⁵⁷	“
4.827 ± 0.007		V95 ⁶⁶	NRQCD
4.84 ± 0.08		JP99 ⁶⁷	“
		MY99 ⁶⁸	“
4.88 ± 0.10		H99 ⁶⁹	“
4.80 ± 0.06		PP98 ⁷⁰	“
		BS99 ⁷¹	“
	4.26 ± 0.11	H00 ⁶³	lattice QCD (average)

Table 4: The b quark mass from SVZ and NRQCD sum rules and the lattice QCD average.

where $Q = c, b$, $H = D_{(s)}, B_{(s)}$ and $q = u, d(s)$, in the same normalization as f_π defined in Eq. (65). An accurate calculation of these decay constants is very important for heavy flavor phenomenology, and QCD sum rules were among the first analytical methods to predict f_B and f_D .^{3,4,72} In these sum rules, perturbative $\mathcal{O}(\alpha_s)$ corrections and $d \leq 6$ condensates were taken in account.

We would like to emphasize two aspects. Firstly, the result for f_B is very sensitive to the value of the b -quark pole mass. The latter is extracted from the analysis of the Υ system discussed in the previous subsection. Lowering the b -quark mass by 100 MeV increases f_B by 30 to 40 MeV. The heavy quark mass dependence is less significant in the determination of f_D . Secondly, the resummation of leading logarithmic contributions in the sum rule for f_B , obtained in the framework of HQET, revealed that α_s has to be taken at a low energy scale, $\mu \simeq 1$ GeV, rather than at $\mu \simeq m_b$.^{73,74} In full QCD with finite b -quark mass, the optimal position of the scale, which has to be determined from higher orders of QCD perturbation theory, remains an unsolved problem. Current sum rule calculations use a somewhat intermediate scale, equal to the Borel parameter: $\mu^2 = M^2 \simeq 3 - 5$ GeV². The shift from m_b to lower scales produces another significant increase of f_B . In the case of f_D this effect is again milder.

In Table 5, we collect several results and compare them with the recent lattice QCD determinations. Notice that the account of the abovementioned effects has produced larger values for f_B than in the original calculations.

The most recent sum rule results presented in Table 5 correspond to the following intervals:

$$f_D = 180 \pm 30 \text{ MeV}, \quad f_B = 170 \pm 30 \text{ MeV}, \quad (80)$$

f_D (MeV)	f_B (MeV)	Ref.
189 ± 49	158 ± 25	DP87 ⁷⁵
173 ± 22	168 ± 18	D93 ⁷⁶
200 ± 20	180 ± 30	KRWY99 ^{77,78}
$195 \pm 10^{+22}_{-10}$	$161 \pm 16^{+24}_{-13}$	UKQCD99 ⁷⁹
$216 \pm 11^{+5}_{-4}$	$173 \pm 13^{+34}_{-2}$	APE00 ⁸⁰
$220 \pm 3^{+2}_{-24}$	$218 \pm 5^{+5}_{-41}$	UKQCD00 ⁸¹

Table 5: D and B meson leptonic decay constants f_D and f_B from QCD sum rules and lattice QCD.

where the rather large uncertainties suggest that there is still a room for an improvement, as we shall argue below.

The ratios f_{D_s}/f_D and f_{B_s}/f_B are calculated by including $\mathcal{O}(m_s)$, SU(3)-flavor symmetry breaking corrections in the sum rules. In these ratios, the dependence on the heavy quark mass, as well as the effects of the radiative $\mathcal{O}(\alpha_s)$ corrections, are less significant. A compilation of various determinations is presented in Table 6; again, one can try to summarize the results as²⁵

$$f_{D_s}/f_D = 1.19 \pm 0.08, \quad f_{B_s}/f_B = 1.16 \pm 0.09. \quad (81)$$

The sum rule predictions for f_{D_s} and f_D have to be compared with the results of the experimental measurements: $f_{D_s} = 280 \pm 19 \pm 28 \pm 34$ MeV and $f_D = 300^{+180+80}_{-150-40}$ MeV, respectively.²⁴ The data are still too uncertain to challenge theory.

The decay constants of the vector mesons D^* and B^* , defined by the matrix elements:

$$\langle 0 | \bar{q} \gamma_\mu Q | H^* \rangle = m_{H^*} f_{H^*} \epsilon_\mu^{(H^*)} \quad (82)$$

($Q = c, b$, $H^* = D^*, B^*$) have also been updated.⁷⁷

$$f_{D^*} = 270 \pm 35 \text{ MeV}, \quad f_{B^*} = 195 \pm 35 \text{ MeV}. \quad (83)$$

The corresponding matrix elements for the orbitally excited heavy mesons have

f_{D_s}/f_D	f_{B_s}/f_B	Ref.
1.21 ± 0.06	1.22 ± 0.02	D93 ⁷⁶
	1.09 ± 0.03	BCNP94 ⁸²
1.15 ± 0.04	1.16 ± 0.04	N94 ⁸³
$1.17 \pm 0.03 \pm 0.03$	$1.20 \pm 0.04 \pm 0.03$	HL96 ⁸⁴
$1.15 \pm 0.04^{+0.02}_{-0.03}$	$1.16 \pm 0.06^{+0.02}_{-0.03}$	UKQCD99 ⁷⁹
$1.11 \pm 0.01^{+0.1}_{-0}$	$1.14 \pm 0.02^{+0.1}_{-0.1}$	APE00 ⁸⁰
$1.09 \pm 0.01^{+0.05}_{-0.02}$	$1.11 \pm 0.01^{+0.05}_{-0.03}$	UKQCD00 ⁸¹

Table 6: The ratios f_{D_s}/f_D and f_{B_s}/f_B : QCD sum rules (the four upper lines) versus lattice QCD predictions (the three lower lines).

been determined, both for finite heavy quark mass⁸⁵ and in HQET as discussed below in Sec. 3.9.

Is it possible to improve the determination of the heavy meson decay constants? The analysis of the heavy-light quark systems does not allow an accurate, independent determination of the heavy quark masses, the latter should be obtained from the heavy quarkonium channels. However, once the accuracy of the b and c quark masses is increased, this immediately reduces the uncertainty of the heavy meson decay constants. The issue of α_s corrections and of their proper scale and resummation requires further investigations, at least in the case of f_B . In this case, the $\mathcal{O}(\alpha_s)$ corrections in the sum rule seem to be unusually large, and one may speculate that anomalously large soft parts of perturbative diagrams should be somehow separated. Furthermore, the contribution of the $d = 7$ $\langle GG\bar{q}q \rangle$ condensate in the same sum rule is proportional to the heavy quark mass and could be sizeable, hence, it should be taken into account. Finally, improvement of the duality approximation for the hadronic spectral density is possible when enough experimental information on radially excited B and D resonances will be available.

3.4 B_c meson

The studies of the charmonium system, in particular the determination of the masses and decay rates of J/ψ , η_c and χ_c , were among the first applications of

the SVZ method and provided the first physical predictions of this approach. It is worth reminding the successful prediction of the mass of η_c .¹ The analysis was then extended to the bottomonium system ($\Upsilon, \eta_b, \chi_b, \dots$). With this rich experience in analyzing heavy quarkonia, QCD sum rules can be used to investigate the B_c meson, the state with open beauty and charm observed recently by the CDF Collaboration.⁸⁶ From the point of view of quark-gluon interactions, B_c is intermediate between the $\bar{c}c$ and $\bar{b}b$ systems, and it shares with the two heavy quarkonia common dynamical properties. For example, it is possible to consider the heavy quark and antiquark as nonrelativistic particles, and describe the bound state, adding then the relativistic corrections. On the other hand, B_c , being the lightest hadron with open beauty and charm, decays weakly. Therefore, it provides us with a rather unique possibility of investigating weak decay form factors in a quarkonium system.

In the framework of QCD sum rules, B_c is investigated using the interpolating current $j_5 = i \bar{c} \gamma_5 b$. The analysis of the two-point correlator is very similar to that discussed in Sec. 2, including the gluon condensate and the $O(\alpha_s)$ correction, and summing up the Coulomb part of this correction in the nonrelativistic approximation. Various calculations of the B_c leptonic constant yield results in the range $f_{B_c} = 300 - 420$ MeV.^{87,88} Clearly, the accuracy of this determination can still be improved. This would be an important outcome, since the purely leptonic mode $B_c \rightarrow \ell \bar{\nu}$ can be used to access the CKM matrix element V_{cb} . Concerning the semileptonic B_c decays, such as $B_c \rightarrow J/\psi(\eta_c) \ell \nu$ and $B_c \rightarrow B_s^{(*)} \ell \nu$, they have been investigated by three-point sum rules,^{88,89} following the method we shall illustrate below. In particular, in this framework it is possible⁸⁹ to derive the relations among the form factors determined by the heavy-quark spin symmetry, i.e. exploiting the decoupling of the spin of the heavy quarks in the infinite quark mass limit. The numerical determination of the form factors is still hampered by the absence of $\mathcal{O}(\alpha_s)$ corrections, which are currently estimated in the nonrelativistic Coulomb approximation at the zero-recoil point.⁸⁹ Abundant B_c production is expected at hadron colliders, and a careful experimental investigation of this system will be possible in the near future.⁹⁰ B_c will represent an interesting testing ground for the QCD sum rule approach, and therefore the refinement of the theoretical predictions concerning this system should be in the working plans of the sum rule practitioners.

3.5 Ioffe currents and sum rules for baryons

QCD sum rules for baryons suggested by Ioffe⁹¹ provide an important demonstration of the universality of the method, generalizing it from the quark-

antiquark states to the three-quark states. To construct the correlation functions^{91,92} one needs a baryon current, that is, a composite operator having the same quantum numbers as a given baryon. For the proton, several possibilities were studied:

$$J^N(x) = \epsilon_{abc}(u^{aT}(x)\mathcal{C}\gamma_\mu u^b(x))\gamma_5\gamma^\mu d^c(x) \quad (84)$$

or

$$J'^N(x) = \epsilon_{abc}(u^{aT}(x)\mathcal{C}\sigma_{\mu\nu}u^b(x))\gamma_5\sigma^{\mu\nu}d^c(x) \quad , \quad (85)$$

where a, b, c are color indices and \mathcal{C} is the charge conjugation matrix. Other possible quark currents involve derivatives. Some criteria have to be adopted to single out the optimal interpolating current for a particular baryon. The first criterion is to choose a current with a minimal number of derivatives, in order to deal with low-dimensional spectral densities and, consequently, to minimize the contribution of the excited states. Furthermore, the currents should maximize the projection onto the considered baryon state. This can be done, for example, by considering linear combinations of the interpolating currents, with the coefficient suitably chosen in order to maximize the overlap. Finally, it is possible to choose currents in such a way that the two-point functions are dominated by the perturbative contribution, with the condensate terms producing a hierarchical set of corrections. This last requirement suggests to use the current (84), instead of (85), to interpolate the proton. Studying the two-point correlation function

$$\Pi(q) = i \int e^{iq \cdot x} \langle 0 | T \{ J^N(x) \bar{J}^N(0) \} | 0 \rangle = \Pi_1(q^2) + \not{q} \Pi_2(q^2) \quad (86)$$

and neglecting the contribution of the continuum and of higher dimensional condensates, an astonishingly simple expression for the nucleon mass can be obtained:⁹¹

$$m_N^3 \simeq -2(2\pi)^2 \langle \bar{q}q \rangle (\mu = 1\text{GeV}) \quad , \quad (87)$$

in agreement with experiment.

With a little effort, one defines the interpolating currents for the $L = 0$ baryonic octet:

$$\begin{aligned} J^\Sigma(x) &= \epsilon_{abc}(u^{aT}(x)\mathcal{C}\gamma_\mu u^b(x))\gamma_5\gamma^\mu s^c(x) \quad , \\ J^\Xi(x) &= -\epsilon_{abc}(s^{aT}(x)\mathcal{C}\gamma_\mu s^b(x))\gamma_5\gamma^\mu u^c(x) \quad , \\ J^\Lambda(x) &= \sqrt{\frac{2}{3}}\epsilon_{abc} \left[(u^{aT}(x)\mathcal{C}\gamma_\mu s^b(x))\gamma_5\gamma^\mu d^c(x) - (d^{aT}(x)\mathcal{C}\gamma_\mu s^b(x))\gamma_5\gamma^\mu u^c(x) \right] \quad , \end{aligned} \quad (88)$$

and for the $L = 0$ decuplet:

$$J_\mu^\Delta(x) = \epsilon_{abc}(u^{aT}(x)\mathcal{C}\gamma_\mu u^b(x))u^c(x) \quad ,$$

$$\begin{aligned}
J_\mu^{\Sigma^*}(x) &= \sqrt{\frac{1}{3}}\epsilon_{abc}\left[2(u^{aT}(x)\mathcal{C}\gamma_\mu s^b(x))u^c(x) + (u^{aT}(x)\mathcal{C}\gamma_\mu u^b(x))s^c(x)\right], \\
J_\mu^{\Xi^*}(x) &= \sqrt{\frac{1}{3}}\epsilon_{abc}\left[2(s^{aT}(x)\mathcal{C}\gamma_\mu u^b(x))s^c(x) + (s^{aT}(x)\mathcal{C}\gamma_\mu s^b(x))u^c(x)\right], \\
J_\mu^\Omega(x) &= \epsilon_{abc}(s^{aT}(x)\mathcal{C}\gamma_\mu s^b(x))s^c(x).
\end{aligned} \tag{89}$$

The $\mathcal{O}(\alpha_s)$ radiative corrections to the two-point functions of baryon currents are known for three massless quarks,⁹³ and have been worked out also for the case of baryons containing one heavy and two massless quarks.⁹⁴ This opens up interesting perspectives for more precise determinations of the baryon properties, both in the light quark and in the heavy quark sector. Let us remind the reader that the analysis of the two-point correlator of baryonic currents was of prime importance for determining some characteristics of the QCD vacuum. As a matter of fact, from the fit of the masses of baryons belonging to the $L = 0$ octet and decuplet, it was possible to determine the values of the mixed quark-gluon condensate (49) and of the $SU(3)$ -flavor breaking parameter $\gamma = \langle \bar{s}s \rangle / \langle \bar{q}q \rangle - 1 \simeq -0.2$.⁴

The extension to the case of baryons containing charm and beauty quarks is also straightforward. In the heavy quark sector, open problems concern the spectra of baryons containing more than one heavy (c and b) quark. These baryons will be experimentally observed and investigated at hadron colliders. Two-point correlation functions of heavy-baryon currents allow one to predict the spectrum of these states.⁹⁵ For an overview of sum rule applications to the baryonic problems, and for an analysis of the features of various three-quark interpolating currents one can consult the available reviews.⁹⁶

An important technique for the studies of the baryon dynamics is *the method of external fields*,⁹⁷ in which two-point correlators in the external static fields (such as magnetic field) are introduced. Originally, many static properties of nucleons, such as magnetic moments, or nucleon matrix elements of axial-vector currents and other operators have been successfully calculated. The limits of this review do not allow us to discuss this technique and its applications in more detail. A thorough presentation can be found, e.g., in the lecture by Ioffe.⁷ To demonstrate the variety of problems that can be solved by employing the external field method or the closely related approach of the soft-pion field, let us mention some recent applications. In the light baryon sector, attention has been recently paid to the properties of negative parity baryons, such as $N^*(1535)$. In particular, the experimental analysis has shown a suppression of the strong $N^*N\pi$ coupling and an enhancement of the $N^*N\eta$ coupling. Interestingly, estimates of these couplings using the two-point correlators in the external (soft) pion field are in agreement with this observation.⁹⁸

Other strong pion-baryon couplings have been analyzed by the same method.⁹⁹

3.6 Three-point correlation functions: form factors and decay amplitudes

The method of QCD sum rules can be generalized in order to calculate the hadronic matrix elements of electromagnetic and weak transitions. In this case one starts from three-point vacuum correlation functions and uses double dispersion relations. This approach has been extensively used, both for light and heavy hadrons. The applications include the pion electromagnetic form factor,¹⁰⁰ radiative charmonium decays such as $J/\psi \rightarrow \eta_c \gamma$,¹⁰¹ D and B semileptonic and flavor-changing neutral current (FCNC) transitions^{102–107} and, more recently, the radiative decays $\phi \rightarrow (\eta, \eta') \gamma$.¹⁰⁸

In order to discuss the advantages and the difficulties of three-point sum rules, let us outline, as an example, the calculation¹⁰⁰ of the pion electromagnetic form factor defined by the matrix element:

$$\langle \pi(p') | j_\mu^{em} | \pi(p) \rangle = F_\pi(q^2)(p + p')_\mu, \quad (90)$$

where $q = p' - p$ and j_μ^{em} is the electromagnetic current

$$j_\mu^{em} = e_u \bar{u} \gamma_\mu u + e_d \bar{d} \gamma_\mu d. \quad (91)$$

The starting point is the correlator of j_μ^{em} with two pion-interpolating currents (66):

$$\begin{aligned} T_{\mu\nu\lambda}(p, p') &= (i)^2 \int d^4x d^4y e^{i(p' \cdot x - p \cdot y)} \langle 0 | T \{ j_\mu^{(\pi)\dagger}(x) j_\lambda^{em}(0) j_\nu^{(\pi)}(y) \} | 0 \rangle \\ &= p'_\mu p_\nu (p + p')_\lambda T(p^2, p'^2, q^2) + \dots, \end{aligned} \quad (92)$$

where the momenta p , p' and q flow through the axial-vector and the electromagnetic currents, respectively. In Eq. (92) we have only shown the relevant kinematical structure, the others being denoted by the ellipses.

Inserting in Eq. (92) two complete sets of hadronic states with the quantum numbers of the pion one obtains the dispersion relation:

$$\begin{aligned} T(p^2, p'^2, q^2) &= \frac{f_\pi^2 F_\pi(q^2)}{(m_\pi^2 - p^2)(m_\pi^2 - p'^2)} + \int_{R_{12}} ds ds' \frac{\rho^h(s, s')}{(s - p^2)(s' - p'^2)} \\ &+ P_1(p^2) \int_{R_2} ds' \frac{\rho_2(s')}{s' - p'^2} + P_2(p'^2) \int_{R_1} ds \frac{\rho_1(s)}{s - p^2}, \end{aligned} \quad (93)$$

where the double dispersion integral receives contributions from the excited and continuum states located in the region R_{12} of the (s, s') plane. The terms

containing the polynomials P_1 and P_2 arise from subtractions in the dispersion relation, and, therefore, two independent Borel transformations in p^2 and p'^2 are needed to get rid of them. The same transformations enhance the double pole term with respect to the double integral in Eq. (93).

On the other hand, the amplitude (92) can be computed by a short-distance expansion, in terms of perturbative and condensate contributions:

$$T(p^2, p'^2, q^2) = \sum_d C^d(p^2, p'^2, q^2, \mu) \langle O_d(\mu) \rangle. \quad (94)$$

The expansion is valid for large spacelike external momenta: $|p^2|, |p'^2| \gg \Lambda_{QCD}^2$; the squared momentum transfer $Q^2 = -q^2$ is also kept large in order to stay far away from the hadronic thresholds in the q^2 -channel. In Fig. 8 we

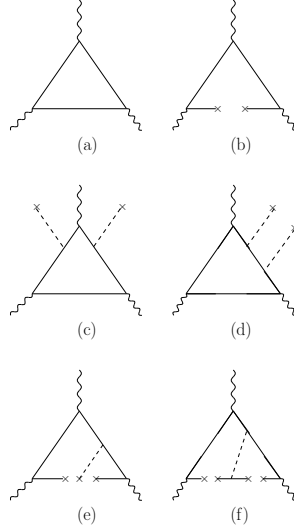


Figure 8: Contributions to the three-point correlator (94): $\mathcal{O}(\alpha_s = 0)$ perturbative term (a) and some nonperturbative corrections (b–f).

depict the perturbative diagram and several contributions of the condensates. In the chiral limit, the contributions of the quark and quark-gluon condensates vanish.

To proceed further, one has to match the expression (94) with the hadronic representation (93). Invoking quark-hadron duality, one approximates the double dispersion integral in the region R_{12} with the perturbative one. After that, the double Borel transformation in p^2, p'^2 is performed, introducing two corresponding parameters M, M' , so that the sum rule for $F_\pi(Q^2)$ reads:

$$f_\pi^2 F_\pi(Q^2) = \frac{1}{\pi^2} \int_{\tilde{R}_{12}} ds ds' \text{Im } C^0(s, s', Q^2) e^{-\frac{s}{M^2} - \frac{s'}{M'^2}} + \sum_{d=3}^n C^d(M^2, M'^2, Q^2, \mu) \langle O_d(\mu) \rangle. \quad (95)$$

The domain $\tilde{R}_{12}(s_0^\pi)$, characterized by the threshold s_0^π , is determined by the duality approximation and by the procedure of subtracting the contributions of excited and continuum states. More specifically, taking $M' = M$ and considering the contribution of condensates up to $d = 6$, yields the following sum rule:¹⁰⁰

$$F_\pi(Q^2) = \frac{4}{f_\pi^2} \left[\int_{\tilde{R}_{12}} ds ds' \rho_0(s, s', Q^2) e^{-\frac{s+s'}{M^2}} + \frac{\alpha_s}{48\pi M^2} \langle G_{\mu\nu}^a G_{\mu\nu}^a \rangle + \frac{52\pi}{81M^4} \alpha_s \langle \bar{\psi}\psi \rangle^2 \left(1 + \frac{2Q^2}{13M^2}\right) \right], \quad (96)$$

where

$$\rho_0(s, s', Q^2) = \frac{3Q^4}{16\pi^2} \frac{1}{\lambda^{7/2}} [3\lambda(\sigma + Q^2)(\sigma + 2Q^2) - \lambda^2 - 5Q^2(\sigma + Q^2)^3], \quad (97)$$

$\lambda = (s + s' + Q^2)^2 - 4ss'$ and $\sigma = s + s'$.

The numerical analysis of (96) uses the values of condensates given in Sec. 2 and the threshold s_0^π inferred from the two-point sum rule (67). For intermediate values of the momentum transfer, $Q^2 = 1 \div 3 \text{ GeV}^2$ the appropriate range of Borel parameter is $0.7 < M^2 < 1.7 \text{ GeV}^2$, where the sensitivity to the duality approximation is low and where there is a hierarchy of power corrections, the criteria adopted in the analysis of two-point SVZ sum rules in Sec. 2. For larger values of Q^2 the contributions of the higher-dimensional condensates containing terms $\sim Q^2/M^2$ overwhelm the contributions of the low-dimensional terms. Therefore, the three-point sum rule (96) cannot be used to predict the large Q^2 behavior of $F_\pi(Q^2)$. The reason of the failure can be traced back to the truncated local condensate approximation, which is too crude to reproduce the physical mechanisms governing the exclusive $\gamma^* \pi \rightarrow \pi$ transition.^k We shall return to this point in Sec. 4. On the other hand, there

^k As one remedy solving this problem it was suggested to use (model-dependent) nonlocal condensates.¹⁰⁹

is no doubt that the sum rule (96) is reliable in the region $Q^2 = 1 \div 3 \text{ GeV}^2$, where also the numerical result $Q^2 F_\pi(Q^2) \simeq 0.3 \text{ GeV}^2$ is in agreement with the experimental data (the latter are presented in Fig. 11).

The calculation of the heavy meson form factors follows the same strategy as outlined above. Let us begin with some useful definitions. The matrix elements governing the weak transitions of D meson to a pseudoscalar $P = K, \pi$ and vector $V = K^*, \rho$ final state are:

$$\langle P(p') | \bar{q} \gamma_\mu c | D(p) \rangle = f_{DP}^+(q^2) (p + p')_\mu + f_{DP}^-(q^2) (p - p')_\mu, \quad (98)$$

and

$$\begin{aligned} \langle V(p', \lambda) | \bar{q} \gamma_\mu (1 - \gamma_5) c | D(p) \rangle &= \frac{2V^{DV}(q^2)}{m_D + m_V} \epsilon_\mu^{\alpha\beta\gamma} \epsilon_\alpha^{(V)*} p_\beta p'_\gamma \\ &- i(m_D + m_V) A_1^{DV}(q^2) \epsilon_\mu^{(V)*} + \frac{iA_2^{DV}(q^2)}{m_D + m_V} (\epsilon^{(V)*} \cdot p) (p + p')_\mu \\ &+ i \frac{2m_V}{q^2} [A_3^{DV}(q^2) - A_0^{DV}(q^2)] (\epsilon^{(V)*} \cdot p) (p - p')_\mu, \end{aligned} \quad (99)$$

where $\epsilon_\mu^{(V)*}$ is the polarization vector of V ,

$$A_3^{DV}(q^2) = \frac{m_D + m_V}{2m_V} A_1^{DV}(q^2) - \frac{m_D - m_V}{2m_V} A_2^{DV}(q^2) \quad (100)$$

and $A_3^{DV}(0) = A_0^{DV}(0)$.

Each of the form factors introduced above can be studied by introducing an appropriate three-point correlation function. For example, the form factor f_{DK}^+ can be computed from

$$T_{\mu\lambda}(p, p') = (i)^2 \int d^4x d^4y e^{i(p' \cdot x - p \cdot y)} \langle 0 | T \{ j_\lambda^{(K)}(x) \bar{s}(0) \gamma_\mu c(0) j_5^{(D)}(y) \} | 0 \rangle, \quad (101)$$

where D and K mesons are interpolated by the corresponding currents $j_5^{(D)} = i \bar{c} \gamma_5 u$ and $j_\lambda^{(K)} = \bar{u} \gamma_\lambda \gamma_5 s$, respectively. In this case, due to the presence of a large scale m_c , the accessible region of the squared momentum transfer q^2 includes also small positive values: $q^2 \ll m_c^2$. There is another important difference with respect to the sum rule for the pion form factor: In the OPE for the correlator (101), the most important nonperturbative effects are due to the quark and quark-gluon condensates, and are described by the diagrams in Fig. 8b,e. The contributions of the gluon condensate and of the four-quark condensates are negligible. The subsequent steps include the use of quark-hadron duality and the double Borel transformation in p^2, p'^2 . The Borel

parameters M, M' are now kept different, since they correspond to heavy and light mass scales, respectively. The sum rule has the form:

$$\frac{m_D^2 f_D f_K}{m_c} f_{DK}^+(q^2) e^{-\frac{m_D^2}{M^2} - \frac{m_K^2}{M'^2}} = \frac{1}{\pi^2} \int_{\tilde{R}_{12}} ds ds' \text{Im } C_{DK}^0(s, s', q^2, \mu) e^{-\frac{s}{M^2} - \frac{s'}{M'^2}} + \sum_{d=3}^n C_{DK}^d(M^2, M'^2, q^2, \mu) \langle O_d(\mu) \rangle. \quad (102)$$

The explicit expressions for the Wilson coefficients C_{DK}^d can be found in the literature.^{103–105} The threshold parameters s_0^D and s_0^K determining the domain $\tilde{R}_{12}(s_0^D, s_0^K)$ can be inferred, together with f_D and f_K , from the study of the corresponding two-point correlation functions.

		$f_{DP}^+(0)$	$A_1^{DV}(0)$	$A_2^{DV}(0)$	$V^{DV}(0)$
$D \rightarrow K$	exp. ¹¹⁰	0.60 ± 0.15			
$D \rightarrow K^*$	exp. ¹¹¹	0.76 ± 0.03	0.50 ± 0.15 0.58 ± 0.03	0.60 ± 0.15 0.41 ± 0.06	1.1 ± 0.25 1.06 ± 0.09
$D \rightarrow \pi$		0.50 ± 0.15			
$D \rightarrow \rho$			0.5 ± 0.2	0.4 ± 0.1	1.0 ± 0.2

Table 7: Form factors of the weak $D \rightarrow P, V$ transitions at $q^2 = 0$. The experimental numbers are obtained assuming the nearest pole dominance for the form factors.

In Table 7 we present a set of results obtained at $q^2 = 0$.^{103,104,105} The q^2 dependence of the form factors can be predicted, although the procedure is non-trivial since one should stay far from the thresholds appearing in the double dispersion relation. The q^2 dependence of A_1 and A_2 turns out to be quite mild; on the contrary, the dependence of f^+ and V is compatible with the nearest pole dominance. The predictions, within their uncertainties, are in agreement with experiment. Note that the form factor f_{DK}^+ is important for an independent determination of the CKM parameter $|V_{cs}|$ from the semileptonic $D \rightarrow K l \nu_l$ decays.²⁴

In order to predict the form factors of B transitions to light mesons (π, K, ρ), one has to replace $c \rightarrow b$ and $D \rightarrow B$ in the above sum rules yielding results for semileptonic^{105,112,113} and FCNC B transitions.^{106,107} The method can be easily generalized to different processes and final states, including orbital excitations, and has provided interesting predictions. An example is the

determination^{114,106,107} of the form factors relevant for the FCNC $B \rightarrow K^*\gamma$ and $B \rightarrow K^*\ell^+\ell^-$ decays:

$$\begin{aligned} \langle K^*(p', \lambda) | \bar{s} \sigma_{\mu\nu} q^\nu b_R | B(p) \rangle &= i \epsilon_{\mu\nu\alpha\beta} \epsilon^{*\nu} p^\alpha p'^\beta T_1(q^2) \\ &+ \frac{1}{2} [e_\mu^* (m_B^2 - m_{K^*}^2) - \epsilon^* \cdot q (p + p')_\mu] T_2(q^2) \\ &+ \frac{\epsilon^* \cdot q}{2} \left(q_\mu - \frac{q^2}{m_B^2 - m_{K^*}^2} (p + p')_\mu \right) T_3(q^2), \end{aligned} \quad (103)$$

where $b_R = 1/2(1 + \gamma_5)b$, $q = p - p'$. The result^{106,107} $T_1(0) = 0.35 \pm 0.05$ allowed to predict the ratio $\Gamma(B \rightarrow K^*\gamma)/\Gamma(b \rightarrow s\gamma) = 0.17 \pm 0.05$, which agrees with the experimental measurements.^l

However, a close inspection of the general structure of three-point sum rules for heavy-light transitions reveals a difficulty which is manifest in the parametric m_b dependence of the various terms of the short-distance expansion. An example is the form factor A_1 in the $B \rightarrow \rho$ matrix element. In the limit of large m_b , one observes that the coefficients of the quark and quark-gluon condensates grow with m_b faster than the coefficient of the perturbative contribution. This is another manifestation of the difficulty in approximating the OPE expansion by the first few terms, revealed in the sum rule for the pion form factor at large Q^2 . The physical origin of this difficulty can be traced back to the mechanisms of producing the light state in the heavy meson decay, for large heavy quark mass.¹¹⁸ Of course, this problem could be irrelevant for the actual value of the b -quark mass, and for particular processes and final states: an example is the transition $B \rightarrow \pi$. However, in order to avoid the problem *ab initio*, an operator expansion on the light-cone can be used to describe heavy-light transitions, as explained in the next Section.

Concerning $b \rightarrow c$ transitions, B decays to charmed states ($B \rightarrow D^{(*)}, D^{**}$) were investigated in early papers^{85,119} for finite c and b quark masses. Since that time, the common attention has shifted towards approaches incorporating the heavy quark flavor and spin symmetry, with the development of appropriate sum rules in HQET (see Sect. 3.9). Our opinion is that three-point sum rules for $b \rightarrow c$ transitions and finite quark masses represent a viable approach complementary to HQET, which allows one to control the accuracy of the heavy quark limit.¹²⁰ Actually, in the finite-mass sum rules the important contributions of hard-gluon exchanges in the diagram in Fig. 8a are not yet available.

^lRecent results for the exclusive $B \rightarrow K^*\gamma$ transitions are: $\mathcal{B}(B^0 \rightarrow K^{*0}\gamma) = (4.55_{-0.68}^{+0.7} \pm 0.34) \cdot 10^{-5}$ and $\mathcal{B}(B^+ \rightarrow K^{*+}\gamma) = (3.76_{-0.83}^{+0.89} \pm 0.28) \cdot 10^{-5}$.¹¹⁵ For the inclusive decay, the most recent measurements give: $\mathcal{B}(b \rightarrow s\gamma) = (3.15 \pm 0.35 \pm 0.36 \pm 0.26) \cdot 10^{-4}$,¹¹⁶ and $\mathcal{B}(b \rightarrow s\gamma) = (3.11 \pm 0.35 \pm 0.80 \pm 0.72) \cdot 10^{-4}$.¹¹⁷

With the current progress of methods for computing many-loop diagrams, it should become possible to calculate these two-loop three-point diagrams with different quark masses.

3.7 Hadron structure functions

A standard application of QCD to the hadronic structure functions is to study their logarithmic dependence on the momentum transfer Q^2 using the perturbative evolution equations. The initial conditions for these equations are usually parametrized and fitted to the experimental data at some intermediate value of Q^2 . A direct analytical calculation of structure functions remains a challenging task. It is therefore very important that QCD sum rules are in a position to solve this problem, albeit approximately and within a limited range of the Bjorken variable. The method was suggested by Ioffe¹²¹ and was originally applied to the nucleon structure functions, to obtain, in particular, the valence u and d quark-parton distributions in the nucleon at intermediate Q^2 . The idea is to consider the four-point correlator

$$T_{\mu\nu}^{\pm} = -i \int d^4x d^4y d^4z e^{iq \cdot x} e^{ip \cdot (z-y)} \langle 0 | T \{ J^N(y) j_{\mu}^{\mp}(x) j_{\nu}^{\pm}(0) \bar{J}^N(z) \} | 0 \rangle, \quad (104)$$

$j_{\mu}^{-} = \bar{d}\gamma_{\mu}(1 - \gamma_5)u$ and $j_{\mu}^{+} = \bar{u}\gamma_{\mu}(1 - \gamma_5)d$ being the weak quark currents, and J^N the nucleon interpolating current (84). Inserting complete sets of

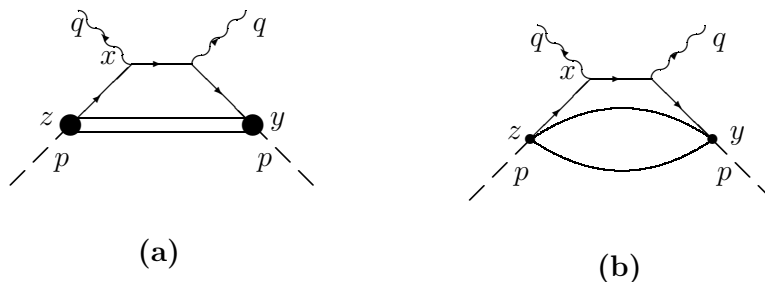


Figure 9: Four-point correlator in Eq. (104) (a) and its perturbative part (b).

states with the nucleon quantum numbers and picking up the ground state, one encounters the forward scattering amplitude:

$$T_{\mu\nu}^N = -i \int d^4x e^{iq \cdot x} \langle N | T \{ j_{\mu}^{\mp}(x) j_{\nu}^{\pm}(0) \} | N \rangle, \quad (105)$$

which is directly related to the nucleon structure function $F_2(x_{Bj}, Q^2)$ measured in deep inelastic neutrino-nucleon scattering. The key observation¹²¹ is that the imaginary part of the correlator (104)

$$\text{Im } T_{\mu\nu} = \frac{1}{2i} [T_{\mu\nu}(p^2, q^2, s + i\epsilon) - T_{\mu\nu}(p^2, q^2, s - i\epsilon)] \quad (106)$$

($s = (p+q)^2$) can be expanded at short distances in the range of large Euclidean momenta p and q : $Q^2 = -q^2 \simeq 10 \text{ GeV}^2$ and $|p^2| \simeq 1 \text{ GeV}^2 \ll Q^2$. For example, considering the lowest order perturbative diagram in Fig. 9b and taking the imaginary part of this diagram in s , one notices that the quark virtualities in the t channel are of the order of $p^2 x_{Bj}$, with $x_{Bj} = Q^2/2p \cdot q$ being the Bjorken variable. Therefore, the quarks are far off-shell if x_{Bj} is not too small.

The OPE for the correlation function (104) is obtained¹²² in a standard way in terms of perturbative and condensate contributions. In this calculation one retains only the leading powers in the ratio $|p^2|/Q^2$ accounting for the leading twist in the structure functions (parton distributions). The dispersion relation is taken in one variable p^2 , which is the virtuality of the baryon current. One then performs a Borel transformation in p^2 and separates the contribution of the lowest-lying nucleon state from the contributions of the other poles and of the continuum. This is a rather sensitive point of the procedure, because, even after the Borel transformation, there is still a contamination of the ground-state term by "parasitic" contributions in the dispersion relation.^m The range of the Bjorken variable, which is accessible to the method, does not include small $x_{Bj} \simeq 0$, where OPE breaks down. The region $x_{Bj} \simeq 1$ is also out of the reach of this method, simply because it is the resonance region in the s channel.

With all such caveats, the valence quark distributions in the nucleon have been computed: $u_v(x_{Bj})$ in the region $0.2 < x_{Bj} < 0.7$ and $d_v(x_{Bj})$ in the region $0.3 < x_{Bj} < 0.5$.¹²² The accuracy of the calculation is at the level of 50%; within this accuracy the result is in agreement with the parton distributions extracted from experimental data. The mere fact that an analytical expression containing quark and gluon condensates reproduces rather subtle dynamical features of the nucleon is impressive and promising.

Estimates of the polarized structure functions $g_1(x_{Bj})$ and $g_2(x_{Bj})$ obtained by the same method¹²⁴ can be presented as average values in the (rather

^mRecently, in calculating the valence quark distribution in the pion, this problem was solved¹²³ by considering a more complicated kinematical configuration of the 4-point correlator, with two different virtualities of interpolating currents. In this case double dispersion relations and double Borel transformation are applicable, eliminating all "parasitic" terms and improving the accuracy of the sum rule.

narrow) accessible ranges of the variable x_{Bj} .⁷

$$\overline{g_1(x_{Bj})}(0.5 < x_{Bj} < 0.7) = 0.05 \pm 50\% \quad (107)$$

$$\overline{g_2(x_{Bj})}(0.5 < x_{Bj} < 0.8) = -0.05 \pm 50\%. \quad (108)$$

These estimates are in a reasonable agreement with the data in the same intervals of the Bjorken variable:

$$\overline{g_1(x_{Bj})}(0.5 < x_{Bj} < 0.7) = 0.08 \pm 0.02,^{125} \quad (109)$$

$$\overline{g_1(x_{Bj})}(0.4 < x_{Bj} < 0.7) = 0.08 \pm 0.02 \pm 0.01,^{126} \quad (110)$$

and

$$\overline{g_2(x_{Bj})}(0.5 < x_{Bj} < 0.8) = -0.037 \pm 0.020 \pm 0.003\%,^{127} \quad (111)$$

Having an approximate but reliable method to calculate the structure functions at intermediate x_{Bj} , it is interesting to apply it to a structure function which is completely unknown and not even directly measurable in deep inelastic scattering. This is the case of the chirality-violating structure function $h_1(x_{Bj})$ which characterizes the transverse spin dynamics in the nucleon.¹²⁸ The dominant, u -quark contribution to the proton structure function h_1 has been estimated¹²⁹ employing an appropriate four-point correlator. The prediction, in the region $0.3 < x_{Bj} < 0.5$, is:

$$\overline{h_1(x_{Bj})}(0.3 < x_{Bj} < 0.5) = 0.5 \pm 50\%. \quad (112)$$

The photon structure function $F_{2\gamma}(x_{Bj}, Q^2)$ can also be obtained¹³⁰ starting from the correlator of four electromagnetic currents with two different virtualities q^2 and p^2 . The imaginary part of this correlator, which determines the structure function of the photon with a virtuality p^2 , is calculated in a form of a condensate expansion, and in the approximation of small p^2/Q^2 . In order to obtain the structure function of the real photon, a dispersion relation in p^2 is used, expressing the virtual photon structure function in terms of the integral over hadronic states and employing the quark-hadron duality. The analyticity of the dispersion relation in p^2 permits the extrapolation to $p^2 = 0$. This method allows one to separate the hard and soft (hadronic) parts in the photon structure function. The hard part corresponds to the pointlike quark-photon interaction, whereas the soft (hadronic) part receives contributions from the interactions of the photon with quark-antiquark states at large distances. The duality threshold s_0^p serves as an effective boundary of this separation. The result for the structure function $F_{2\gamma}(x_{Bj}, Q^2)$, predicted in the

range $0.2 < x_{Bj} < 0.7$ and at $Q^2 \sim$ a few GeV^2 ¹³⁰ agrees with the experimental data. This agreement is impressive, because all inputs in this calculation are fixed by two-point sum rules. Furthermore, in this approach it is possible to calculate the twist 4 corrections to $F_{2\gamma}(x_{Bj}, Q^2)$,¹³¹ and to find the gluon distribution in the photon.¹³²

The four-point correlator with two heavy-light quark currents $j_5 = \bar{Q}\gamma_5 q$ and two electromagnetic heavy quark currents $j_\mu = \bar{Q}\gamma_\mu Q$ ($Q = c$ or b) interpolates a deep inelastic scattering on a heavy meson (D or B). The advantage in this case is that the correlator has a well-defined forward scattering limit, since the $\bar{Q}Q$ states in the t channel are far from $t = 0$. Calculating this correlator in terms of the perturbative part plus condensate expansion and performing the double Borel transformation, it is possible to calculate a few first moments of the heavy quark parton distribution in D, B mesons,¹³³ obtaining, in a certain approximation, also the fragmentation functions of heavy quarks into heavy mesons. The calculation was done for finite quark masses, it would be interesting to repeat it in HQET.

Finally, as a new direction in studying the structure functions, which is, however, out of the scope of our main presentation, one should mention the analysis of parton distributions in terms of a coordinate-space variable called the Ioffe time. These distributions have been obtained for proton and photon, employing the four-point correlation functions and sum rule technique.¹³⁴

3.8 Matrix elements of effective operators

The description of neutral meson oscillations involves a set of important hadronic parameters. The first one is $B_K(\mu)$, defined by the matrix element

$$\langle \bar{K}^0 | (\bar{s}\gamma^\mu(1 - \gamma_5)d)(\bar{s}\gamma_\mu(1 - \gamma_5)d) | K^0 \rangle = 2(1 + \frac{1}{N_c})(f_K m_K)^2 B_K(\mu) \quad (113)$$

and representing the deviation of the $K^0 - \bar{K}^0$ mixing amplitude from the vacuum saturation approximation. A similar definition holds for $B_{d,s}$, and the matrix elements analogous to (113) are expressed in terms of $B_{B_{d,s}}(\mu)$. The leading dependence on the renormalization scale μ is:

$$B_K(\mu) = \hat{B}_K(\alpha_s(\mu))^{\frac{2}{9}} \quad , \quad B_{B_{d,s}}(\mu) = \hat{B}_{B_{d,s}}(\alpha_s(\mu))^{\frac{6}{23}} \quad , \quad (114)$$

\hat{B}_i being renormalization invariant quantities.

There are two different methods to determine \hat{B}_K . The first one is based on the analysis of the two-point correlator of the $\Delta S = 2$ four-quark operator $O_{\Delta S=2} = (\bar{s}\gamma^\mu(1 - \gamma_5)d)(\bar{s}\gamma_\mu(1 - \gamma_5)d)$, with the hadronic spectral function

receiving a contribution from the KK intermediate state. The second method consists in the calculation of the three-point function of $O_{\Delta S=2}$ and of the interpolating currents for K^0 and \bar{K}^0 . The determination of \hat{B}_K from the two-point sum rule yields $\hat{B}_K = 0.55 \pm 0.09$,¹³⁵ while three-point sum rules give $\hat{B}_K = 0.4 - 0.9$.¹³⁶

Similar two- and three-point sum rules involving the relevant operator $O_{\Delta B=2} = (\bar{b}\gamma^\mu(1 - \gamma_5)d)(\bar{b}\gamma^\mu(1 - \gamma_5)d)$ are employed to obtain the parameter \hat{B}_{B_d} . The results are compatible with the vacuum saturation approximation, namely $\hat{B}_{B_d} = 1.00 \pm 0.15$.¹³⁷ All these calculations suffer from the uncertainties related to the neglect of nonfactorizable α_s corrections. Notice that an accurate knowledge of the ratio $r = f_{B_d}^2 \hat{B}_{B_d} / f_{B_s}^2 \hat{B}_{B_s}$ is nowadays indispensable for the analysis of the CKM unitarity triangle using information on B_d and B_s oscillations. In this ratio, several uncertainties (from b -quark mass, radiative corrections, thresholds, etc.) should cancel out. Therefore, a direct extraction of the parameter r from the ratios of sum rules deserves to be worked out.

3.9 QCD sum rules in HQET

QCD sum rules are frequently applied in the framework of the Heavy Quark Effective Theory (HQET). One considers the correlation functions of quark currents, where the heavy quarks are represented by their effective fields $h_v(x)$, v being the heavy quark four-velocity.ⁿ An example is the calculation of the parameter \hat{F} related to the B meson leptonic decay constant f_B by the equation:

$$f_B = \hat{C}(m_b) \hat{F} \left[1 - \frac{A}{m_b} + \mathcal{O}\left(\frac{1}{m_b^2}\right) \right], \quad (115)$$

where the coefficient $\hat{C}(m_b)$ can be computed in perturbation theory. To determine \hat{F} , the SVZ method can be applied to the two-point correlation function:

$$\Pi(\omega) = i \int d^4x e^{ik \cdot x} \langle 0 | T \{ j_M^\dagger(x) j_M(0) \} | 0 \rangle \quad (116)$$

where $\omega = 2v \cdot k$ and $j_M(x) = \bar{h}_v(x) i \gamma_5 q(x)$ is the interpolating current of the pseudoscalar heavy-light mesons in HQET. Due to the heavy quark spin symmetry, \hat{F} can also be computed from the two-point correlation function of the vector currents $j_V(x) = \bar{h}_v(x) (\gamma_\mu - v_\mu) q(x)$ interpolating heavy-light 1^- mesons. The procedure starts from writing down a dispersion relation for

ⁿA more detailed discussion of HQET with the relation of the effective fields $h_v(x)$ to the heavy quark fields $Q(x)$ can be found in the chapter by De Fazio in this book.

(116) in the variable ω :

$$\Pi(\omega) = \frac{\hat{F}^2}{2\bar{\Lambda} - \omega} + \int_{s_h}^{\infty} d\nu \frac{\rho^h(\nu)}{\nu - \omega} + \text{subtractions}, \quad (117)$$

isolating the ground state contribution from the integral over the excited states and the continuum. The parameter $\bar{\Lambda} = m_B - m_b$ represents the binding energy of the light degrees of freedom in the heavy meson. The dispersion relation (117) is then matched with the QCD expression, obtained for negative ω in terms of a perturbative term and condensate contributions:

$$\Pi(\omega) = \Pi_{pert}(\omega) + \sum_d C_d \frac{\langle O_d \rangle}{(-\omega)^d} . \quad (118)$$

Finally, the Borel transformation is performed and, invoking quark-hadron duality, the contribution of higher states and of the continuum are approximated by the perturbative contribution above the threshold s_h .

Another example is the calculation of the Isgur-Wise function $\xi(y)$. At the leading order in the $1/m_{b,c}$ expansion, this function parametrizes the semileptonic $B \rightarrow D^{(*)}$ matrix elements. The form factor ξ can be obtained from the sum rule for the three-point correlation function:^{74,138,139}

$$\Xi(\omega, \omega', y) = i \int d^4x d^4x' \exp^{i(k \cdot x - k' \cdot x')} \langle 0 | T \{ j_{M'}^\dagger(x) J_\mu(0) j_M(x') \} | 0 \rangle, \quad (119)$$

$y = v \cdot v'$ being the product of the initial and final meson four-velocities and $J_\mu = \bar{h}_{v'} \gamma_\mu h_v$. Similar analyses can be applied to the form factors $\tau_{1/2}(y)$, $\tau_{3/2}(y)$, etc, of B transitions to orbitally excited charm mesons.

There are several advantages in applying QCD sum rules in HQET. For example, the relatively simple form of the Feynman rules in the effective theory allows to compute two-loop radiative corrections, not only for two-point correlators, such as (116), but also for three-point ones similar to (119).^{139,140,141} As we mentioned in Sec.3.6, such corrections are not yet available for finite quark masses in the three-point functions. Furthermore, a systematic renormalization group improvement in the current correlators can be performed; this is important, for example, in determining the choice of the scale of α_s corrections in the calculation of the HQET parameters.

Let us briefly mention a few numerical results obtained in this framework. For the parameters \hat{F} and A defined in Eq. (115) the sum rule predictions^{73,74,142–144} are, typically,

$$\hat{F} = 0.40 \pm 0.06 \text{ GeV}^{\frac{3}{2}}, \quad A = 0.9 \pm 0.2 \text{ GeV}. \quad (120)$$

The parameter $\bar{\Lambda} = 570 \pm 70 \text{ MeV}$ ¹⁴⁴ is consistent with the determination of m_b from the bottomonium system.^o The analogous quantities $\bar{\Lambda}^+$ and $\bar{\Lambda}'$ have been computed for the $0^+, 1^+$ and $1^+, 2^+$ heavy-light doublets, respectively, with the results $\bar{\Lambda}^+ \simeq \bar{\Lambda}' = 0.9 - 1.0 \text{ GeV}$.¹⁴⁵ Combining this result with the calculation of $\bar{\Lambda}$ one can infer a prediction of the mass of P-wave $\bar{q}Q$ states which is consistent with the experimental data.

The mass splitting between the lowest-lying 1^- and 0^- states is related to the chromomagnetic interaction parameter λ_2 ; the result^{74,146,147} $m_{(1-)}^2 - m_{(0-)}^2 = 0.46 \pm 0.14 \text{ GeV}^2$ fits well to the experimental measurement.

More involved is the determination of the HQET parameter λ_1 , related to the kinetic energy of the b -quark in the B meson, where the results still have a large uncertainty.^{146,147} The role of nondiagonal contributions (i.e. matrix elements between different radial excitations) to the double dispersion relation has to be better understood.¹⁴⁸

The Isgur-Wise form factors $\xi(y)$ and $\tau_{\frac{1}{2}}(y)$ have been computed at the next-to leading order in α_s ,^{140,141} the functions $\tau_{\frac{3}{2}}(y)$ and $\tau_{\frac{5}{2}}(y)$ are known at the leading order in the strong coupling constant,¹⁴⁵ together with the form factors of subleading terms in the inverse heavy quark mass expansion.^{139,149}

The analysis has been extended to baryons containing one heavy quark, with the determination of the binding energy $\bar{\Lambda}_{\Lambda_b}$, the kinetic energy of the heavy quark in the heavy baryon and four-quark matrix elements on the Λ_b ,¹⁵⁰ the Isgur-Wise form factor governing the semileptonic $\Lambda_b \rightarrow \Lambda_c$ transition,¹⁵¹ and the matrix elements of decays such as $\Lambda_b \rightarrow p\ell\nu$ and $\Lambda_b \rightarrow \Lambda\ell^+\ell^-$.¹⁵²

It would be interesting to enlarge the field of applications of HQET sum rules by analyzing also four-point correlators with heavy-light currents in order to determine the heavy and light quark distributions in the heavy hadrons.

4 Light-Cone Sum Rules

4.1 The basics of the method

The method of light-cone sum rules (LCSR)^{153–155} is a fruitful hybrid of the SVZ technique and the theory of hard exclusive processes.^{156–158} The basic idea is to expand the products of currents near the light-cone. This procedure involves a partial resummation of local operators and avoids certain irregularities of the truncated OPE in the three-point sum rules. In recent years, the LCSR approach proved very useful in calculating various hadronic transition

^oFor a more detailed discussion of the definition of $\bar{\Lambda}$ and its relation to the b quark mass see the chapter by Uraltsev in this book.

form factors. Within this approach, one is able to take into account both hard scattering and soft (end-point)¹⁵⁹ contributions.

While SVZ sum rules employ vacuum-to-vacuum correlation functions, the starting object of LCSR is different. One considers a correlation function which is a T-product of two quark currents sandwiched between vacuum and an on-shell state.¹⁶⁰ The latter can be a light-quark hadron (pion, kaon, ρ , K^* , nucleon) or a photon. A physical example is provided by the process $e^+e^- \rightarrow \pi^0 e^+e^-$. The hadronic part of this reaction is a fusion of two virtual photons into a single π^0 via quark e.m. currents. The corresponding amplitude, shown schematically in Fig. 10a, has the structure of a typical LCSR correlation function:

$$\begin{aligned} F_{\mu\nu}(p, q) &= i \int d^4x e^{-iq \cdot x} \langle \pi^0(p) | T \{ j_\mu^{em}(x) j_\nu^{em}(0) \} | 0 \rangle \\ &= \epsilon_{\mu\nu\alpha\beta} p^\alpha q^\beta F(Q^2, (p-q)^2), \end{aligned} \quad (121)$$

where p is the pion momentum, q and $(p-q)$ are the photon momenta, $Q^2 = -q^2$, j_μ^{em} is the quark electromagnetic current (91) and F is the invariant amplitude encoding the dynamics of the process. The chiral limit is adopted and $p^2 = m_\pi^2 = 0$.

To derive the LCSR, one has to calculate the correlation function (121) in QCD, in the region of large Q^2 and $|(p-q)^2|$ and to use dispersion relation to match the result of this calculation with hadronic matrix elements. Let us explain this procedure in more detail. Using unitarity in the channel of the current j_ν^{em} with the momentum $p-q$, i.e., inserting the complete set of hadronic states, one derives a dispersion relation for (121) in the variable $(p-q)^2$ keeping the second variable Q^2 fixed:

$$\begin{aligned} F_{\mu\nu}(p, q) &= 2 \frac{\langle \pi^0(p) | j_\mu^{em} | \rho^0(p-q) \rangle \langle \rho^0(p-q) | j_\nu^{em} | 0 \rangle}{m_\rho^2 - (p-q)^2} \\ &+ \frac{1}{\pi} \int_{s_0^h}^{\infty} ds \frac{Im F_{\mu\nu}(Q^2, s)}{s - (p-q)^2}. \end{aligned} \quad (122)$$

In the above, the ground-state contribution of the ρ meson contains the hadronic matrix element determining the $\gamma^* \rho \rightarrow \pi$ transition form factor multiplied by the ρ meson decay constant: $\langle \rho^0(p-q) | j_\nu^{em} | 0 \rangle = (f_\rho/\sqrt{2}) m_\rho \epsilon_\nu^{(\rho)*}$. The dispersion integral includes the contributions of excited and continuum states at $s > s_0^h$. The coefficient 2 takes into account the contribution of ω meson which is approximately equal to that of ρ . Calculating the amplitude $F_{\mu\nu}$ in QCD,

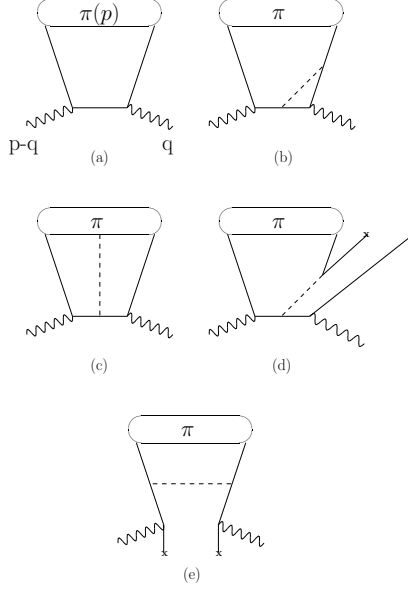


Figure 10: Light-cone expansion of the correlation function (121).

one then applies the standard SVZ technique: the Borel transformation in the variable $(p - q)^2$ and quark-hadron duality. The resulting sum rule allows to obtain the $\gamma^* \rho \rightarrow \pi$ form factor and to determine its dependence on the momentum transfer Q^2 .

The correlation function (121) can be calculated by expanding the T product of quark currents near the light-cone $x^2 = 0$. This expansion is different from the local OPE used before and, as we shall see below, incorporates summation of infinite series of local operators.

Before proceeding with the light-cone expansion, we first have to convince ourselves that at sufficiently large $Q^2 = -q^2$ and $|(p - q)^2|$ the dominant part of the integrand in the correlation function (121) stems from the region near the light-cone $x^2 = 0$. Importantly, the pion momentum p does not need to vanish. Hence, the invariant variable $\nu = q \cdot p = (q^2 - (p - q)^2)/2$ can also be large:

$$|\nu| \sim |(p - q)^2| \sim Q^2 \gg \Lambda_{CD}^2. \quad (123)$$

It is convenient to define the ratio ξ

$$\xi = 2\nu/Q^2, \quad (124)$$

so that the region (123) corresponds to finite values of this ratio, $\xi \sim 1$. Consider a reference frame where the pion three-momentum \vec{p} is finite but small as compared to the photon virtualities: $|\vec{p}| \sim \mu$, $|p_0| \sim \mu$ and $\mu^2 \ll Q^2, \nu$. In this frame, $q_0 \sim Q^2\xi/(4\mu) + O(\mu)$ and the argument $q \cdot x$ of the exponential function in Eq. (121) can be approximated as:

$$q \cdot x = q_0 x_0 - q_3 x_3 \simeq \frac{Q^2\xi}{4\mu} x_0 - \left(\sqrt{\frac{Q^4\xi^2}{16\mu^2} + Q^2} \right) x_3 \simeq \frac{Q^2\xi}{4\mu} (x_0 - x_3) - \frac{2\mu}{\xi} x_3.$$

In order to avoid strong oscillations of the integrand, one has to demand $x_0 - x_3 \sim 4\mu/(Q^2\xi)$, and simultaneously $x_3 \sim \xi/(2\mu)$. These two conditions yield

$$x_0^2 \simeq (x_3 + 4\mu/Q^2\xi)^2 \simeq x_3^2 + 4/Q^2 + O(\mu^2/Q^4),$$

and, hence, $x^2 \sim 1/Q^2 \rightarrow 0$ in the region (123). At the same time, there is no short-distance dominance, because $x_0 \sim x_3 \sim \xi/(2\mu) \gg 1/\sqrt{Q^2}$, indicating that an expansion in local operators around $x = 0$ is not applicable^p

To proceed, let us calculate the leading-order contribution to the light-cone OPE of the correlator (121) corresponding to the diagram in Fig. 10a. For simplicity we consider only the u -quark part of the currents without the electromagnetic charge factor. Contracting the u quark fields in (121), using the propagator of the free massless quark

$$iS_0(x, 0) = \langle 0 | T\{u(x)\bar{u}(0)\} | 0 \rangle = \frac{i \not{x}}{2\pi^2 x^4}, \quad (125)$$

and transforming $\gamma_\mu \gamma_\alpha \gamma_\nu \rightarrow -i\epsilon_{\mu\alpha\nu\rho} \gamma^\rho \gamma_5 + \dots$, we obtain

$$F_{\mu\nu}(p, q) = -i\epsilon_{\mu\nu\alpha\rho} \int d^4x \frac{x^\alpha}{\pi^2 x^4} e^{-iq \cdot x} \langle \pi^0(p) | \bar{u}(x) \gamma^\rho \gamma_5 u(0) | 0 \rangle. \quad (126)$$

To investigate the structure of the nonlocal quark-antiquark operator in Eq. (126), let us expand it in local operators around $x = 0$:

$$\bar{u}(x) \gamma_\rho \gamma_5 u(0) = \sum_r \frac{1}{r!} \bar{u}(0) (\overleftarrow{D} \cdot x)^r \gamma_\rho \gamma_5 u(0). \quad (127)$$

^p One may still use the local OPE for the soft pion, $p = 0$ ($\xi = 0$). In this case, (121) reduces to a one-variable amplitude similar to (2) and the short-distance dominance follows from the arguments presented in Section 2.1.

The matrix elements of these operators have the following general decomposition:

$$\begin{aligned} \langle \pi^0(p) | \bar{u} \overleftarrow{D}_{\alpha_1} \overleftarrow{D}_{\alpha_2} \dots \overleftarrow{D}_{\alpha_r} \gamma_\rho \gamma_5 u | 0 \rangle = & (-i)^r p_{\alpha_1} p_{\alpha_2} \dots p_{\alpha_r} p_\rho M_r \\ & + (-i)^r g_{\alpha_1 \alpha_2} p_{\alpha_3} \dots p_{\alpha_r} p_\rho M'_r + \dots \end{aligned} \quad (128)$$

In the above, the first term is totally symmetric and traceless (at $p^2 = 0$) and contains only 4-vectors. There are other terms containing one or more $g_{\alpha_i \alpha_k}$, one of them displayed explicitly. Substituting the decomposition (127) in (126), integrating over x and using the definitions (128) and (124) one obtains

$$F(Q^2, (p-q)^2) = \frac{1}{Q^2} \sum_{r=0}^{\infty} \xi^r M_r + \frac{4}{Q^4} \sum_{r=2}^{\infty} \frac{\xi^{r-2}}{r(r-1)} M'_r + \dots \quad (129)$$

Since the variable $\xi \sim 1$ in a generic exclusive kinematics with $p \neq 0$, all terms should be kept in each series in this expression. We have explicitly confirmed the qualitative conclusion made above: the expansion of F in local operators cannot be truncated at any finite order. One has to take into account and to sum up an infinite series of matrix elements M_r , M'_r, \dots of local operators. On the other hand, there is a distinct hierarchy on the r.h.s. of (129). The second term containing M'_r and further similar terms are suppressed by powers of a small parameter $1/Q^2$ as compared with the first term containing M_r . A closer investigation reveals that the difference between the local operators entering the first and the second term in (129) is in their *twist*. Twist is defined as the difference between the dimension and the spin of a traceless and totally symmetric local operator. The lowest twist of the operators entering (128) is equal to two, simply because the operator without derivatives has dimension 3 and Lorentz spin 1. Furthermore, after taking the matrix elements, the twist 2 components of the operators contribute only to the first, symmetric and traceless term of Eq. (128), containing M_r . After multiplying both parts of Eq. (128) by $g_{\alpha_1 \alpha_2}$ it becomes clear that the matrix elements M'_r receive their contributions from the twist 4 operators, the lowest-dimension operator being $\bar{u}(\overleftarrow{D})^2 \gamma_\rho \gamma_5 u$. We conclude that one has to treat the nonlocal operator in Eq. (126) by expanding it near the light-cone $x^2 = 0$ in components corresponding to different twists.

In the leading order of this expansion, at $x^2 = 0$ (and $p^2 = 0$), the matrix element in Eq. (126) has the following parametrization:

$$\langle \pi^0(p) | \bar{u}(x) \gamma_\mu \gamma_5 u(0) | 0 \rangle_{x^2=0} = -i p_\mu \frac{f_\pi}{\sqrt{2}} \int_0^1 du e^{iup \cdot x} \varphi_\pi(u, \mu), \quad (130)$$

where the function $\varphi_\pi(u, \mu)$ is the pion *light-cone distribution amplitude* of twist 2, normalized to unity: $\int_0^1 \varphi_\pi(u, \mu) du = 1$.⁹ The normalization scale μ emerges due to the logarithmic dependence on x^2 and reflects the light-cone separation between the quark and antiquark fields in the operator. At $x = 0$, Eq. (130) is simply reduced to the matrix element (65) defining the pion decay constant. Furthermore, expanding both sides of Eq. (130) and comparing the l.h.s. with the expansions (127) and (128) we find that the moments of $\varphi_\pi(u)$ are related to the matrix elements of local twist-2 operators:

$$M_r = -i \frac{f_\pi}{\sqrt{2}} \int_0^1 du u^r \varphi_\pi(u, \mu). \quad (131)$$

The function $\varphi_\pi(u)$, multiplied by f_π , is a universal nonperturbative object encoding the long-distance dynamics of the pion. Together with the corresponding higher-twist distribution amplitudes, $\varphi_\pi(u)$ plays a similar role as the vacuum condensates play in SVZ sum rules.

Substituting the definition (130) in Eq. (126), integrating over x , restoring the electromagnetic charge factor and adding the d -quark part we obtain the correlation function in the twist 2 approximation:

$$F^{(tw2)}(Q^2, (p-q)^2) = \frac{\sqrt{2}f_\pi}{3} \int_0^1 \frac{du \varphi_\pi(u, \mu)}{\bar{u}Q^2 - u(p-q)^2}, \quad (132)$$

where $\bar{u} = 1 - u$. Note that this representation has the form of a convolution

$$F^{(tw2)}(Q^2, (p-q)^2) = \frac{\sqrt{2}f_\pi}{3} \int_0^1 du \varphi_\pi(u, \mu) T(Q^2, (p-q)^2, u, \mu) \quad (133)$$

of the hard scattering amplitude T with the distribution amplitude φ_π . The scale μ plays the role of the factorization scale which separates the contributions at $x^2 < 1/\mu^2$ entering the hard scattering amplitude from the long-distance effects at $x^2 > 1/\mu^2$ parametrized by the distribution amplitude. At zeroth order in α_s , the hard amplitude

$$T^{(0)}(Q^2, (p-q)^2, u) = \frac{1}{\bar{u}Q^2 - u(p-q)^2} \quad (134)$$

⁹ The complete definition includes the path-ordered factor necessary for gauge invariance: $Pexp\{ig_s \int_0^1 d\alpha x_\mu A^{a\mu}(\alpha x) \lambda^a / 2\}$, which is unity in the light-cone gauge, $x_\mu A^{a\mu} = 0$ employed here.

is μ -independent.

At this point one has to emphasize that the definition (130) is actually almost ten years older than the method of LCSR. It was introduced^{156–158} in perturbative QCD studies of exclusive processes with large momentum transfer. In this approach, $\varphi_\pi(u)$ describes the distribution in the fraction of the longitudinal pion momentum carried by a valence quark in the infinite-momentum frame. The convolution (133) determining the asymptotic limit of the hard exclusive $\gamma^*\gamma^* \rightarrow \pi^0$ amplitude has also been obtained at that time.¹⁵⁶ The $O(\alpha_s)$ correction to T has been calculated¹⁶¹ from the diagrams similar to the one shown in Fig. 10b.

We are now in a position to obtain a sum rule from the dispersion relation (122) matching it with the result of the light-cone expansion. Defining the matrix element

$$\langle \pi^0(p) | j_\mu^{em} | \rho^0(p-q) \rangle = F^{\rho\pi}(Q^2) m_\rho^{-1} \epsilon_{\mu\nu\alpha\beta} \epsilon^{(\rho)\nu} q^\alpha p^\beta, \quad (135)$$

in terms of the transition form factor $F^{\rho\pi}(Q^2)$, we obtain, to leading twist 2 accuracy:

$$\frac{\sqrt{2}f_\rho F^{\rho\pi}(Q^2)}{m_\rho^2 - (p-q)^2} + \int_{s_0^h}^{\infty} ds \frac{\frac{1}{\pi} \text{Im} F(Q^2, s)}{s - (p-q)^2} = \frac{\sqrt{2}f_\pi}{3} \int_0^1 \frac{du \varphi_\pi(u)}{\bar{u}Q^2 - u(p-q)^2}. \quad (136)$$

Furthermore, representing Eq. (132) in a form of the dispersion integral

$$F^{(tw2)}(Q^2, (p-q)^2) = \frac{1}{\pi} \int_0^{\infty} ds \frac{\text{Im} F^{(tw2)}(Q^2, s)}{s - (p-q)^2} \quad (137)$$

with

$$\frac{1}{\pi} \text{Im} F^{(tw2)}(Q^2, s) = \frac{\sqrt{2}f_\pi}{3} \int_0^1 du \varphi_\pi(u) \delta(\bar{u}Q^2 - us), \quad (138)$$

we obtain the duality approximation for the contribution of excited and continuum states:

$$\int_{s_0^h}^{\infty} ds \frac{\frac{1}{\pi} \text{Im} F(Q^2, s)}{s - (p-q)^2} = \int_{s_0^\rho}^{\infty} ds \frac{\frac{1}{\pi} \text{Im} F^{(tw2)}(Q^2, s)}{s - (p-q)^2} = \frac{\sqrt{2}f_\pi}{3} \int_0^{u_0^\rho} \frac{du \varphi_\pi(u)}{\bar{u}Q^2 - u(p-q)^2}, \quad (139)$$

where $u_0^\rho = Q^2/(s_0^\rho + Q^2)$. The duality threshold parameter s_0^ρ can be taken from the SVZ sum rule (60). Using Eq. (139), one can simply subtract the

integral on the l.h.s. of Eq. (136) from the r.h.s. Performing the Borel transformation, we finally obtain the LCSR for the form factor of the $\gamma^* \rho \rightarrow \pi$ transition.¹⁶²

$$F^{\rho\pi}(Q^2) = \frac{f_\pi}{3f_\rho} \int_{u_0^\rho}^1 \frac{du}{u} \varphi_\pi(u, \mu) \exp\left(-\frac{\bar{u}Q^2}{uM^2} + \frac{m_\rho^2}{M^2}\right). \quad (140)$$

The light-cone distribution amplitude φ_π , which is the necessary input for this sum rule, will be discussed below.

To improve the accuracy of Eq. (140), one has to include into the sum rule not only $O(\alpha_s)$ perturbative QCD corrections to the hard amplitude, but also higher twist effects. Physically, the latter take into account both the transverse momentum of the quark-antiquark state and the contributions of higher Fock states in the pion wave function. There are several sources of higher twist corrections in the light-cone expansion. First, one encounters the twist 4 contributions expanding the matrix element (130) at $x^2 = 0$ beyond the leading order:

$$\begin{aligned} \langle \pi(p) | \bar{u}(x) \gamma_\mu \gamma_5 u(0) | 0 \rangle &= -ip_\mu f_\pi \int_0^1 du e^{iup \cdot x} (\varphi_\pi(u) + x^2 g_1(u)) \\ &\quad + f_\pi \left(x_\mu - \frac{x^2 p_\mu}{p \cdot x} \right) \int_0^1 du e^{iup \cdot x} g_2(u), \end{aligned} \quad (141)$$

where $g_{1,2}(u)$ are the light-cone distribution amplitudes of twist 4. Furthermore, the expansion of the quark propagator near the light-cone yields the matrix elements of the quark-antiquark-gluon operators corresponding to three-particle distribution amplitudes (diagram in Fig. 10c). There are also four-quark contributions stemming from the propagator expansion, some of them shown in Fig. 10d. These effects, together with other four-quark diagrams (Fig. 10e) give rise (in the twist 6 approximation) to contributions which can be factorized into a product of the quark condensate and a two-particle distribution amplitude. This effect can be potentially important at intermediate Q^2 and has to be investigated case by case. Nonfactorizable four-quark contributions and all other higher twist terms suppressed by high powers of Q^2 can safely be neglected.^r

Replacing the currents j_μ^{em} in the correlation function (121) by quark currents with different spin-parity and flavor, one is able to interpolate other hadronic transitions involving the pion. This replacement will only change the

^rNote that twist 3 contributions to the correlation function (121) are proportional to m_π^2 and vanish in the chiral limit.

hard scattering amplitude. One and the same set of distribution amplitudes will enter the light-cone expansion of the new correlation function. The idea of combining perturbatively calculable, process-dependent coefficients with a universal long-distance input works here in complete analogy with SVZ sum rules.

4.2 Light-cone distribution amplitudes

As we have seen in the case of $\varphi_\pi(u)$, distribution amplitudes are defined through the vacuum-hadron matrix elements of nonlocal operators composed of a certain number of quark and gluon fields taken at light-like separations. These operators emerge in the light-cone OPE of the T-product of currents. The relevant technique including the quark propagator expansion near the light-cone and the extraction of various twist components is quite general.^{163,164} It shares many common features with the technique used nowadays to study forward and nonforward deep-inelastic amplitudes. The distribution amplitude can be expanded employing the conformal symmetry of massless QCD. The conformal spin (partial wave) decomposition allows to represent each distribution amplitude as a sum of certain orthogonal polynomials in the variable u . The coefficients of these polynomials are multiplicatively renormalizable, and have growing anomalous dimensions, so that, at sufficiently large normalization scale μ , only the first few terms in this expansion are relevant. The part of the distribution amplitude, which does not receive logarithmic renormalization is called *asymptotic*. The discussion of many important aspects of this analysis and of several interesting results obtained in recent years, is beyond the scope of this review, and we refer the reader to the literature.^{165,166} Here, we only present the most important conformal expansion of the leading twist 2 distribution amplitude:

$$\varphi_\pi(u, \mu) = 6u\bar{u} \left[1 + \sum_{n=2,4,\dots} a_n(\mu) C_n^{3/2}(u - \bar{u}) \right], \quad (142)$$

where $C_n^{3/2}$ are the Gegenbauer polynomials (for a derivation, see, e.g., Ref. 167). The coefficients a_n are multiplicatively renormalizable:

$$a_n(\mu) = a_n(\mu_0) \left(\frac{\alpha_s(\mu)}{\alpha_s(\mu_0)} \right)^{\gamma_n/\beta_0}, \quad (143)$$

and

$$\gamma_n = C_F \left[-3 - \frac{2}{(n+1)(n+2)} + 4 \left(\sum_{k=1}^{n+1} \frac{1}{k} \right) \right] \quad (144)$$

are the anomalous dimensions.¹⁶⁷ At $\mu \rightarrow \infty$, $a_n(\mu)$ vanish, and the limit $a_n = 0$ corresponds to the asymptotic distribution amplitude

$$\varphi_\pi^{(as)}(u) = 6u\bar{u} . \quad (145)$$

The values of the nonasymptotic coefficients a_n at a certain intermediate scale μ_0 can be estimated from two-point sum rules¹⁶⁷ for the moments $\int u^n \varphi_\pi(u, \mu) du$ at low n . This method is attractive because it employs nonperturbative information encoded in quark and gluon condensates. However, in practice the two-point sum rule determination of a_n is not very accurate. One can also determine or, at least, restrict the nonasymptotic coefficients from the light-cone sum rules for measured hadronic quantities. Some examples will be discussed below. Regarding other methods, lattice QCD has an almost unexplored potential to calculate distribution amplitudes.¹⁶⁸ Furthermore, φ_π was evaluated in the instanton vacuum model, at a low normalization scale.¹⁶⁹ Interestingly, this calculation has produced a distribution close to the asymptotic one.

Twist 3 and 4 distribution amplitudes for the pion have also been worked out.^{165,170} Use of the QCD equations of motion^{165,171} yields rigorous relations between three- and two-body distribution amplitudes of the same twist, considerably reducing the number of independent parameters.

To apply LCSR to hadronic matrix elements involving other pseudoscalar mesons (K, η), one has to assess the SU(3)-violation effects in the light-cone expansion. There are several sources of such effects. The virtual s -quark propagator creates twist 3 contributions proportional to m_K^2 , which differ from the analogous $O(m_\pi^2)$ effects in the case of u, d quarks; the ratio of nonperturbative parameters f_K/f_π is larger than unity by about 20 %; finally, the asymmetry between strange and nonstrange quark momentum distributions in the kaon has to be taken into account by introducing nonzero odd coefficients a_1, a_3, \dots in the Gegenbauer expansion (142) for $\varphi_K(u)$.

The light-cone analysis for the vector mesons (ρ, ω, K^*, ϕ) has been worked out, including the update of the twist 2,¹⁷² and a detailed study of twist 3 and 4 distribution amplitudes,¹⁶⁶ taking into account the finite meson-mass effects. The distribution amplitudes for other than pseudoscalar and vector mesons still need to be determined. It is already possible to apply LCSR to hadronic matrix elements involving nucleons, since the nucleon higher twist distribution amplitudes have been classified and studied.¹⁷³ Finally, studies of the two-pion light-cone distribution amplitudes¹⁷⁴ extend the field of applications of the LCSR method to the exclusive processes with two pions.¹⁷⁵

To complete our survey, let us mention the photon light-cone distribution amplitudes. They are important for many applications of LCSR to exclusive

processes, where the photon is emitted at large distances. The photon distribution amplitudes were used, e.g., in the early study of the weak radiative transition $\Sigma \rightarrow p\gamma$.¹⁵³ In particular, the leading twist-2 distribution amplitude of the photon has the following definition:

$$\langle \gamma | \bar{u}(x) \sigma_{\alpha\beta} u(0) | 0 \rangle = e_u \langle \bar{u}u \rangle \int_0^1 du \varphi_\gamma(u) F_{\alpha\beta}(uq, x), \quad (146)$$

where $F_{\alpha\beta}(q, x) = (\epsilon_\beta q_\alpha - \epsilon_\alpha q_\beta) e^{iq \cdot x}$ is the photon field strength tensor, and the asymptotic distribution amplitude is $\varphi_\gamma(u) = 6\chi u(1-u)$. The nonperturbative parameter $\chi \simeq -4 \text{ GeV}^2$ (at $\mu = 1 \text{ GeV}$) normalizing this distribution in units of the quark condensate density, can be determined from two-point sum rules with experimentally known hadronic parts. The update of this parameter and of higher twist photon distribution amplitudes is desirable.

4.3 LCSR for the pion form factor

An example of the application of LCSR is the calculation of the pion electromagnetic form factor defined in Eq. (90). The original sum rule¹⁷⁶ was recently improved¹⁷⁷ by calculating the $O(\alpha_s)$ perturbative contribution of twist 2 and the factorizable twist 6 corrections. The starting object is the vacuum-pion correlation function similar to (121), but containing a pion interpolating current $j_\nu^{(\pi)}$ instead of j_ν^{em} . The resulting LCSR, at zeroth order in α_s and in the twist 2 approximation, reads:¹⁷⁶

$$F_\pi(Q^2) = \int_{u_0^\pi}^1 du \varphi_\pi(u, \mu_u) \exp\left(-\frac{\bar{u}Q^2}{uM^2}\right) \xrightarrow{Q^2 \rightarrow \infty} \frac{\varphi'_\pi(0, M^2)}{Q^4} \int_0^{s_0^\pi} ds s e^{-s/M^2}, \quad (147)$$

where $\varphi'_\pi(0) = -\varphi'_\pi(1)$, and $u_0^\pi = Q^2/(s_0^\pi + Q^2)$, s_0^π is the duality threshold in the pion channel, taken from Eq. (67). The factorization scale $\mu_u^2 = \bar{u}Q^2 + uM^2$ corresponds to the average quark virtuality in the correlation function. This sum rule has a regular behavior at large Q^2 : the $1/Q^4$ dependence of Eq. (147) at $Q^2 \rightarrow \infty$ corresponds to the soft end-point mechanism, provided that the integration region shrinks to the point $u = 1$.

At $O(\alpha_s)$, one recovers the leading $\sim 1/Q^2$ asymptotic behavior corresponding to the hard scattering mechanism. Including this contribution in the LCSR and retaining the first two terms of the sum rule expansion in powers

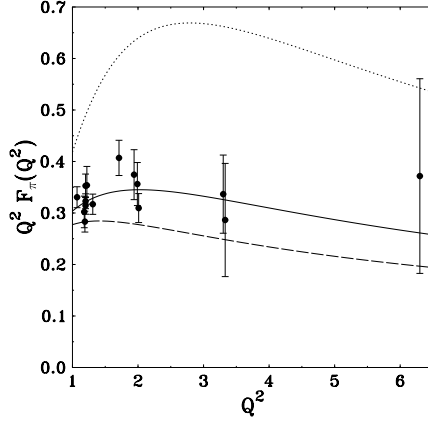


Figure 11: The light-cone sum rule predictions for the pion electromagnetic form factor using asymptotic (dashed), CZ (dotted) distribution amplitude and the fit to the data (solid). Q^2 is in GeV^2 .

of $1/Q^2$ one obtains:¹⁷⁷

$$F_\pi(Q^2) = \frac{2\alpha_s}{3\pi Q^2} \int_0^{s_0} ds e^{-s/M^2} \int_0^1 du \frac{\varphi_\pi(u)}{\bar{u}} + \varphi'_\pi(0) \int_0^{s_0} \frac{ds s e^{-s/M^2}}{Q^4} + O\left(\frac{\alpha_s}{Q^4}\right). \quad (148)$$

The $O(1/Q^2)$ term in (148) coincides with the well known expression for the asymptotics of the pion form factor:^{156–158}

$$F_\pi(Q^2) = \frac{8\pi\alpha_s f_\pi^2}{9Q^2} \left| \int_0^1 du \frac{\varphi_\pi(u)}{\bar{u}} \right|^2, \quad (149)$$

obtained by the convolution of two twist-2 distribution amplitudes $\varphi_\pi(u)$ of the initial and final pion with the $O(\alpha_s)$ quark hard-scattering kernel. This coincidence can be easily traced provided that the SVZ sum rule (67) for f_π yields in the leading order $\int_0^{s_0} ds e^{-s/M^2} = 4\pi^2 f_\pi^2$, and that $\int_0^1 du \varphi_\pi^{\text{as}}(u)/\bar{u} = 3$.

In addition to the twist 4 terms,¹⁷⁶ the factorizable twist 6 contributions determined by the quark condensate density, have been calculated and turned out to be small.¹⁷⁷ Adding twist 4,6 terms to the twist 2 (leading and $O(\alpha_s)$) parts yields the LCSR prediction for $F_\pi(Q^2)$ shown in Fig. 11¹⁷⁷ for the

pion distribution amplitude (142) with two choices: $a_2 = 0$ (asymptotic) and $a_2(1 \text{ GeV}) = 2/3$ (the CZ distribution¹⁶⁷). For the twist 4 distribution amplitude, their asymptotic expressions are taken, which provides a sufficient accuracy. The fit of the LCSR to the experimental data¹⁷⁸ (with only $a_2 \neq 0$) yields

$$a_2(1 \text{ GeV}) = 0.12 \pm 0.07^{+0.05}_{-0.07}, \quad (150)$$

where the first (second) uncertainty is experimental (theoretical). Within errors, this determination is compatible with the asymptotic distribution amplitude.

Similar to the pion elastic form factor F_π , the LCSR for other transition form factors involving the pion have been obtained, including $\gamma^* \rho \rightarrow \pi$ (chosen as a study case in Sec. 4.1),¹⁶² and $\gamma^* \pi \rightarrow a_1$.¹⁷⁹ Transition form factors of the pion to other light mesons are still unexplored within the LCSR method.

Finally, LCSR contributed to the study of the $\gamma^* \gamma \rightarrow \pi$ transition. The corresponding form factor is simply equal to the amplitude Eq. (121) at zero virtuality of one of the photons: $F^{\gamma\pi}(Q^2) \equiv F(Q^2, 0)$. Since the real photon is a long-distance object, the form factor $F^{\gamma\pi}(Q^2)$ contains nonperturbative contributions which are beyond the light-cone expansion of two electromagnetic quark currents. The leading $1/Q^2$ asymptotics of $F^{\gamma\pi}(Q^2)$ is well known¹⁵⁶ and given by Eq. (132) at $(p - q)^2 \rightarrow 0$. The calculation of the contributions suppressed by powers of $1/Q^2$ is a nontrivial task, at least when using three-point QCD sum rules and short-distance OPE.¹⁸⁰ Within LCSR approach, one possibility not yet exploited is to employ the photon distribution amplitudes. Another way to estimate the $\gamma^* \gamma \rightarrow \pi$ form factor is to use the hadronic dispersion relation (136) where the resonance term is determined by the LCSR (140) and the integral over higher states is estimated using duality.¹⁶² One can analytically continue this relation to $(p - q)^2 \rightarrow 0$ provided that it does not contain subtraction terms. The result shown in Fig. 12¹⁶² again has a better agreement with the experimental data^{181,182} in the case of the asymptotic pion distribution amplitude. The $O(\alpha_s)$ correction^{161,183} decreases the leading order (twist 2,4) result by 15-20% leaving some room for nonasymptotic coefficients. The fit to the data yields $a_2 = 0.12 \pm 0.03$ at $\mu = 2.4 \text{ GeV}$ (if all other coefficients are neglected).¹⁸³

Summarizing, the LCSR studies indicate that the twist 2 distribution amplitude of the pion is close to its asymptotic shape, already at intermediate scales. More precise data on various form factors involving pion are needed to increase the accuracy of this determination.

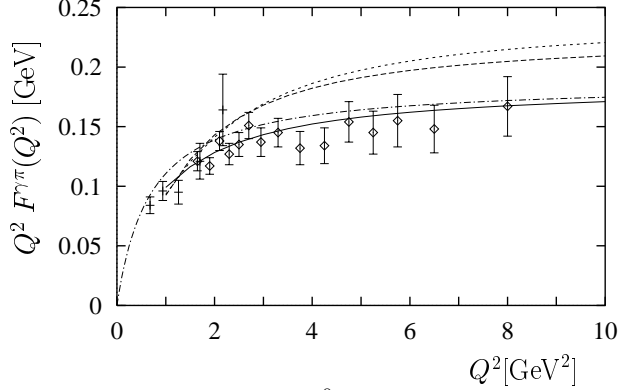


Figure 12: Form factor of the $\gamma^*\gamma \rightarrow \pi^0$ transition calculated with the asymptotic (solid), CZ ($a_2(\mu_0) = 2/3$; long dashed) and BF($a_2(\mu_0) = 2/3$, $a_4(\mu_0) = 0.4$; short-dashed) distribution amplitude of the pion (where $\mu_0 = 0.5$ GeV) in comparison with the experimental data points. The dash-dotted line corresponds to the Brodsky-Lepage interpolation formula.

4.4 Strong Couplings

The correlation function (121) can also be used to calculate the strong $\rho\omega\pi$ coupling, defined by the hadronic matrix element

$$\langle \pi^0(p)\omega(-q) | \rho^0(p-q) \rangle = \epsilon^{\mu\nu\alpha\beta} \epsilon_\mu^{(\omega)} \epsilon_\nu^{(\rho)} p_\alpha q_\beta g_{\omega\rho\pi}. \quad (151)$$

The idea is to employ the analyticity of the amplitude $F(q^2, (p-q)^2)$ in two independent invariant variables q^2 and $(p-q)^2$, the squares of momenta flowing through the two channels of electromagnetic currents. Inserting in these channels the complete sets of hadronic states with the quantum numbers of ω and ρ , one obtains a double dispersion relation:

$$F_{\mu\nu}(p, q) = \frac{\langle \pi^0(p)\omega(-q) | \rho^0(p-q) \rangle \langle 0 | j_\mu^{em} | \omega(-q) \rangle \langle \rho^0(p-q) | j_\nu^{em} | 0 \rangle}{(m_\omega^2 - q^2)(m_\rho^2 - (p-q)^2)} + \{\omega \leftrightarrow \rho\} \\ + \int_{R_{12}} ds_1 ds_2 \frac{\rho_{\mu\nu}^h(s_1, s_2)}{(s_2 - q^2)(s_1 - (p-q)^2)} + \dots, \quad (152)$$

where $\rho_{\mu\nu}^h$ is the double spectral density of the excited and continuum states and R_{12} is the region occupied by these states in the (s_1, s_2) -plane. Eq. (152) is very similar to the double dispersion relation (93) used in Sec. 3 for the three-point correlation function. The terms arising from subtractions are denoted by ellipses. The ground-state resonance contribution includes two (approximately equal) combinations of ρ and ω . Substituting the definition (151) in the above

relation and expressing the matrix elements of the electromagnetic currents through the decay constants $f_{\rho,\omega}$ yields the dispersion relation for the invariant amplitude:

$$F(q^2, (p-q)^2) = \frac{f_\rho f_\omega g_{\omega\rho\pi}}{(m_\omega^2 - q^2)(m_\rho^2 - (p-q)^2)} + \dots \quad (153)$$

To obtain the sum rule, one has to match Eq. (153) to the light-cone expansion (132), in the region of large $|q^2|$ and $|(p-q)^2|$. The double dispersion integral over continuum and excited states can be replaced by its dual counterpart, obtained by integrating the double imaginary part of $F(q^2, (p-q)^2)$ over a certain region in the (s_1, s_2) -plane. The lower boundary is $s_{1,2} = 0$ and the upper boundary is characterized by a single threshold parameter s_0^ρ (again assuming that $s_0^\omega \simeq s_0^\rho$). The shape of this region is not very important because the double imaginary part of the amplitude $Im_{s_1} Im_{s_2} F(s_1, s_2)$ obtained from (132) is concentrated on the diagonal $s_1 = s_2$. A detailed discussion of this procedure is available in the literature.^{184,185}

Furthermore, one applies the Borel transformations with respect to the variables q^2 and $(p-q)^2$, introducing two independent Borel parameters M_1 and M_2 , respectively. The following formula is useful for this derivation:

$$\mathcal{B}_{M_1^2} \mathcal{B}_{M_2^2} \frac{(l-1)!}{(-\bar{u}q^2 - u(p-q)^2)^l} = (M^2)^{2-l} \delta(u - u_0), \quad (154)$$

where $M^2 = M_1^2 M_2^2 / (M_1^2 + M_2^2)$ and $u_0 = M_1^2 / (M_1^2 + M_2^2)$. It is natural to take $M_1^2 = M_2^2 = 2M^2$, i.e. $u_0 = 1/2$, having in mind almost equal mass scales in the ρ and ω channels. After Borel transformation, all subtraction terms vanish and the sum rule converts into a simple relation:

$$g_{\omega\rho\pi} = \frac{\sqrt{2}f_\pi}{f_\rho^2 m_\rho^2} e^{m_\rho^2/M^2} M^2 (1 - e^{-s_0^\rho/M^2}) \varphi_\pi(1/2) + O(\alpha_s) + \text{higher twists}, \quad (155)$$

where we used $f_\omega \simeq f_\rho/3$, and the subtracted exponent is the result of the quark-hadron duality approximation. The twist 4,6 terms not shown explicitly have also been calculated,¹⁵⁴ whereas the $O(\alpha_s)$ correction is not yet available. The interesting point is that the sum rule for the strong coupling is determined by the value of the light-cone distribution amplitude at the middle point $u = 1/2$. This value is particularly sensitive to the nonasymptotic coefficients a_{2n} . Therefore, the sum rule (155) together with analogous relations for other measured strong couplings (like the LCSR for the πNN coupling¹⁵⁴) is useful for constraining the nonasymptotic parts of distribution amplitude. For

the asymptotic φ_π the numerical result $g_{\omega\rho\pi} = 12.5 \pm 2 \text{ GeV}^{-1}$ obtained from Eq. (155) agrees with the experimental value $g_{\omega\rho\pi} = 14 \pm 2 \text{ GeV}^{-1}$.²⁴

The method of external fields, briefly mentioned in Sec. 3.5, also allows to calculate $g_{\omega\rho\pi}$.¹⁸⁶ In fact, this method corresponds to the soft pion limit of the light-cone expansion.¹⁸⁴ In this limit one can apply a short-distance expansion in terms of local operators with increasing dimensions. From that one may argue that sum rules in the external field can still be used for determinations of the strong couplings if the pion is soft, say, $p_\pi \sim 100 \text{ MeV}$. On the other hand, the external field technique is not applicable in cases when the pion has a relatively large momentum, like, e.g., in the $\rho \rightarrow \pi\pi$ decay, whereas LCSR work for any pion momentum. Moreover, in the one-variable dispersion relation used in the external field approach, the contributions containing transitions between the ground and excited states remain unsuppressed after Borel transformation, thus, reducing the accuracy of the sum rule.

4.5 Heavy-to-light form factors and couplings

During the last years, LCSR have been extensively used to predict the form factors of various transitions of heavy (B, D) to light (π, K, ρ, K^*, \dots) hadrons. Reviews describing these studies are available.^{185,187} Here we only briefly outline the main points, and present some recent results.

Let us consider, as an example, the calculation of the form factor $f_{B\pi}^+(q^2)$ (the definition is similar to Eq. (98)). The underlying correlation function in this case is

$$\begin{aligned} F_\mu(p, q) &= i \int dx e^{iq \cdot x} \langle \pi(p) | T \{ \bar{u}(x) \gamma_\mu b(x), m_b \bar{b}(0) i \gamma_5 d(0) \} | 0 \rangle \\ &= F(q^2, (p+q)^2) p_\mu + \tilde{F}(q^2, (p+q)^2) q_\mu, \end{aligned} \quad (156)$$

where the weak current $\bar{u} \gamma_\mu b$ is combined with the current $\bar{b} i \gamma_5 d$ interpolating the B meson. The leading order in α_s corresponds to the diagram in Fig. 10a with the virtual b quark. In the twist 2 approximation, one obtains, for the relevant invariant amplitude,

$$F(q^2, (p+q)^2) = m_b f_\pi \int_0^1 \frac{du \varphi_\pi(u, \mu_b)}{m_b^2 - \bar{u}q^2 - u(p+q)^2}. \quad (157)$$

Comparison of this expression with the result (132) for the correlator of the light-quark currents nicely demonstrates the universality of the method: both expressions are determined by one and the same distribution amplitude φ_π . The hard scattering amplitudes are different, the one in Eq. (157) being generated by the heavy quark propagator. Also the factorization scale of φ_π in

Eq. (157) should be adjusted to the characteristic virtualities of the heavy quark.

The LCSR is obtained by matching the light-cone expansion of F with the dispersion relation in the B channel. The result reads:^{155,188}

$$f_{B\pi}^+(q^2) = \frac{1}{2m_B^2 f_B} e^{m_B^2/M^2} m_b^2 f_\pi \int_{u_0^B}^1 \frac{du}{u} \exp\left(-\frac{m_b^2 - q^2(1-u)}{uM^2}\right) \varphi_\pi(u, \mu_b) + O(\alpha_s) + \text{higher twists}, \quad (158)$$

where $u_0^B = (m_b^2 - q^2)/(s_0^B - q^2)$, s_0^B being the duality-threshold parameter in the B channel. This sum rule is valid at q^2 , sufficiently lower than m_b^2 , in order to stay far away from the hadronic states in the channel of the weak current. In contrast to the case of the LCSR for the pion form factor, the twist 3 contributions, not shown explicitly in Eq. (158), are important.

Importantly, LCSR (158) has a regular behavior in the $m_b \rightarrow \infty$ limit. If one employs the scaling relations for mass parameters and decay constants: $m_B = m_b + \bar{\Lambda}$, $s_0^B = m_b^2 + 2m_b\omega_0$, $M^2 = 2m_b\tau$, $f_B = \hat{f}_B/\sqrt{m_B}$, where $\bar{\Lambda}$, ω_0 , τ and \hat{f}_B are independent of m_b , the LCSR can be expanded in the heavy mass. The higher-twist corrections either scale with the same power of m_b as the leading-twist term, or they are suppressed by extra powers of m_b . Furthermore, the asymptotic scaling behavior sharply differs at small and large momentum transfers: at $q^2 = 0$ one has $f^+(0) \sim m_b^{-3/2}$,¹⁵⁵ and at $p^2 = m_b^2 - 2m_b\chi$, where χ does not scale with m_b , $f^+(p^2) \sim m_b^{1/2}$.¹⁸⁹ Hence, the large p^2 behavior is consistent with the asymptotic dependence predicted in HQET for the region of small pion momentum.¹⁹⁰ Another important feature is that, similar to case of the pion form factor, the heavy-to-light form factors calculated from LCSR receive contributions from both soft and hard mechanisms of the exclusive transition.¹⁹¹

At the current accuracy, Eq. (158) includes the $O(\alpha_s)$ correction to the twist 2 term^{192,193} and all twist 3 and 4 quark-antiquark and quark-antiquark-gluon contributions.^{188,184} Concerning the numerical analysis of this LCSR, one has to mention that the sensitivity of $f^+(q^2)$ to m_b is considerably reduced if f_B and s_0^B are taken from the two-point sum rule considered in Sec. 3.3. There is also a spectacular cancelation between $O(\alpha_s)$ corrections to these two sum rules. Furthermore, the sensitivity to the light-cone distribution amplitudes is also not high because in the sum rule (158) these normalized distributions are convoluted with relatively smooth coefficient functions over a wide region of u starting from ~ 0.5 to 1. In particular, the result obtained from the sum rule (158) is less sensitive to the values of nonasymptotic coefficients in

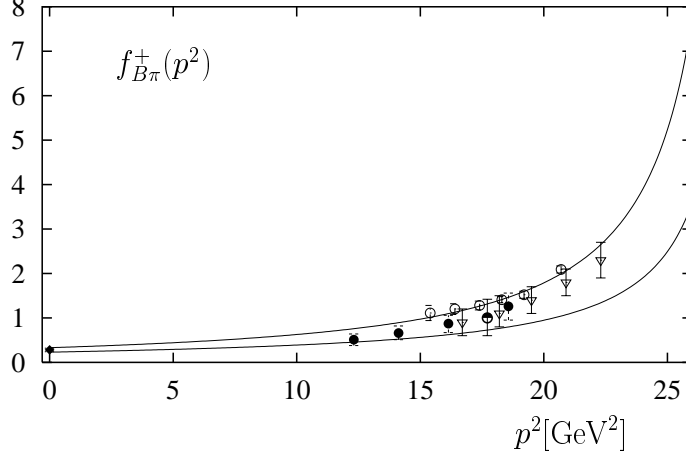


Figure 13: The LCSR predictions for the $B \rightarrow \pi$ transition form factor in comparison to lattice results. The solid curves indicate the size of the LCSR uncertainties.

the distribution amplitude φ_π , than the LCSR result for the pion form factor. A typical overall uncertainty of heavy-to light form factors obtained by this method amounts to 15-20 %, if one employs constraints on nonasymptotic coefficients $a_{2,4,\dots}$ provided by the comparison of the LCSR for the pion form factors (F_π , $F^{\gamma\pi}$) and for the strong couplings with experimental data. To somewhat reduce this uncertainty, one needs better determination of these coefficients. It is also important to calculate the $O(\alpha_s)$ correction to the twist 3 contribution in Eq. (158).

The same correlation function (156) can be used to estimate the $B^*B\pi$ coupling, defined as $\langle \bar{B}^{*0}(q)\pi^-(p) | B^-(p+q) \rangle = -g_{B^*B\pi}(p \cdot \epsilon^{(B^*)})$, from the double dispersion relation in B and B^* channels, as explained in Sec. 4.4. The corresponding LCSR reads:¹⁸⁴

$$f_{B^*}g_{B^*B\pi} = \frac{1}{m_B^2 m_{B^*} f_B f_{B^*}} e^{\frac{m_B^2 + m_{B^*}^2}{2M^2}} m_b^2 f_\pi M^2 \left(e^{-\frac{m_b^2}{M^2}} - e^{-\frac{s_0^B}{M^2}} \right) \varphi_\pi(1/2, \mu_b) + O(\alpha_s) + \text{higher twists}. \quad (159)$$

Here again the NLO accuracy in twist 2 has recently been achieved.⁷⁷ In Fig. 13⁷⁸ the form factor $f_{B\pi}^+(q^2)$, obtained using Eqs. (158) and (159), is displayed in comparison with the recent lattice results (see references in the original paper⁷⁸). Other applications of LCSR include the $B \rightarrow K$,^{188,194}

$B \rightarrow \rho, K^*, \phi$ form factors of weak and FCNC transitions.^{118,195,196} Fig. 14¹⁹⁶ shows, for example, the recent predictions on the form factors of $B \rightarrow K^*$ transition. It is easy to convert the sum rules for B mesons to the corresponding sum rules for D mesons by replacing b with c , and $B^{(*)}$ with $D^{(*)}$ in Eqs. (158) and (159). The $D \rightarrow \pi, K$ form factors (the latter being quite sensitive to the SU(3)-flavor violation) calculated within this method^{104,184,78} are in a good agreement with the experiment and with the lattice QCD. In

\hat{g}	$g_{D^*D\pi}$	$g_{B^*B\pi}$	method	Ref.
0.22 ± 0.06	10.5 ± 3.0	22 ± 7	LCSR (NLO)	KRWY99 ⁷⁷
0.39 ± 0.16	9 ± 1 11 ± 2	32 ± 6 20 ± 4 28 ± 6	SP (LO) ” ‘ ”	O89 ¹⁹⁷ CNDDFG95 ¹⁹⁸ BBKR ¹⁸⁴
$0.27^{+0.04+0.05}_{-0.02-0.02}$			χ PT+data	S98 ¹⁹⁹
$0.42 \pm 0.04 \pm 0.08$			lattice QCD	UKQCD98 ²⁰⁰

Table 8: Strong $B^*B\pi$ and $D^*D\pi$ couplings from LCSR and from the sum rules in the soft pion limit (SP) compared with some recent results of other methods. The scale-independent coupling is defined as $\hat{g} = f_\pi g_{H^*H\pi}/2m_H$, $H = B, D$.

Table 8 the sum rule predictions for the strong couplings $g_{D^*D\pi}$ and $g_{B^*B\pi}$ are compared with the result obtained on the lattice, and with the recent prediction of χ PT constrained by experimental data. A compilation of results of many other approaches is also available.¹⁸⁴ LCSR have been applied to obtain the strong couplings $g_{D^*D\rho}$ and $g_{B^*B\rho}$,²⁰¹ as well as the matrix elements for the radiative transitions between heavy mesons ($B^* \rightarrow B\gamma$)²⁰² and heavy baryons.²⁰³ The strong couplings of negative and positive parity heavy mesons and pions have also been determined, both in the heavy quark mass limit and for finite c and b quark masses, with predictions on the widths of 0^+ , 1^+ and 2^+ charmed and beauty mesons.^{204,205} LCSR with photon distribution amplitudes have been employed to estimate the long-distance contributions to $B \rightarrow \rho\gamma$ weak radiative decays.²⁰⁶

Finally, it is important to mention the use of QCD sum rules for the analysis of exclusive nonleptonic decays of heavy mesons. Nowadays, these decays

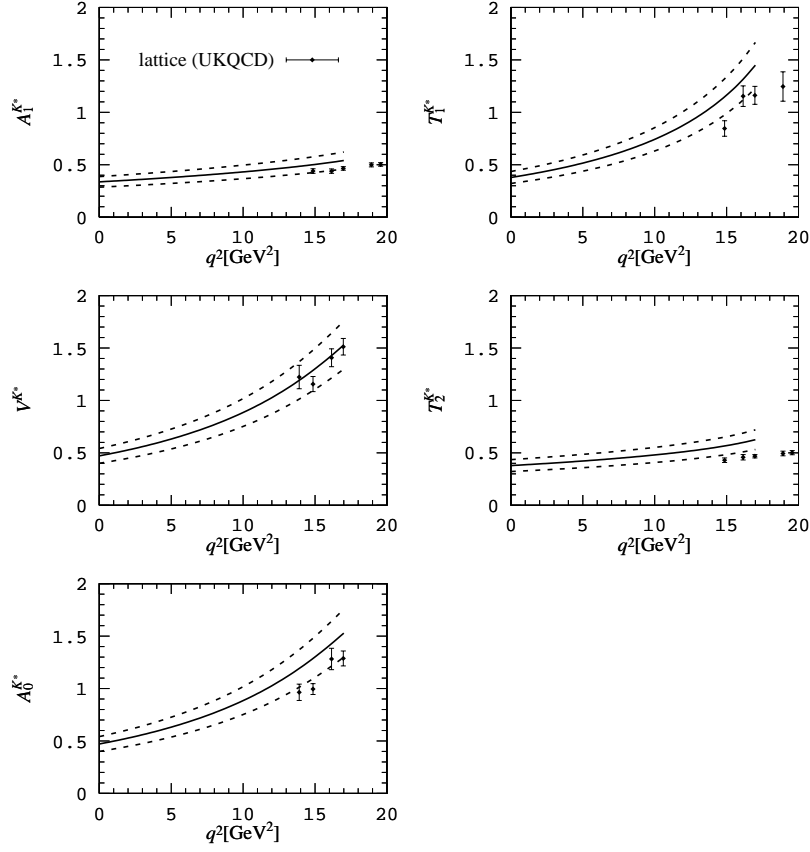


Figure 14: LCSR predictions for the $B \rightarrow K^*$ transition form factors. The dashed lines indicate theoretical uncertainties, the points represent lattice QCD results.

attract a lot of attention, being one of the main objects for studying the mechanism of CP-violation. The form factors and decay constants calculated from LCSR and SVZ sum rules can immediately be used for estimates of the non-leptonic decay amplitudes in the factorization approximation, in particular, for assessing the violation of the $SU(3)$ -flavor (or U -spin) symmetry in various B -decays. More subtle effects, such as violation of factorization, annihilation and penguins can, in principle, also be treated within the sum rule framework. First attempts to analyze nonfactorizable effects in B and D decays and related long distance effects in $B \rightarrow K^* \gamma$ decays employed short-distance OPE.^{185,207,208} The LCSR have only been partially used in order to obtain the form factors of effective operators emerging in the short-distance expansion of correlation functions.²⁰⁹ It would be extremely interesting to continue these studies trying to create a framework where the light-cone OPE is consistently employed at all stages of calculation.

5 Summary

In this review we have tried to present a concise and updated picture of QCD sum rules and their applications. This was not an easy task, because after more than twenty years of development, the manifold of works using this method resembles a large tree with many branches penetrating into different fields of QCD and hadron phenomenology. Some of the branches are quite distant with respect to each other, and in order to find the relevant papers one has to search not only in the hep-ph, but also in the hep-th and nucl-th electronic archives. Nevertheless, the procedure used in all these applications is essentially one and the same, formulated in the original work:¹ A) construct a correlation function, B) calculate it at some Euclidean scale using the operator product expansion and C) match it with the hadronic dispersion integral. Above, in Sec.2, we have described this procedure step by step, deriving the SVZ sum rule for the decay constant f_ρ as a study case.

The applications of QCD sum rules considered in this review cover only a part of the work done in this field. Following our particular line of discussion, we could have missed some important references. The aim of our presentation was not just to demonstrate how the problems of hadron phenomenology are treated within this method, but to help the reader to assess the current status of QCD sum rules in general. Let us try to formulate the main conclusions of our discussion:

- QCD sum rules, together with experimental data on hadronic spectral densities can successfully be used to determine quark masses and universal nonperturbative parameters, such as vacuum condensates;

- Within the sum rule framework, operating with a handful of inputs, one is able to reproduce many hadronic observables, such as decay constants, form factors and parton distributions, in a reasonable agreement with the experimental data;

- The accuracy of the method is essentially limited. Nevertheless, since the correlation functions are field-theoretic objects defined in QCD and related to hadrons via rigorous dispersion relations, the theoretical uncertainties can be traced and estimated;

- Today QCD sum rules are not limited by the “classical” SVZ approach based on two-point correlators. As we have seen, combining the sum rule technique with the light-cone expansion, it is possible to develop the LCSR method which avoids certain problems of the local condensate expansion and adequately describes QCD mechanisms of exclusive hadronic transitions.

Concerning the open problems, the major one is to reduce theoretical uncertainties in the inputs and in the procedure. Here QCD sum rules alone are not sufficient. Interaction with other nonperturbative methods is very important, e.g. lattice QCD determination of condensates or light-cone distributions. Some new experimental results of hadron physics could be very helpful. As we have seen, accurate measurements of the form factors of light hadrons will allow us to fix the nonasymptotic coefficients in the light-cone distribution amplitudes. Furthermore, a better knowledge of excited hadronic resonances with different quantum numbers could reduce systematic uncertainties introduced by the quark-hadron duality approximation. One may even suggest dedicated experimental studies. For example, semileptonic decays of charmed mesons can provide important information about the resonances in the $K\pi$ and $K\pi\pi$ system with different spin-parities.

To outline the future perspectives of the method, let us give only one important example. In order to extract fundamental parameters of the electroweak theory and to search for new physics employing the current and future data on exclusive B and D decays, accurate predictions on the heavy meson decay amplitudes are needed. Approximate QCD methods are the only tools we have at our disposal, and the analytical method of QCD sum rules has, undoubtedly, a large unexplored potential in this field.

Acknowledgments

We are grateful to M. Shifman for offering us to write this review. Numerous discussions with our colleagues, with whom we collaborated on different applications of QCD sum rules during many years, are acknowledged. We thank P. Ball and N. Paver for useful remarks on the manuscript. A.K. is grateful to

the High Energy Group at the Niels Bohr Institute for hospitality and support during the initial stage of this work.

References

1. M. A. Shifman, A. I. Vainshtein and V. I. Zakharov, *Nucl. Phys. B* **147**, 385, 448 (1979).
2. V. A. Novikov, M. A. Shifman, A. I. Vainshtein and V. I. Zakharov, *Nucl. Phys. B* **191**, 301 (1981).
3. V. A. Novikov, L. B. Okun, M. A. Shifman, A. I. Vainshtein, M. B. Voloshin and V. I. Zakharov, *Phys. Rept.* **41**, 1 (1978).
4. L. J. Reinders, H. Rubinstein and S. Yazaki, *Phys. Rept.* **127**, 1 (1985).
5. M. A. Shifman, “*Vacuum structure and QCD sum rules*”, North-Holland (1992).
6. E. V. Shuryak, *Rev. Mod. Phys.* **65**, 1 (1993).
7. B. L. Ioffe, in “*The spin structure of the nucleon*”, edited by B. Frois, V.W. Hughes, N. de Groot, World Scientific (1997), hep-ph/9511401.
8. M. Shifman, *Prog. Theor. Phys. Suppl.* **131**, 1 (1998).
9. S. Narison, “*QCD Spectral Sum Rules*”, World Scientific (1989).
10. E. de Rafael, Lectures at Les Houches Summer School, Session 68, Les Houches, France (1997), hep-ph/9802448.
11. V. A. Novikov, M. A. Shifman, A. I. Vainshtein and V. I. Zakharov, *Fortsch. Phys.* **32**, 585 (1985).
12. S. Narison and E. de Rafael, *Phys. Lett. B* **103**, 57 (1981).
13. J. Schwinger, “*Particles, sources and fields*”, Addison-Wesley (1973).
14. M.B. Voloshin, *Sov. J. Nucl. Phys.* **29** 703 (1979).
15. P. Pascual and R. Tarrach, “*QCD: Renormalization For The Practitioner*,” Springer (1984).
16. M. S. Dubovikov and A. V. Smilga, *Nucl. Phys. B* **185**, 109 (1981).
17. K. G. Chetyrkin, A. L. Kataev and F. V. Tkachev, *Phys. Lett. B* **85**, 277 (1979);
M. Dine and J. Sapirstein, *Phys. Rev. Lett.* **43**, 668 (1979);
S. G. Gorishnii, A. L. Kataev and S. A. Larin, *JETP Lett.* **53**, 127 (1991); *Phys. Lett. B* **259**, 144 (1991);
L. R. Surguladze and M. A. Samuel, *Phys. Rev. Lett.* **66**, 560 (1991).
18. S. N. Nikolaev and A. V. Radyushkin, *Phys. Lett. B* **110**, 476 (1982);
Nucl. Phys. B **213**, 285 (1983); *Phys. Lett. B* **124**, 243 (1983).
19. V. A. Novikov, M. A. Shifman, A. I. Vainshtein, M. B. Voloshin and V. I. Zakharov, *Nucl. Phys. B* **237**, 525 (1984).
20. V.M. Belyaev and B.L. Ioffe, *Sov. Phys. JETP* **56**, 493 (1982).

21. M. V. Polyakov and C. Weiss, *Phys. Rev. D* **57**, 4471 (1998).
22. A. G. Oganesian, *Phys. Atom. Nucl.* **61**, 1359 (1998).
23. B. V. Geshkenbein and M. S. Marinov, *Sov. J. Nucl. Phys.* **30**, 726 (1979).
24. D.E. Groom et al., (Particle Data Group) *Eur. Phys. J. C* **15**, 1 (2000).
25. “*The BaBar physics book: Physics at an asymmetric B factory*”, P. F. Harrison and H. R. Quinn eds., SLAC-R-0504.
26. H. Leutwyler, *Phys. Lett. B* **378**, 313 (1996).
27. K. G. Chetyrkin, *Phys. Lett. B* **390**, 309 (1997).
28. V.L. Eletsky and B.L. Ioffe, *Phys. Rev. D* **48**, 1441 (1993);
C. Adami, E.G. Drukarev and B.L. Ioffe, *Phys. Rev. D* **48**, 2304 (1993).
29. J. Bijnens, J. Prades and E. de Rafael, *Phys. Lett. B* **348**, 226 (1995).
30. F.J. Yndurain, *Nucl. Phys. B* **517**, 324 (1998).
31. C.A. Dominguez and E. de Rafael, *Ann. Phys.* **174**, 372 (1987).
32. S. Narison, *Phys. Lett. B* **216**, 191 (1989).
33. J. Prades, *Nucl. Phys. B (Proc. Suppl.)* **64**, 253 (1998).
34. B.J. Gough et al., *Phys. Rev. Lett.* **79**, 1622 (1997).
35. D. Becirevich, V. Gimenez, V. Lubicz, G. Martinelli, *Phys. Rev. D* **61**, 114507 (2000).
36. A. Ali Khan et al., hep-lat/0004010.
37. K.G. Chetyrkin, C.A. Dominguez, D. Pirjol, K. Schilcher, *Phys. Rev. D* **51**, 5090 (1995).
38. M. Jamin and M. Münz, *Z. Phys. C* **66**, 633 (1995).
39. K.G. Chetyrkin, D. Pirjol and K. Schilcher, *Phys. Lett. B* **404**, 337 (1997).
40. D. Aston et al., *Nucl. Phys. B* **296**, 493 (1988).
41. P. Colangelo, F. De Fazio, G. Nardulli and N. Paver, *Phys. Lett. B* **408**, 340 (1997).
42. M. Jamin, *Nucl. Phys. B (Proc. Suppl.)* **64**, 250 (1998).
43. Previous determinations can be found in: S. Narison, N. Paver E. de Rafael and D. Treleani, *Nucl. Phys. B* **212**, 365 (1983);
C.A. Dominguez, C. van Gend and N. Paver, *Phys. Lett. B* **253**, 241 (1991);
S.C. Generalis, *J. Phys. G* **16** L117 (1990);
S. Narison, *Phys. Lett. B* **358**, 113 (1995).
44. K. Maltman, *Phys. Lett. B* **462**, 195 (1999).
45. T. Bhattacharya, R. Gupta and K. Maltman, *Phys. Rev. D* **57**, 5455 (1998).
46. C. A. Dominguez, L. Pirovano and K. Schilcher, *Nucl. Phys. B (Proc. Suppl.)* **74**, 313, (1999).

47. K.J. Chetyrkin, J.H. Kühn and A.A. Pivovarov, *Nucl. Phys. B* **533**, 473 (1998).
48. A. Pich and J. Prades, *JHEP* **9910**:004 (1999).
49. J.G. Korner, F. Krajewski and A.A. Pivovarov, hep-ph/0003165.
50. J. Kambor and K. Maltman, hep-ph/0005156.
51. N. Eicker et al., *Phys. Lett. B* **407**, 290 (1997).
52. S. Aoki et al., *Phys. Rev. Lett.* **82**, 4392 (1999).
53. M. Göckeler et al., *Phys. Rev. D* **62**, 054504 (2000).
54. J. Garden et al., *Nucl. Phys. B* **571**, 237 (2000).
55. Other determinations of the charm quark mass can be found in: J.S. Bell and R.A. Bertlmann, *Nucl. Phys. B* **187**, 285 (1981);
S. Narison, *Phys. Lett. B* **197**, 405 (1987), **216**, 191 (1989).
56. C.A. Dominguez, G.R. Gluckman and N. Paver, *Phys. Lett. B* **333**, 184 (1994).
57. S. Narison, *Phys. Lett. B* **341**, 73 (1994).
58. K. G. Chetyrkin, J. H. Kuhn and M. Steinhauser, *Nucl. Phys. B* **505**, 40 (1997).
59. L. Giusti (APE Coll.), *Nucl. Phys. B (Proc. Suppl.)* **63**, 167 (1998).
60. A. S. Kronfeld, *Nucl. Phys. B (Proc. Suppl.)* **63**, 311 (1998).
61. K. Hornbostel (NRQCD Coll.), *Nucl. Phys. B (Proc. Suppl.)* **73**, 339 (1999).
62. Other calculations of m_b can be found in: R.A. Bertlmann, *Nucl. Phys. B* **204**, 387 (1982);
M.B. Voloshin and Yu.M. Zaitsev, *Sov. Phys. Usp.* **30**, 53 (1987).
63. S. Hashimoto, *Nucl. Phys. B (Proc. Suppl.)* **83**, 3 (2000).
64. M. Beneke, hep-ph/9911490.
65. C.A. Dominguez and N. Paver, *Phys. Lett. B* **293**, 197 (1992).
66. M.A. Voloshin, *Int. J. Mod. Phys. A* **10**, 2865, (1995).
67. M. Jamin and A. Pich, *Nucl. Phys. B Proc. Suppl.* **74**, 300 (1999).
68. K. Melnikov and A. Yelkhovsky, *Phys. Rev. D* **59**, 114009 (1999).
69. A. Hoang, *Phys. Rev. D* **59**, 014039 (1999).
70. A.A. Penin and A.A. Pivovarov, *Nucl. Phys. B* **549**, 217 (1999).
71. M. Beneke and A. Signer, *Phys. Lett. B* **471**, 233 (1999).
72. D. J. Broadhurst, *Phys. Lett. B* **101**, 423 (1981);
T.M. Aliev and V.L. Eletsky, *Sov. J. Nucl. Phys.* **38**, 936 (1983).
73. X. Ji and M. J. Musolf, *Phys. Lett. B* **257**, 409 (1991);
D. J. Broadhurst and A. G. Grozin, *Phys. Lett. B* **274**, 421 (1992);
E. Bagan, P. Ball, V.M. Braun and H.G. Dosch, *Phys. Lett. B* **278**, 457 (1992)
74. M. Neubert, *Phys. Rev. D* **45**, 2451 (1992).

75. C.A. Dominguez and N. Paver, *Phys. Lett. B* **197**, 423 (1987), (E) *B* **199**, 596 (1987).
76. C.A. Dominguez, in *Proceedings of the Third Workshop on the Tau-Charm Factory*, Marbella, Spain, Ed. J. Kirkby and R. Kirkby, Editions Frontières, p. 357 (1993).
77. A. Khodjamirian, R. Rückl, S. Weinzierl and O. Yakovlev, *Phys. Lett. B* **457**, 245 (1999).
78. A. Khodjamirian, R. Rückl, S. Weinzierl, C. W. Winhart and O. Yakovlev, to appear in *Phys. Rev. D*, hep-ph/0001297.
79. L. Lellouch et al. (UKQCD Coll.), hep-ph/9912322.
80. A. Abada et al. (APE Coll.), *Nucl. Phys. B (Proc. Suppl.)* **83**, 268 (2000).
81. K. C. Bowler et al., (UKQCD Collaboration), hep-lat/0007020.
82. P. Blasi, P. Colangelo, G. Nardulli and N. Paver, *Phys. Rev. D* **49**, 238 (1994).
83. S. Narison, *Phys. Lett. B* **322**, 247 (1994).
84. T. Huang and C.W. Luo, *Phys. Rev. D* **53**, 5042 (1996).
85. P. Colangelo, G. Nardulli, A. A. Ovchinnikov and N. Paver, *Phys. Lett. B* **269**, 201 (1991).
86. CDF Collab., F. Abe et al., *Phys. Rev. Lett.* **81**, 2432 (1998); *Phys. Rev. D* **58**, 112004 (1998).
87. S. Narison, *Phys. Lett. B* **210**, 238 (1988);
V. V. Kiselev and A. V. Tkabladze, *Sov. J. Nucl. Phys.* **50**, 1063 (1989);
T. M. Aliev and O. Yilmaz, *Nuovo Cim. A* **105**, 827 (1992);
M. Chabab, *Phys. Lett. B* **325**, 205 (1994);
S. Reinshagen and R. Rückl, CERN-TH-6879-93.
88. P. Colangelo, G. Nardulli and N. Paver, *Z. Phys. C* **57**, 43 (1993);
E. Bagan et al., *Z. Phys. C* **64**, 57 (1994);
V. V. Kiselev and A. V. Tkabladze, *Phys. Rev. D* **48**, 5208 (1993).
89. V. V. Kiselev, A. A. Likhoded and A. I. Onishchenko, *Nucl. Phys. B* **569**, 473 (2000);
V. V. Kiselev, A. E. Kovalski and A. A. Likhoded, hep-ph/0002127.
90. P. Ball et al., “*B decays at the LHC*”, hep-ph/0003238.
91. B. L. Ioffe, *Nucl. Phys. B* **188**, 317 (1981); *Z. Phys. C* **18**, 67 (1983).
92. Y. Chung, H. G. Dosch, M. Kremer and D. Shall, *Nucl. Phys. B* **197**, 55 (1982); *Z. Phys. C* **15**, 367 (1982).
93. A. A. Ovchinnikov, A. A. Pivovarov and L. R. Surguladze, *Int. J. Mod. Phys. A* **6**, 2025 (1991).
94. S. Groote, J. G. Körner and O. I. Yakovlev, *Phys. Rev. D* **55**, 3016 (1997);

- S. Groote, J. G. Körner and A. A Pivovarov, *Phys. Rev. D* **61**, 071501 (2000).
95. V. V. Kiselev and A. E. Kovalsky, hep-ph/0005019.
 96. T. D. Cohen and R. J. Furnstal, *Prog. Part. Nucl. Phys.* **35**, 221 (1995);
D. B. Leinweber, *Ann. Phys.* **254**, 328 (1997).
 97. B. L. Ioffe and A. V. Smilga, *JETP Lett.* **37**, 298 (1983); *Nucl. Phys. B* **232**, 109 (1984);
I. I. Balitsky and A. V. Yung, *Phys. Lett. B* **129**, 328 (1983).
 98. M. Oka, D. Jido and A. Hosaka, *Nucl. Phys. A* **629**, 156C (1998).
 99. H. Kim, T. Dai, S. H. Lee, M. Oka and S. H. Lee, *Nucl. Phys. A* **662**, 371 (2000);
M. C. Birse and B. Krippa, *Phys. Rev. C* **54**, 3240 (1996).
 100. B. L. Ioffe and A. V. Smilga, *Nucl. Phys. B* **216**, 373 (1983);
V. A. Nesterenko and A. V. Radyushkin, *Phys. Lett. B* **115**, 410 (1982).
 101. A. Y. Khodjamirian, *Phys. Lett. B* **90**, 460 (1980), *Sov. J. Nucl. Phys.* **39**, 614 (1984);
V. A. Beilin and A. V. Radyushkin, *Nucl. Phys. B* **260**, 61 (1985).
 102. T. M. Aliev, V. L. Eletsky and Y. I. Kogan, *Sov. J. Nucl. Phys.* **40**, 527 (1984).
 103. P. Ball, V. M. Braun, H. G. Dosch and M. Neubert, *Phys. Lett. B* **259**, 481 (1991);
 104. P. Ball, V. M. Braun and H. G. Dosch, *Phys. Rev. D* **44**, 3567 (1991).
 105. P. Ball, *Phys. Rev. D* **48**, 3190 (1993).
 106. P. Colangelo, C. A. Dominguez, G. Nardulli and N. Paver, *Phys. Lett. B* **317**, 183 (1993);
P. Ball, hep-ph/9308244.
 107. P. Colangelo, F. De Fazio, P. Santorelli and E. Scrimieri, *Phys. Rev. D* **53**, 3672 (1996); *Phys. Lett. B* **395**, 339 (1997).
 108. F. De Fazio and M. R. Pennington, *JHEP* **0007**, 051 (2000).
 109. A. P. Bakulev and A. V. Radyushkin, *Phys. Lett. B* **271**, 223 (1991).
 110. A. Ryd, in Proc. of 7th International Symposium on Heavy Flavor Physics, Santa Barbara, (1997).
 111. E. M. Aitala *et al.* [Fermilab E791 Collaboration], *Phys. Rev. Lett.* **80**, 1393 (1998).
 112. P. Colangelo, F. De Fazio and P. Santorelli, *Phys. Rev. D* **51**, 2237 (1995).
 113. T. M. Aliev and M. Savci, *Phys. Lett. B* **456**, 256 (1999).
 114. C. A. Dominguez, N. Paver and Riazuddin, *Phys. Lett. B* **214**, 459 (1988).
 115. T. E. Coan *et al.* [CLEO Collaboration], *Phys. Rev. Lett.* **84**, 5283

- (2000).
116. S. Ahmed *et al.* [CLEO Collaboration], hep-ex/9908022.
 117. R. Barate *et al.* [ALEPH Collaboration], *Phys. Lett. B* **429**, 169 (1998).
 118. P. Ball and V. M. Braun, *Phys. Rev. D* **55**, 5561 (1997).
 119. A. A. Ovchinnikov and V. A. Slobodenyuk, *Sov. J. Nucl. Phys.* **50**, 891 (1989);
V. N. Baier and A. G. Grozin, *Z. Phys. C* **47**, 669 (1990).
 120. P. Ball, *Phys. Lett. B* **281**, 133 (1992).
 121. B. L. Ioffe, *JETP Lett.* **42**, 327 (1985).
 122. V. M. Belyaev and B. L. Ioffe, *Nucl. Phys. B* **310**, 548 (1988); **313**, 647 (1989).
 123. B. L. Ioffe and A. G. Oganesian, *Eur. Phys. J. C* **13**, 485 (2000)
 124. V.M. Belyaev and B. L. Ioffe, *Int. J. Mod. Phys. A* **6** 1533 (1992).
 125. K. Abe *et al.* [E143 Collaboration], *Phys. Rev. Lett.* **74**, 346 (1995); **75**, 25 (1995).
 126. D. Adams *et al.* [Spin Muon Collaboration (SMC)], *Phys. Lett. B* **329**, 399 (1994).
 127. K. Abe *et al.* [E143 Collaboration], *Phys. Rev. Lett.* **76**, 587 (1996).
 128. R. L. Jaffe and X. Ji, *Phys. Rev. Lett.* **67**, 552 (1991).
 129. B. L. Ioffe and A. Khodjamirian, *Phys. Rev. D* **51**, 3373 (1995).
 130. A. S. Gorsky, B. L. Ioffe, A. Yu. Khodjamirian and A. Oganesian, *Z. Phys. C* **44**, 523 (1989).
 131. A. S. Gorsky, B. L. Ioffe and A. Y. Khodjamirian, *Z. Phys. C* **53**, 299 (1992).
 132. B. L. Ioffe and A. Oganesian, *Z. Phys. C* **69**, 119 (1995).
 133. G. L. Balaian, A. Y. Khodjamirian and A. G. Oganesian, *Sov. J. Nucl. Phys.* **49**, 682 (1989);
A. Y. Khodjamirian and A. G. Oganesian, *Z. Phys. C* **48**, 519 (1990).
 134. V. Braun, P. Gornicki and L. Mankiewicz, *Phys. Rev. D* **51**, 6036 (1995);
S. Hofmann, L. Mankiewicz and A. Schafer, *Z. Phys. A* **359**, 157 (1997).
 135. S. Narison, *Phys. Lett. B* **351**, 369 (1995).
 136. K. G. Chetyrkin, A. L. Kataev, A. B. Krasulin and A. A. Pivovarov, *Phys. Lett. B* **174**, 104 (1986);
R. Decker, *Nucl. Phys. B* **277**, 660 (1986);
L. J. Reinders and S. Yazaki, *Nucl. Phys. B* **288**, 789 (1987);
N. Bilic, C. A. Dominguez and B. Guberina, *Z. Phys. C* **39**, 351 (1988).
 137. S. Narison and A. A. Pivovarov, *Phys. Lett. B* **327**, 341 (1994).
L. J. Reinders and S. Yazaki, *Phys. Lett. B* **212**, 245 (1988);
A. A. Ovchinnikov and A. A. Pivovarov, *Phys. Lett. B* **207**, 333 (1988).
 138. A. V. Radyushkin, *Phys. Lett. B* **271**, 218 (1991).

139. E. Bagan, P. Ball and P. Gosdzinsky, *Phys. Lett. B* **301**, 249 (1993).
140. M. Neubert, *Phys. Rev. D* **47**, 4063 (1993).
141. P. Colangelo, F. De Fazio and N. Paver, *Phys. Rev. D* **58**, 116005 (1998).
142. V. Eletsky and E. Shuryak, *Phys. Lett. B* **276**, 191 (1992).
143. P. Ball, *Nucl. Phys. B* **421**, 593 (1994).
144. M. Neubert, *Phys. Rept.* **245**, 259 (1994).
145. P. Colangelo, G. Nardulli and N. Paver, *Phys. Lett. B* **293**, 207 (1992);
Y. Dai and M. Huang, *Phys. Rev. D* **59**, 034018 (1999);
P. Colangelo, F. De Fazio and G. Nardulli, *Phys. Lett. B* **478**, 408 (2000).
146. P. Ball and V. M. Braun, *Phys. Rev. D* **49**, 2472 (1994).
147. M. Neubert, *Phys. Lett. B* **322**, 419 (1994).
148. I. Bigi, M. Shifman and N. Uraltsev, *Ann. Rev. Nucl. Part. Sci.* **47**, 591 (1997).
149. M. Neubert, *Phys. Rev. D* **46**, 3914 (1992);
M. Neubert, Z. Ligeti and Y. Nir, *Phys. Lett. B* **301**, 101 (1993); *Phys. Rev. D* **47**, 5060 (1993);
M. Huang, C. Li and Y. Dai, *Phys. Rev. D* **61**, 054010 (2000).
150. P. Colangelo, C. A. Dominguez, G. Nardulli and N. Paver, *Phys. Rev. D* **54**, 4622 (1996);
P. Colangelo and F. De Fazio, *Phys. Lett. B* **387**, 371 (1996).
151. Y. Dai, C. Huang, M. Huang and C. Liu, *Phys. Lett. B* **387**, 379 (1996);
R. S. Marques de Carvalho, F. S. Navarra, M. Nielsen, E. Ferreira and H. G. Dosch, *Phys. Rev. D* **60**, 034009 (1999).
152. C. Huang, C. Qiao and H. Yan, *Phys. Lett. B* **437**, 403 (1998);
C. Huang and H. Yan, *Phys. Rev. D* **59**, 114022 (1999).
153. I. I. Balitsky, V. M. Braun and A. V. Kolesnichenko, *Nucl. Phys. B* **312**, 509 (1989).
154. V. M. Braun and I. E. Filyanov, *Z. Phys. C* **44**, 157 (1989).
155. V. L. Chernyak and I. R. Zhitnitsky, *Nucl. Phys. B* **345**, 137 (1990).
156. G. P. Lepage and S. J. Brodsky, *Phys. Lett. B* **87**, 359 (1979); *Phys. Rev. D* **22**, 2157 (1980); *Phys. Rev. D* **24**, 1808 (1981).
157. A. V. Efremov and A. V. Radyushkin, *Phys. Lett. B* **94**, 245 (1980);
Theor. Math. Phys. **42**, 97 (1980).
158. V. L. Chernyak and A. R. Zhitnitsky, *JETP Lett.* **25**, 510 (1977); *Sov. J. Nucl. Phys.* **31**, 544 (1980);
159. N. Isgur and C.H. Llewellyn Smith, *Phys. Lett. B* **217**, 535 (1989);
A.V. Radyushkin, *Nucl. Phys. A* **527** 153C (1991); *Nucl. Phys. A* **532** 141 (1991).
160. The first studies of this type of correlation functions in the context of

- QCD sum rules are in: N. S. Craigie and J. Stern, *Nucl. Phys. B* **216**, 209 (1983);
N. S. Craigie, N. Paver and Riazuddin, *Z. Phys. C* **30**, 69 (1986).
161. F. del Aguila and M. K. Chase, *Nucl. Phys. B* **193**, 517 (1981);
E. Braaten, *Phys. Rev. D* **28**, 524 (1983);
E.P. Kadantseva, S.V. Mikhailov and A.V. Radyushkin, *Sov. J. Nucl. Phys.* **44**, 326 (1986).
 162. A. Khodjamirian, *Eur. Phys. J. C* **6**, 477 (1999).
 163. I. I. Balitsky, *Phys. Lett. B* **124**, 230 (1998).
 164. I. I. Balitsky and V. M. Braun, *Nucl. Phys. B* **311**, 541 (1989).
 165. V. M. Braun and I. E. Filyanov, *Z. Phys. C* **48**, 239 (1990).
 166. P. Ball, V. M. Braun, Y. Koike and K. Tanaka, *Nucl. Phys. B* **529**, 323 (1998);
P. Ball and V. M. Braun, *Nucl. Phys. B* **543**, 201 (1999).
 167. V. L. Chernyak and A. R. Zhitnitsky, *Phys. Rept.* **112**, 173 (1984).
 168. U. Aglietti *et al.*, *Phys. Lett. B* **441**, 371 (1998)
 169. V. Y. Petrov and P. V. Pobylitsa, hep-ph/9712203;
V. Y. Petrov *et al.* *Phys. Rev. D* **59**, 114018 (1999).
 170. P. Ball, *JHEP* **9901**, 010 (1999).
 171. A. S. Gorsky, *Yad. Fiz.* **45**, 824 (1987).
 172. P. Ball and V. M. Braun, *Phys. Rev. D* **54**, 2182 (1996).
 173. V. Braun, R. J. Fries, N. Mahnke and E. Stein, hep-ph/0007279.
 174. M. Diehl, T. Gousset, B. Pire and O. Teryaev, *Phys. Rev. Lett.* **81**, 1782 (1998);
M. V. Polyakov, *Nucl. Phys. B* **555**, 231 (1999).
 175. N. Kivel and L. Mankiewicz, hep-ph/0008168.
 176. V. Braun and I. Halperin, *Phys. Lett. B* **328**, 457 (1994).
 177. V. M. Braun, A. Khodjamirian and M. Maul, *Phys. Rev. D* **61**, 073004 (2000).
 178. C.J. Bebek *et al.*, *Phys. Rev. D* **17**, 1693 (1978);
S.R. Amendolia *et al.*, *Nucl. Phys. B* **277**, 168 (1986).
 179. V. M. Belyaev, *Z. Phys. C* **65**, 93 (1995).
 180. A. V. Radyushkin and R. T. Ruskov, *Nucl. Phys. B* **481**, 625 (1996).
 181. H. J. Behrend *et al.* [CELLO Collaboration], *Z. Phys. C* **49**, 401 (1991).
 182. J. Gronberg *et al.* [CLEO Collaboration], *Phys. Rev. D* **57**, 33 (1998).
 183. A. Schmedding and O. Yakovlev, hep-ph/9905392.
 184. V. M. Belyaev, V. M. Braun, A. Khodjamirian and R. Rückl, *Phys. Rev. D* **51**, 6177 (1995).
 185. A. Khodjamirian and R. Ruckl, in *Heavy Flavors*, 2nd edition, eds., A.J. Buras and M. Linder, World Scientific (1998), hep-ph/9801443.

186. V. L. Eletsky, B. L. Ioffe and Y. I. Kogan, *Phys. Lett. B* **122**, 423 (1983);
V. L. Eletskii, Y. I. Kogan, *Z. Phys. C* **20**, 357 (1983).
187. V. M. Braun, hep-ph/9911206.
188. V. M. Belyaev, A. Khodjamirian and R. Rückl, *Z. Phys. C* **60**, 349 (1993).
189. A. Khodjamirian, R. Rückl and C. W. Winhart, *Phys. Rev. D* **58**, 054013 (1998).
190. N. Isgur and M. B. Wise, *Phys. Rev. D* **41**, 151 (1990); *Phys. Rev. D* **42**, 2388 (1990).
191. V.M. Braun, in "Rostock 97, Progress in heavy quark physics"(1997), pp. 105-118, hep-ph/9801222.
192. A. Khodjamirian, R. Rückl, S. Weinzierl and O. Yakovlev, *Phys. Lett. B* **410**, 275 (1997).
193. E. Bagan, P. Ball and V. M. Braun, *Phys. Lett. B* **417**, 154 (1998).
194. P. Ball, *JHEP* **9809**, 005 (1998).
195. A. Ali, V. M. Braun and H. Simma, *Z. Phys. C* **63**, 437 (1994).
196. P. Ball, V. M. Braun, *Phys. Rev. D* **58**, 094016 (1998).
197. A. A. Ovchinnikov, *Sov. J. Nucl. Phys.* **50**, 519 (1989).
198. P. Colangelo, G. Nardulli, A. Deandrea, N. Di Bartolomeo, R. Gatto and F. Feruglio, *Phys. Lett. B* **339**, 151 (1994).
199. I. W. Stewart, *Nucl. Phys. B* **529**, 62 (1998).
200. G. M. de Divitiis et al., *JHEP* **9810**, 010 (1998).
201. T. M. Aliev, D. A. Demir, E. Iltan and N. K. Pak, *Phys. Rev. D* **53**, 355 (1996).
202. T. M. Aliev, E. Iltan and N. K. Pak, *Z. Phys. C* **73**, 293 (1997).
203. S. Zhu and Y. Dai, *Phys. Rev. D* **59**, 114015 (1999).
204. P. Colangelo, F. De Fazio, G. Nardulli, N. Di Bartolomeo and R. Gatto, *Phys. Rev. D* **52**, 6422 (1995).
205. P. Colangelo and F. De Fazio, *Eur. Phys. J. C* **4**, 503 (1998);
Y. Dai and S. Zhu, *Phys. Rev. D* **58**, 074009 (1998).
206. A. Khodjamirian, G. Stoll and D. Wyler, *Phys. Lett. B* **358**, 129 (1995);
A. Ali and V. M. Braun, *Phys. Lett. B* **359**, 223 (1995).
207. B. Blok and M. Shifman, *Sov. J. Nucl. Phys.* **45**, 135, 301, 522 (1987);
Nucl. Phys. B **389**, 534 (1993); **399**, 441, 459 (1993).
208. A. Khodjamirian, R. Rückl, G. Stoll and D. Wyler, *Phys. Lett. B* **402**, 167 (1997).
209. I. Halperin, *Phys. Lett. B* **349**, 548 (1995);
A. Khodjamirian and R. Rückl, in "Continuous Advances in QCD 1998",
ed. A.V. Smilga, p. 287-303, World Scientific (1998), hep-ph/9807495.